SUMMARY OF PROFESSIONAL ACCOMPLISHMENTS

Magdalena Skurzok

Faculty of Physics, Astronomy and Applied Computer Science
Jagiellonian University

Cracow, 15th September 2023

Table of Contents

1 Personal data

1.1 Name and Surname

Magdalena Skurzok

1.2 Affiliation

Faculty of Physics, Astronomy and Applied Computer Science
Jagiellonian University in Cracow
ul. Łojasiewicza 11
30-348 Cracow

1.3 Diplomas and academic degrees

- Ph.D. degree in physics (with distinction)
  Jagiellonian University, Cracow, 2016
  Thesis entitled: *Search for η-mesic helium via dd* $\rightarrow {}^3He n\pi^0$ *reaction by means of the WASA-at-COSY facility*
  Supervisor: prof. dr hab. Paweł Moskal

- MSc degree in physics (with distinction)
  Jagiellonian University, Cracow, 2010
  Thesis entitled: *Feasibility study of η-mesic nuclei production by means of the WASA-at-COSY and COSY-TOF facilities*
  Supervisor: prof. dr hab. Paweł Moskal

1.4 Education and employment in scientific institutions

from 2021	Assistant Professor, Faculty of Physics, Astronomy and Applied Computer Science, Jagiellonian University
2018 - 2020	Post-doctoral Fellowship, Laboratori Nazionali di Frascati - Instituto Nazionale di Fisica Nucleare (LNF-INFN), Frascati, Italy
2017 - 2018	Research Assistant in the frame of research grant SONATA financed by the National Science Center, Faculty of Physics, Astronomy and Applied Computer Science, Jagiellonian University

2014 - 2016 Research Assistant in the frame of research grant PRELUDIUM financed by the National Science Center, Faculty of Physics, Astronomy and Applied Computer Science, Jagiellonian University

2010 - 2015 Ph.D. Studies in Applied Nuclear Physics and Innovative Technologies as a part of International Doctoral Projects financed by the Foundation for Polish Science, Faculty of Physics, Astronomy and Applied Computer Science, Jagiellonian University

2005 - 2010 Master studies in Physics, Faculty of Physics, Astronomy and Applied Computer Science, Jagiellonian University

2002 - 2005 Antoni Osuchowski High School in Cieszyn, mathematical-physical profile

2 Scientific achievement constituting the basis for the habilitation procedure

The basis of my habilitation is a series of eleven publications. They concern experimental studies of exotic bound systems in the form of mesic nuclei and mesonic atoms. The investigation of such objects is crucial; they provide valuable information on the interactions of mesons with nucleons in vacuum and nuclear matter and interactions of mesons with nuclei. This information is pivotal for the verification and testing of available theoretical models. The performed studies may have significant consequences in various sectors of physics, from nuclear physics to astrophysics.

2.1 Title of scientific achievement

As the scientific achievement (set out in art. 16 point 2 of the act from 14.03.2003 on academic degrees and titles and degrees and titles in the field of art, Dz. U. 2017 r. poz. 1789), I present a series of 11 thematically related scientific publications entitled:

Investigation of exotic nuclear matter in the form of mesic nuclei and mesonic atoms

2.2 A series of publications constituting a scientific achievement

Impact Factor (IF) and ministerial points are given for the year of publication. The total number of citations (on 15 September 2023) is taken from the Web of Science.

[H1] P. Adlarson, W. Augustyniak, W. Bardan, M. Bashkanov, F.S. Bergmann, M. Berłowski, H. Bhatt, A. Bondar, M. Büscher, H. Calén, I. Ciepał, H. Clement,

E. Czerwiński, K. Demmich, R. Engels, A. Erven, W. Erven, W. Eyrich, P. Fedorets, K. Föhl, K. Fransson, F. Goldenbaum, A. Goswami, K. Grigoryev, C.O. Gullström, L. Heijkenskjöld, V. Hejny, N. Hüsken, L. Jarczyk, T. Johansson, B. Kamys, N.G. Kelkar, G. Kemmerling, G. Khatri, A. Khoukaz, A. Khreptak, D.A. Kirillov, S. Kistryn, H. Kleines, B. Kłos, W. Krzemień, P. Kulessa, A. Kupść, A. Kuzmin, K. Lalwani, D. Lersch, B. Lorentz, A. Magiera, R. Maier, P. Marciniewski, B. Mariański, H.P. Morsch, P. Moskal, H. Ohm, E. Perez del Rio, N.M. Piskunov, D. Prasuhn, D. Pszczel, K. Pysz, A. Pyszniak, J. Ritman, A. Roy, Z. Rudy, O. Rundel, S. Sawant, S. Schadmand, I. Schätti-Ozerianska, T. Sefzick, V. Serdyuk, B. Shwartz, K. Sitterberg, T. Skorodko, **M. Skurzok**, J. Smyrski, V. Sopov, R. Stassen, J. Stepaniak, E. Stephan, G. Sterzenbach, H. Stockhorst, H. Ströher, A. Szczurek, A. Trzciński, R. Varma, M. Wolke, A. Wrońska, P. Wüstner, A. Yamamoto, J. Zabierowski, M. J. Zieliński, J. Złomańczuk, P. Żuprański, M. Żurek

Search for η-mesic ^4He in the $dd \to {}^3He n\pi^0$ and $dd \to {}^3He p\pi^-$ reactions with the WASA-at-COSY facility

Nucl. Phys. A 959, 102 (2017)

IF: 1.992, no. citations: 33, ministerial points: 25

I estimate my contribution at approx. 80%.

I am the leading and corresponding author of the article. My contribution consisted of (i) co-coordinating the dedicated WASA-at-COSY experiment in 2010 at Forschungszentrum Jülich (Germany) by active participation in the preparation for the measurements (preparation and tests of the detection system, data acquisition system, triggers) as well as their execution and monitoring (participation in the experimental shifts), (ii) independently developing and performing the data analysis (preparation of dedicated Monte Carlo simulations and analysis of the data collected during the experiment) as well as (iii) interpretation of the results. I prepared the publication. According to the rules of the WASA-at-COSY Collaboration, the list of authors is given in alphabetical order regardless of their contribution to the publication preparation.

[H2] **M. Skurzok**, P. Moskal, N. G. Kelkar, S. Hirenzaki, H. Nagahiro, N. Ikeno

Constraining the optical potential in the search for η-mesic ^4He

Phys. Lett. B 782, 6 (2018)

IF: 4.162, no. citations: 14, ministerial points: 40

I estimate my contribution at approx. 80%.

I am the leading and corresponding author of the article. My contribution consisted of (i) independently developing and conducting a comparative analysis of the data collected in the WASA-at-COSY experiment (which I participated in and co-coordinated) at Forschungszentrum Jülich (Germany) with the theoretical model developed by a group from Nara Women's University in Japan, and (ii) the interpretation of the results. I prepared the publication.

[H3] N. G. Kelkar, H. Kamada, **M. Skurzok**
N-N-N model calculations for experimental η-mesic ^{3}He searches*
Int. J. Mod. Phys. E 28, No. 8, 1950066 (2019)
IF: 1.036, no. citations: 3, ministerial points: 70
I estimate my contribution at approx. 20%.
My contribution consisted of (i) preparing and performing Monte Carlo simulations based on a theoretical model developed by a research group from the University of Los Andes, Bogotá (Colombia), to determine the geometric acceptance of the WASA detector for the measurement of the considered process and (ii) participating in the interpretation of the results.

[H4] **M. Skurzok**, S. Hirenzaki, S. Kinutani, H. Konishi, P. Moskal, H. Nagahiro, O. Rundel
Non-mesonic decay of the η-mesic ^{3}He via $pd \to {}^3He2\gamma(6\gamma)$ reaction
Nucl. Phys. A 993, 121647 (2020)
IF: 1.683, no. citations: 4, ministerial points: 100
I estimate my contribution at approx. 60%.
I am the leading and corresponding author of the article. My contribution consisted of (i) proposing the subject of research on the description of a new mechanism for the mesic nuclei decay, (ii) participating in the development of the theoretical model in collaboration with the research group from the Nara Women's University, and (iii) developing and performing dedicated Monte Carlo simulations to study the feasibility of investigating the proposed mechanism in the WASA-at-COSY experiment, which I independently coordinated in 2014 at Forschungszentrum Jülich (Germany). I prepared the publication.

[H5] P. Adlarson, W. Augustyniak, W. Bardan, M. Bashkanov, S. D. Bass, M. Berłowski, A. Bondar, M. Büscher, H. Calén, I. Ciepał, H. Clement, E. Czerwiński, R. Engels, A. Erven, W. Erven, W. Eyrich, P. Fedorets, K. Föhl, K. Fransson, F. Goldenbaum, A. Goswami, K. Grigoryev, L. Heijkenskjöld, V. Hejny, S. Hirenzaki, L. Jarczyk, T. Johansson, B. Kamys, N. G. Kelkar, G. Kemmerling, A. Khreptak, D.A. Kirillov, S. Kistryn, H. Kleines, B. Kłos, W. Krzemień, P. Kulessa, A. Kupść, K. Lalwani, D. Lersch, B. Lorentz, A. Magiera, R. Maier, P. Marciniewski, B. Mariański, H.P. Morsch, P. Moskal, H. Ohm, W. Parol, E. Perez del Rio, N.M. Piskunov, D. Prasuhn, D. Pszczel, K. Pysz, J. Ritman, A. Roy, O. Rundel, S. Sawant, S. Schadmand, I. Schätti-Ozerianska, T. Sefzick, V. Serdyuk, B. Shwartz, T. Skorodko, **M. Skurzok**, J. Smyrski, V. Sopov, R. Stassen, J. Stepaniak, E. Stephan, G. Sterzenbach, H. Stockhorst, H. Ströher, A. Szczurek, A. Trzciński, M. Wolke, A. Wrońska, P. Wüstner, A. Yamamoto, J. Zabierowski, M. J. Zieliński, J. Złomańczuk, P. Żuprański, M. Żurek
Search for η-mesic ^{3}He with the WASA-at-COSY facility in the $pd \to {}^3He2\gamma$ and $pd \to {}^3He6\gamma$ reactions
Phys. Lett. B 802, 135205 (2020)
IF: 4.771, no. citations: 5, ministerial points: 140

I estimate my contribution at approx. 60%.
I am the leading and corresponding author of the article. My contribution consisted of (i) participating in the preparation of the scientific proposal for the experiment (ii) independently coordinating the WASA-at-COSY experiment in 2014 at Forschungszentrum Jülich (Germany) by active participation in the preparation of the measurement (preparation and tests of the detection system, data acquisition system, triggers, data monitoring software) and their execution and monitoring (participation in the experimental shifts), (iii) developing and performing data analysis with Mr Oleksandr Rundel, who did his Ph.D. thesis under my supervision as an auxiliary supervisor (performing dedicated Monte Carlo simulations and analysis of data collected during the experiment) as well as (iv) results interpretation. I took a significant part in the article edition. According to the rules of the WASA-at-COSY Collaboration, the list of authors is given in alphabetical order regardless of their contribution to the publication preparation.

[H6] N. G. Kelkar, D. Bedoya Fierro, H. Kamada, **M. Skurzok**
Study of the N momentum distribution for experimental η-mesic ^{3}He searches*
Nucl. Phys. A 996, 121698 (2020)
IF: 1.683, no. citations: 3, ministerial points: 100
I estimate my contribution at approx. 20%.
My contribution consisted of (i) preparing and performing Monte Carlo simulations based on a theoretical model developed by a research group from the University of Los Andes, Bogotá (Colombia), to determine the geometric acceptance of the WASA detector for the measurement of the considered process and (ii) participating in the interpretation of the results.

[H7] P. Adlarson, W. Augustyniak, M. Bashkanov, S. D. Bass, F. S. Bergmann, M. Berłowski, A. Bondar, M. Büscher, H. Calén, I. Ciepał, H. Clement, E. Czerwiński, K. Demmich, R. Engels, A. Erven, W. Erven, W. Eyrich, P. Fedorets, K. Föhl, K. Fransson, F. Goldenbaum, A. Goswami, K. Grigoryev, L. Heijkenskjöld, V. Hejny, N. Hüsken, S. Hirenzaki, T. Johansson, B. Kamys, N. G. Kelkar, G. Kemmerling, A. Khoukaz, A. Khreptak, D. A. Kirillov, S. Kistryn, H. Kleines, B. Kłos, W. Krzemień, P. Kulessa, A. Kupść, K. Lalwani, D. Lersch, B. Lorentz, A. Magiera, R. Maier, P. Marciniewski, B. Mariański, H.-P. Morsch, P. Moskal, H. Ohm, W. Parol, E. Perez del Rio, N. M. Piskunov, D. Prasuhn, D. Pszczel, K. Pysz, J. Ritman, A. Roy, O. Rundel, S. Sawant, S. Schadmand, T. Sefzick, V. Serdyuk, B. Shwartz, T. Skorodko, **M. Skurzok**, J. Smyrski, V. Sopov, R. Stassen, J. Stepaniak, E. Stephan, G. Sterzenbach, H. Stockhorst, H. Ströher, A. Szczurek, M. Wolke, A. Wrońska, P. Wüstner, A. Yamamoto, J. Zabierowski, M. J. Zieliński, J. Złomańczuk, M. Żurek
Search for η-mesic ^{3}He with the WASA-at-COSY facility in the $pd \to dp\pi^0$ reaction
Phys. Rev. C 102 no. 4, 044322 (2020)
IF: 3.296, no. citations: 4, ministerial points: 140
I estimate my contribution at approx. 60%.

I am the leading and corresponding author of the article. My contribution consisted of (i) participating in the preparation of the scientific proposal for the experiment (ii) independently coordinating the WASA-at-COSY experiment in 2014 at Forschungszentrum Jülich (Germany) by active participation in the preparation of the measurement (preparation and tests of the detection system, data acquisition system, triggers, data monitoring software) and their execution and monitoring (participation in the experimental shifts), (iii) developing and performing data analysis with Mr Aleksander Khreptak, who did his Ph.D. thesis under my supervision as an auxiliary supervisor (performing dedicated Monte Carlo simulations and analysis of data collected during the experiment) as well as (iv) results interpretation. I took a significant part in the article edition. According to the rules of the WASA-at-COSY Collaboration, the list of authors is given in alphabetical order regardless of their contribution to the publication preparation.

[H8] **M. Skurzok**, A. Scordo, S. Niedźwiecki, A. Baniahmad, M. Bazzi, D. Bosnar, M. Bragadireanu, M. Carminati, M. Cargnelli, A. Clozza, C. Curceanu, L. De Paolis, R. Del Grande, L. Fabbietti, C. Fiorini, C. Guaraldo, M. Iliescu, M. Iwasaki, P. Levi Sandri, J. Marton, M. Miliucci, P. Moskal, K. Piscicchia, F. Sgaramella, H. Shi, M. Silarski, D. L. Sirghi, F. Sirghi, A. Spallone, M. Tüchler, O. Vazquez Doce, J. Zmeskal
Characterization of the SIDDHARTA-2 luminosity monitor
JINST 15, P10010 (2020)
IF: 1.415, no. citations: 10, ministerial points: 70
I estimate my contribution at approx. 80%.
I am the leading and corresponding author of the article. My contribution consisted of (i) developing the design of the luminosity detector for the SIDDHARTA-2 experiment at the LNF-INFN in Italy, (ii) coordinating the construction of the detector at the Institute of Physics of the Jagiellonian University, (iii) active participation in the testing of the detector and the installation of its modules on the beam of the DAΦNE accelerator, (iv) performing the measurements, and (v) independently analyzing the experimental data. I am also a co-author of the program for luminosity monitoring during the SIDDHARTA-2 experiment. I prepared the publication.

[H9] **M. Skurzok**
Search for η-mesic helium with WASA-at-COSY
Acta Phys. Polon. B 51, 33 (2020)
IF: 0.748, no. citations: 3, ministerial points: 40
I estimate my contribution at 100%.
That is single-author conference proceedings in which I summarised the research carried out by the WASA-at-COSY Collaboration in terms of the search for mesic nuclei, in which I actively participated both by coordinating measurements (preparation of experiments and participation in measurements) and by independently performing data analyses (experimental data and Monte Carlo

simulations). I prepared the publication.

[H10] **M. Skurzok**
Status of the search for η-mesic nuclei with particular focus on η-Helium bound states
Few Body Syst. 62, 5 (2021)
IF: 1.844, no. citations: 0, ministerial points: 40
I estimate my contribution at 100%.
That is a single-author review article in which I have summarised my research on mesic nuclei, focusing mainly on the search for η-Helium bound states carried out by the WASA-at-COSY Collaboration, in which I have been actively involved both by coordinating measurements (preparation of experiments and participation in measurements) and by performing data analyses (experimental data and Monte Carlo simulations) myself. The paper also contains an overview of the models developed by the theoretical groups I collaborate with. I prepared the publication.

[H11] K. Piscicchia, **M. Skurzok**, M. Cargnelli, R. Del Grande, L. Fabbietti, J. Marton, P. Moskal, A. Scordo, A. Ramos, D. L. Sirghi, O. Vazquez Doce, J. Zmeskal, S. Wycech, P. Branchini, F. Ceradini, E. Czerwinski, E. De Lucia, S. Fiore, A. Kupść, G. Mandaglio, M. Martini, A. Passeri, V. Patera, E. Perez Del Rio, A. Selce, M. Silarski, C. Curceanu
First simultaneous $K^- p \to (\Sigma^0/\Lambda)\,\pi^0$ cross-sections measurement at 98 MeV/c
article accepted for publication in w Phys. Rev. C (2023)
IF: 3.1, no. citations: 0, ministerial points: 140
I estimate my contribution at approx. 45%.
I am the leading author with Dr. Kristian Piscicchia (equal contribution to the article) and the corresponding author. My contribution consisted of (i) a full analysis of the experimental data collected by the AMADEUS research group to which I belong, (ii) preparation of the dedicated Monte Carlo simulations, and (iii) participation in the discussions and interpretation of the results. The publication was prepared with my significant contribution.

2.3 Discussion of the scientific purposes of the works mentioned above and the achieved results

The citations included in the following section refer to the list of scientific publications included in Section 2.2 (with the prefix "H"), presented at the end of this chapter and in Section 2.1 of the *List of Achievements* (with the prefixes "R", "P", "I").

2.3.1 Introduction

The study of exotic nuclear matter is currently one of the most popular issues in nuclear physics, both from an experimental and theoretical point of view. Many exotic nuclear objects have already been observed, such as, among others, the hypernuclei discovered by

Polish Professors Marian Danysz and Jerzy Pniewski [1], tetraquarks, and pentaquarks observed for the first time by the Belle [2] and LHCb [3, 4] Collaborations, respectively, dibaryons discovered by the WASA-at-COSY [R83,R89,R103] group, and mesonic atoms (pionic and kaonic atoms) observed at the GSI (Germany) and KEK (Japan) research centers [5, 6]. Research into these states of nuclear matter is being carried out at many research centers around the world, such as at the Laboratori Nazionali di Frascati research institute in Italy (LNF-INFN), where the SIDDHARTA-2 [R4,R16,R20] experiment is being carried out to observe kaonic deuterium atoms for the first time in the world, as well as precisely studying the already discovered kaonic atoms of other elements, including hydrogen and helium.

A major experimental challenge is the research for new forms of nuclear matter that have been theoretically predicted but never observed, such as the mesic nuclei [7]. Contrary to mesonic atoms (shown schematically in Fig. 2.1 (a)), in which the Coulomb effects are dominating, they are systems bound by predominantly strong interactions in the case of charged mesons (K^+, K^-) or objects bound only by the strong interactions in the case of neutral mesons (η, η', K^0, ω, ϕ). A scheme of a mesic nucleus is shown in Fig. 2.1 (b).

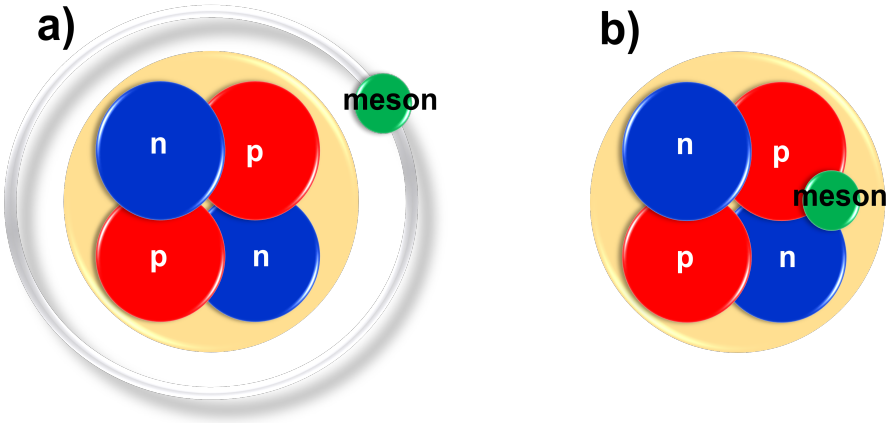

Figure 2.1: Illustrative drawing showing a scheme of a mesonic atom, where a negatively charged meson (π^-, K^-) orbiting around the atomic nucleus interacts with it via Coulomb interaction (a), and a mesonic nucleus, where a strong interaction dominates between the atomic nucleus and the meson (b).

The first signal interpreted so far as originating from kaonic clusters „K^-pp" have recently been observed in measurements of the ^{3}He(K^-,Λp)n reaction carried out at the J-PARC [8] accelerator complex. Independent studies of the possibility of kaonic nuclei production are currently being carried out by the AMADEUS group at LNF-INFN analyzing kaon K^- absorption processes in light atomic nuclei [**H11**,R28,R42,R47]. In contrast, no experiment till now has confirmed the existence of an atomic nucleus bound by a strong interaction with a neutral meson. Among the most promising candidates for such bound systems are the η-mesic nuclei (η, η'), since the η and η' mesons are neutral particles and their interaction with nucleons is strongly attracting [7] (the ηN interaction

is stronger than the η'N [9]). A method with a good chance of discovering a system of bound η meson with the nuclei of helium atoms has been developed by a research group from Jagiellonian University. Dedicated research has been carried out within the framework of the international WASA-at-COSY Collaboration at the Research Centre Forschungszentrum Jülich in Germany [**H1-H7,H9,H10**].

The subject of my scientific activity is the experimental search for the bound states of the η meson with light atomic nuclei and the exploration of kaonic atoms and nuclei by studying the low-energy interactions of negatively charged kaons with nuclear matter. I have carried out this research in collaboration with the experimental groups WASA-at-COSY at the Forschungszentrum Jülich (Germany) and AMADEUS and SIDDHARTA-2 at the Laboratori Nazionali di Frascati LNF-INFN (Italy), as well as with teams of theorists from the Universidad de los Andes in Colombia and Nara Women's University in Japan, respectively.

The study of exotic systems in the form of mesic nuclei and kaonic atoms is extremely important for a deeper understanding of elementary meson-nucleon interactions at low energies (the area of non-perturbative QCD). It allows verification of existing theoretical models/predictions, with consequent impact on the understanding of many unsolved problems in physics, such as chiral symmetry breaking conferring mass to the surrounding matter or the structure of neutron stars.

My contribution to the research mentioned above involves (i) the design, construction, and testing of detectors used in nuclear/particle physics measurements involving accelerator beams, (ii) active participation in the experiments, including as the main coordinator of the measurements, (iii) participation in theoretical studies related to the topics under consideration, and (iv) conducting analyses of experimental data and simulations that resulted in the original results presented in papers [H1-H11]. The aims, topics, and results of my research are presented in detail in the following sections.

2.3.2 Research on η-mesic nuclei

The era of the search for η mesic nuclei, or strongly bound systems of η meson with atomic nuclei, began more than 30 years ago, after Heider and Liu [10] postulated their existence based on the results of an earlier analysis, shown in Ref. [11], demonstrating the strong and attractive nature of the interaction of η meson with nucleons. It was predicted that due to the relatively small value of the determined scattering length $a_{\eta N}$ [11], the η-nucleon bound state could be formed only for nuclei with masses of A$\geq$ 12. However, recent hadron- and photoproduction studies of η mesons have resulted in a wide range of the scattering length ηN values, which does not exclude the formation of strongly bound systems of η meson with light nuclei, such as helium, tritium, and even deuterium (see review articles [7, 12–16]).

Hypothetical η mesic nuclei have been searched for in many experiments, but no clear signatures indicating their existence have been observed so far. However, some experimental indications [15, 16] may point to the possibility of the formation of such

exotic systems.

The discovery of η mesic nuclei would not only be of cognitive interest but would also allow the precise determination of the poorly known ηN scattering length [7,12,13], which would be crucial for a better understanding of elementary η-nucleon interactions in the nuclear medium in the low energy region. Moreover, it would provide an opportunity to elucidate the structure of the η meson since, as the authors of the papers [15,17,18] have shown, the binding of the η meson in nuclear matter is in close relation to the glue content of the singlet component of the quark-gluon wave function of the η meson. The study of the bound states of the η meson with atomic nuclei can also help explore the properties of the N*(1535) baryon resonance in nuclear matter by testing various theoretical models describing its internal structure, including the chiral doublet models [19–21], or the chiral unitarity approach [22–26].

The search for η-mesic nuclei is quite an experimental challenge. It has been taken up by a Krakow research group from the Jagiellonian University, to which the author of this paper belongs, developing an experimental method that allows the search for bound states of the η meson with the nuclei of helium atoms. The research was carried out with exceptional precision within the framework of the international WASA-at-COSY research group at Forschungszentrum Jülich (Germany) using a cooled proton or deuteron beam of the COSY synchrotron and the WASA detection system. The results of these studies presented in papers **[H1-H7,H9,H10]**, with emphasis on my contribution, are described in detail in the second part of this section. The first part, in turn, focuses on presenting the theoretical predictions and the status of other experiments dedicated to the search for the nuclei. The first part, in turn, focuses on presenting theoretical predictions and describing other experiments dedicated to the search for η-mesic nuclei.

2.3.2.1 η-nucleon interaction

The η meson, belonging to the nonet of light pseudoscalar mesons, is an electrically neutral particle, characterized by zero spin and negative parity ($J^\pi = 0^-$), which can decay under both strong and electromagnetic interactions [27]. In the quark model, it is shown (like η') as a superposition of an octet state ($\eta_8 = \frac{1}{\sqrt{6}}(d\bar{d} + u\bar{u} - 2s\bar{s})$) and singlet state ($\eta_1 = \frac{1}{\sqrt{3}}(d\bar{d} + u\bar{u} + s\bar{s})$) of the SU(3) flavour symmetry group ($|\eta >= \eta_8 cos\theta - \eta_1 sin\theta$). The mixing angle θ determined based on phenomenological studies of various decays oscillates between -15° a -20° [28–30], suggesting that the η meson is mainly composed of the octet state, with a small contribution from the singlet state. Observation of the mass of the η' meson ($m_{\eta'}$=957.78±0.06 MeV/c^2 [27]), much larger than the mass determined based on the assumption of pure-quark structure (mixing of SU(3) states), indicates the gluon contribution to the singlet state [15], which, due to the mixing of η-η', also affects the description of the ηN interaction. It was observed that the η meson interacts more strongly with the nucleon than the η' meson [9].

The η - nucleon interaction has been studied for many years considering the possibility of the formation of η-mesic nuclei. The most appropriate way to study such an interaction would be elastic scattering measurements, which, however, are not possible due to the

short lifetimes of η meson ($\tau \leq 5{\cdot}10^{-19}$ s [27]). Therefore, information about the ηN interaction is mainly obtained from experimental data for processes such as $\pi\mathrm{N} \to \eta\mathrm{N}$, $\gamma\mathrm{N} \to \eta\mathrm{N}$ and $\mathrm{NN} \to \mathrm{NN}\eta$ ($pp \to pp\eta$ [31], $pn \to pn\eta$ [32]). The low-energy interaction of the η meson with the nucleon is dominated by the broad baryon resonance N*(1535) ($\Gamma \sim$150 MeV) [27], located just 49 MeV above the threshold for the ηN production, which is strongly coupled to both η and π, as manifested by a sharp rise in the cross-section spectra of pion-nucleon [33, 34], as seen in Fig. 2.2. The ηN scattering amplitude is thus complex, with the imaginary part corresponding to the excitation of the N*(1535) resonance due to the absorption of the η meson by the nucleon.

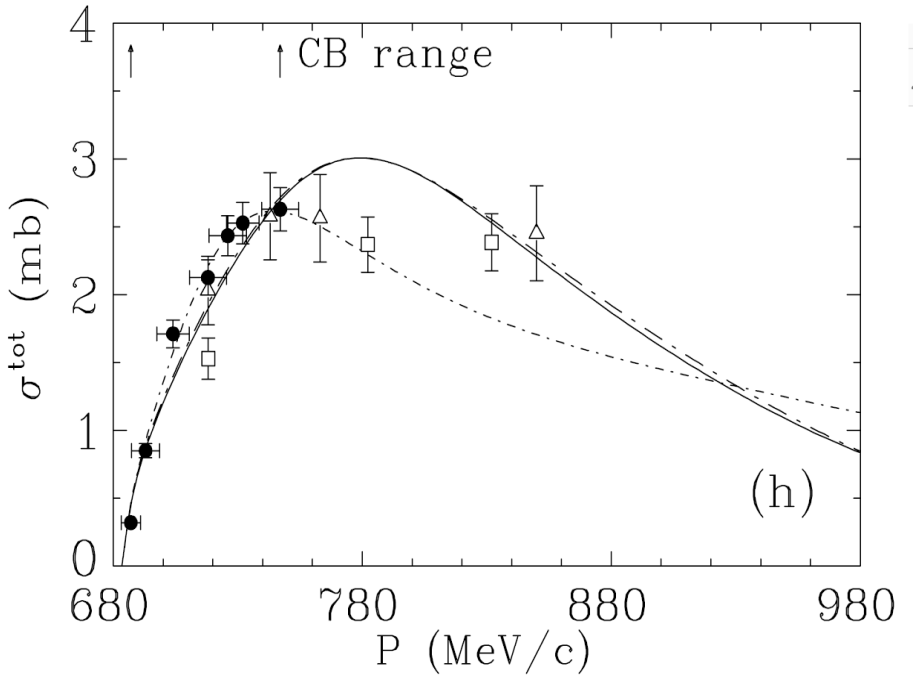

Figure 2.2: The total cross-section for the $\pi^- p \to \eta n$ reaction as a function of the π^- momentum. The experimental data are from measurements described in the papers: [33] (solid circles), [33] (empty triangles) and [36] (open squares). Lines indicate fits of theoretical models (FA02 (solid), I375 (long dashed), and PWA (short dashed)). The figure is adapted from [33].

It is determined mainly phenomenologically by comparing coupled-channels calculations with available experimental data [7, 12, 35]. The first such analysis by Bhalerao and Liu [11] (including the $\eta-$N, $\pi-$N and $\Delta - \pi$ channels) showed that the interaction between the η meson and the nucleon is attractive and strong in the threshold region (s-wave). Photon- and hadron-induced reaction studies carried out so far, based on various theoretical models, abound in a wide range of the $a_{\eta N}$ scattering length values from $(0.18, 0.16i)$ fm to $(1.14, 0.49i)$ fm [7, 12, 13, 34, 35, 37] describing the strength of the interaction potential in the low energy region. The ηN scattering amplitudes for several different interaction models are shown in Fig. 2.3.

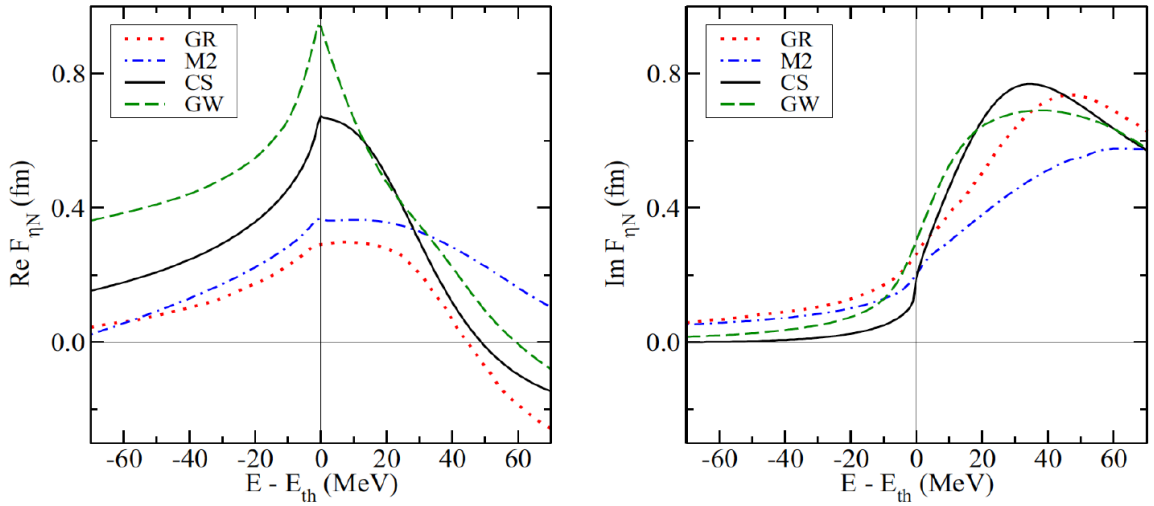

Figure 2.3: Energy dependence of the real (left panel) and imaginary (right panel) parts of the free ηN scattering amplitude determined based on different theoretical models: GW (dashed) [38], CS (solid) [39], M2 (dot-dashed) [40] and GR (dotted) [24,41]. The vertical line denotes the η-nucleon production threshold. The figure is taken from Ref. [42].

Since the calculations are model-dependent, the determined $a_{\eta N}$ scattering lengths cannot be a good indicator of whether or not the η meson can form a bound state with atomic nucleus or not [43]. The results obtained, do not, however, rule out the formation of strongly bound η-nucleus systems even with light nuclei [7, 12–16].

2.3.2.2 η-mesic nuclei in theory - current approaches and predictions

After the discovery of the strong and attractive η-nucleon interaction [11], the possibility of η-mesic nuclei formation was considered and discussed in many theoretical papers, which are summarized in the articles [7, 12, 13, 15, 16][R5]. Many different approaches and predictions have been made about these exotic objects. Selected ones, highlighting the most recent ones involving η-mesic helium nuclei, are presented in this section.

In general, the theoretical search for η-mesic nuclei is based on the use of information about the ηN interaction, obtained from fitting coupled-channel models to experimental data for η meson production, to construct complex η-nucleus potential, or the scattering matrix S [12, 13, 44]. According to non-relativistic quantum mechanics, a bound state occurs when the interaction potential is attractive and the states that are solutions of the radial Schrödinger equation lie on an imaginary axis in the momentum plane ($Im(p) > 0$) (in the so-called "physical sheet" of the scattering matrix) as shown in Fig. 2.4. Mesic nuclei, due to their possible decays and associated inelastic interactions (complex potential), are not stricte bound states but rather quasibound states. Bound (or quasibound) states correspond to poles in the upper part of the second quadrant

of the scattering matrix (in the lower part of the second quadrant there may be poles corresponding to resonances that pass from the third quadrant due to inelastic interactions) [12,13]. The physical sheet of the S-matrix contains poles corresponding to virtual and quasi-virtual states.

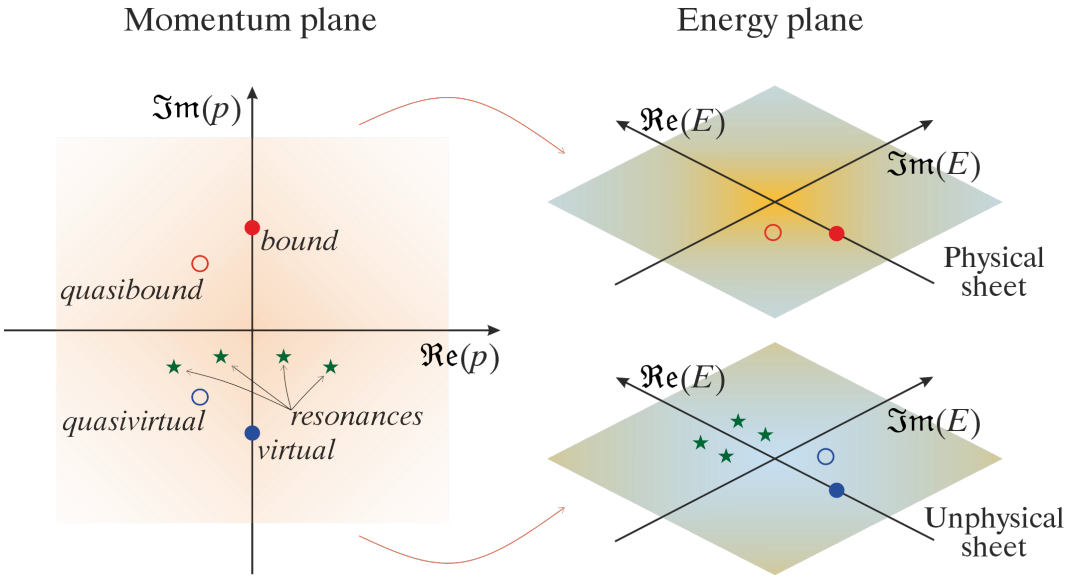

Figure 2.4: The diagram displays the complex planes of momentum (left) and energy (right) with labels indicating the positions of the poles in the scattering matrix (S). The poles correspond to different states: bound (red full circle), quasibound (red empty circle), virtual (blue full circle), quasivirtual (blue empty circle) and resonances (green stars). The figure is adapted from Ref. [R5].

The standard approach, used mainly in the area of heavier η-mesic nuclei, is to construct the corresponding optical potential ($U_{opt} = V + iW$) based on the phenomenologically determined scattering lengths $a_{\eta N}$ and then solve the wave equation [12, 13]. This approach was applied by the precursors of the η-mesic bound states studies [10] by formulating the potential based on the so-called "$T\rho$" approximation ($U_{opt} = -\frac{2\pi}{\mu} T(\eta N \rightarrow \eta N) A\rho(r)$) [13]. Their results indicated the possibility of forming bound states in carbon and a few heavier atomic nuclei (for A$\geq$12). In their subsequent studies, they also considered the optical microscopic potential containing off-shell ηN interaction, which they compared with calculations within the factorization approximation (FA) accounting for the energy shift of the η-nucleon interaction in the nuclear medium. The obtained results indicate that the formation of bound states takes place for interaction energies ηN about 30 MeV below the threshold, which determines the reduction of the binding energy of the ηN system (relative to that determined at the threshold) [45]. Similarly, the widths of bound states strongly depend on the subthreshold dynamics of the ηN interaction.

Other calculations for bound states considering the strong energy dependence of the ηN scattering amplitudes at the threshold and in the subthreshold region are presented

in Ref. [42, 46]. Based on the scattering amplitudes for several interaction models (shown in Fig. 2.3), the binding energies and widths of the bound states of the η meson with atomic nuclei were determined. As shown in Fig. 2.5, with increasing atomic number, the binding energy increases regardless of the model considered, while the width of the meson nucleus is approximately constant. In contrast, the binding energies and widths of the mesic nuclei are smaller than those obtained by the authors of Ref. [45] as well as Ref. [24] (the latter work was based on the chiral unitarity approach).

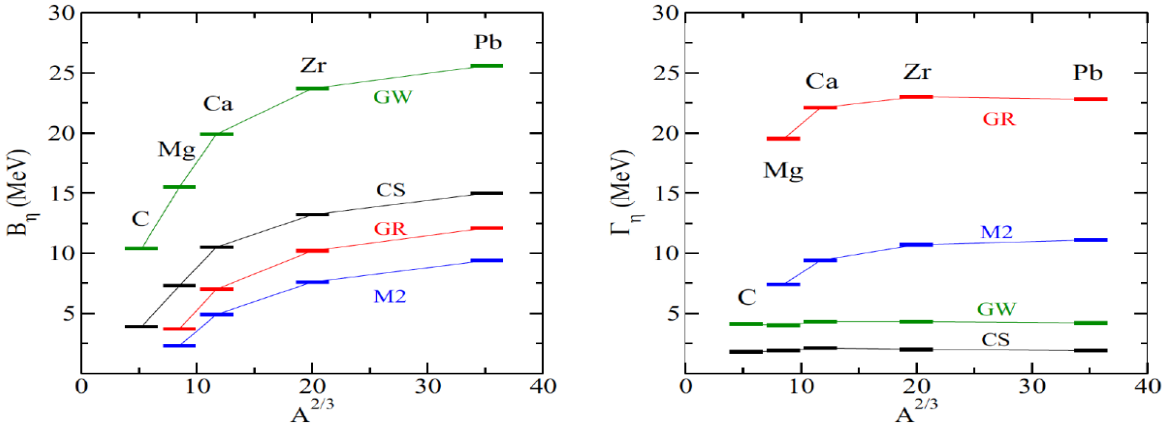

Figure 2.5: Binding energies (left panel) and widths (right panel) of 1s η-nucleus bound states in selected atomic nuclei determined based on different scattering amplitudes shown in Fig. 2.3. Figure is adapted from Ref. [42].

Also worth mentioning is the quark-meson coupling model (QMC) based on quantum chromodynamics. According to it, an immersed η meson inside an atomic nucleus couples with quarks and mixes with the η' meson [17, 47] takes place. The η-nucleus optical potential including the η-η' mixing, $U(r) = m^*_\eta(r) - m_\eta(r)$ [12], is determined based on the mass of the η meson in the medium (m^*_η) obtained by solving the mean-field equations. The solution of the Klein-Gordon equation using the above potential suggested the existence of η-mesic bound states for several closed-shell nuclei like: ^{16}O, ^{40}Ca, ^{90}Zr,^{208}Pb, and also for ^{6}He, ^{11}Be and ^{26}Mg [47, 48].

Current theoretical studies are devoted in particular to light η-mesic nuclei, such as η-mesic helium [49–62]**[H3,H4,H6]**, which are intensively searched by many experimental groups (see Sec. 2.3.2.3). The existence of light η-mesic nuclei can manifest as poles in the S-matrix (Fig. 2.4) translating into constraints on the complex η-nucleus scattering lengths ($a_{\eta-nucleus}$). For a bound system to form, the imaginary part of the scattering length must take on a positive value ($\Im(a_{\eta-nucleus})>0$), while its modulus must be smaller than that of the real part ($|\Im(a_{\eta-nucleus})|<|\Re(a_{\eta-nucleus}|$) [45]. An additional requirement to ensure that the poles of the S-matrix are located in the plane of the bound state, rather than the virtual state, is the negative value of the real part of the scattering length ($\Re(a_{\eta-nucleus})<0$) [13].

The scattering length for the meson nucleus ^{3}He-η, $a_{\eta-^3He}$ = -2.31 + i2.57 fm, obtained from the optical potential approach [49], indicates a strong η-nucleus interaction and the possibility of forming a bound state close to the threshold for η meson production. However, due to the larger value of the imaginary part than the real part, the criterion for the existence of a bound system is not fulfilled.

Feasibility studies of the η-bound state production in light nuclei have been carried out mainly based on models based on the few-body equations [50–52]. One of the earliest works, which considered the coupled ηNN - πNN system in Faddeev three-body equation, resulted in the observation of a pole corresponding to a quasibound state with a mass of 2.430 MeV and a width in the range of 10-20 MeV [52]. This approach was also applied in later analyses of the production of the hypothetical d-η, t-η, ^{3}He-η i ^{4}He-η nuclei, under the finite-rank approximation (FRA) [51]. Quasi-bound states were found for $\Re(a_{\eta N})$ *in* (0.27,0.98) fm. This research has been continued by many groups [53–55], resulting in new values for scattering lengths and thus predictions for light bound systems.

An alternative method used by the authors of the work [12,56] is the so-called Wigner time delay concept. Taking into account the production mechanism of the η meson and the final state interaction (FSI), a time delay for elastic η-nucleus scattering is determined, allowing to locate the bound states of the η meson with the deuteron, ^{3}He and ^{4}He. The results obtained indicate the formation of bound states for small values of $a_{\eta N}$, while large values correspond to the resonances.

Calculations for η systems with several nucleons carried out by the Jerusalem-Prague Collaboration [57–60] based on the Stochastic Variational Method (SVM), taking into account the Minnesota NN potential and the two models of ηN interactions, GW (Green & Wycech) and CS (Cieply & Smejkal), indicate a ^{4}He-η bound state in the case of the GW model, while the issue of the ^{3}He-η system remains in question. In contrast, the authors of the papers [61, 62], fitting existing experimental data $pd(dp) \rightarrow {}^3\mathrm{He}\eta$ and $dd \rightarrow {}^4\mathrm{He}\eta$ with He-η optical potentials, report a weakly bound ^{3}He-η system with a binding energy of $\mathrm{B}_s \sim 0.3$ MeV and width of $\Gamma \sim 3$ MeV, and neither confirm nor exclude the existence of a ^{4}He-η mesic nucleus. Similarly, the analysis presented in Ref. [63], which uses the Alt-Grassberger-Sandhas (AGS) few-body formalism, does not confirm the formation of a ^{4}He-η bound state, while the ^{3}He-η issue remains ambiguous.

Performed theoretical studies (based on various approaches/models) predict the width of η-nucleus bound states in the range from a few to about 50 MeV [10, 13, 20, 24, 35, 42, 45–48, 50, 51, 56, 58–61, 64], including the width of η-mesic helium nuclei, considered in this work, in the range of 1 to 23 MeV [13, 24, 50, 51, 56, 58–61, 64]. Moreover, the widths of η-mesic nuclei are predicted to be larger than their binding energies [24, 51, 57, 61, 62].

As mentioned earlier, the dependence of theoretical calculations on the models used does not allow one to conclude unambiguously whether and which mesonic nuclei exists. It is well illustrated by the example of the η-Helium nuclei, which are the subject of this work. The results obtained from different theoretical approaches are often contradictory, hence, it is not possible to determine whether the η-Helium bound state exists and to determine which of its isotopes ^{4}He or ^{3}He is a better candidate for forming a bound system. There are only experimental indications that it is ^{3}He (see Section 2.3.2.3).

Current phenomenological calculations [65, 66]**[H3,H4,H6]** on the production of

He-η nuclei in dd and pd collisions have been performed for recent experimental data analysis **[H1,H2,H5,H7]**, the results of which are presented in Section 2.3.2.3. Two main mechanisms for the hypothetical η-mesic helium decay were considered: (i) assuming the absorption of the η meson on one of the nucleons inside the helium, followed by its possible propagation in the nucleus through successive excitations of the nucleons to the N*(1535) resonance until it decays into an N-π pair (e.g. $dd \rightarrow (^4\text{He-}\eta)_{bound} \rightarrow \text{N}^*\text{-}^3\text{He} \rightarrow {}^3\text{He}p\pi^-$, $pd \rightarrow (^3\text{He-}\eta)_{bound} \rightarrow \text{N}^*\text{-}d \rightarrow dp\pi^0$) and (ii) by direct decay of the bound η meson while it is still "orbiting" around the atomic nucleus (e.g. $pd \rightarrow (^3\text{He-}\eta)_{bound} \rightarrow {}^3$ He2γ). Schematics of the mechanisms are shown in Fig. 2.6 and Fig. 2.7.

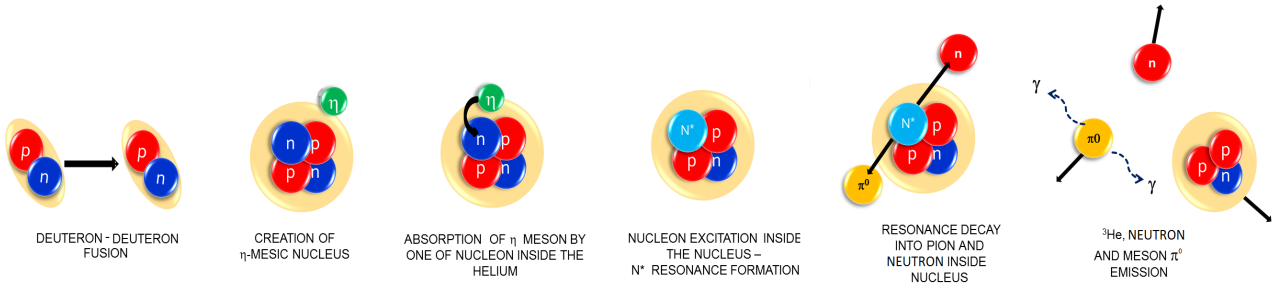

Figure 2.6: Scheme of the production and decay of the ^{4}He-η mesic nuclei in $dd \rightarrow {}^3\text{He}n\pi^0$ reaction. The ^{4}He-η mesic nuclei formed in dd collision decays according to the mechanism (i) described in the text.

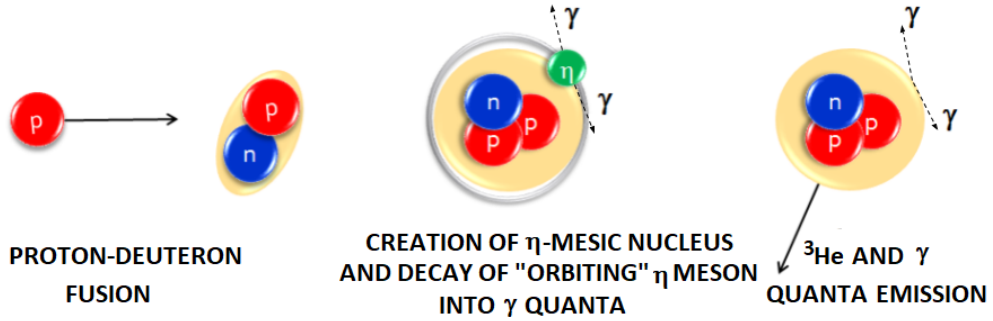

Figure 2.7: Scheme of the production and decay of the ^{3}He-η in $pd \rightarrow {}^3\text{He}2\gamma$ reaction. The ^{3}He mesic nuclei formed in pd collision decays according to the mechanism (ii) described in the text.

In the case of the first mechanism, the kinematics of the particles in the final state depends on the momentum of the N* resonance inside the helium nucleus. The first attempts to determine the momentum distribution of the N* baryon resonance in the N*-^{3}He and N*-NN systems were recently undertaken and described in the articles [65, 66]**[H3,H6]**. The calculations are based on the construction of the NN$^* \rightarrow$

NN* elementary interaction within the π and η meson exchange model, as shown schematically in Fig. 2.8 (taking into account the corresponding coupling constants ηNN*, πNN*). In the case of works [65, 66],combining the elementary interactions with known nuclear densities allowed the determination of the N*-nucleus potential. This potential was successively fitted by the Woods-Saxon form, which made it easier to find the bound state N*-^{3}He and to determine its wave function (solution of the Schrödinger equation), and thus the N* momentum distribution inside the ^{4}He nucleus. In turn, the N*-d momentum distribution was obtained by solving the Schrödinger equation with the N*-deuteron potential determined using a standard technique in scattering theory (based on the scattering amplitude) assuming the "Paris" parameterization [67] of the deuteron wave function [**H6**].

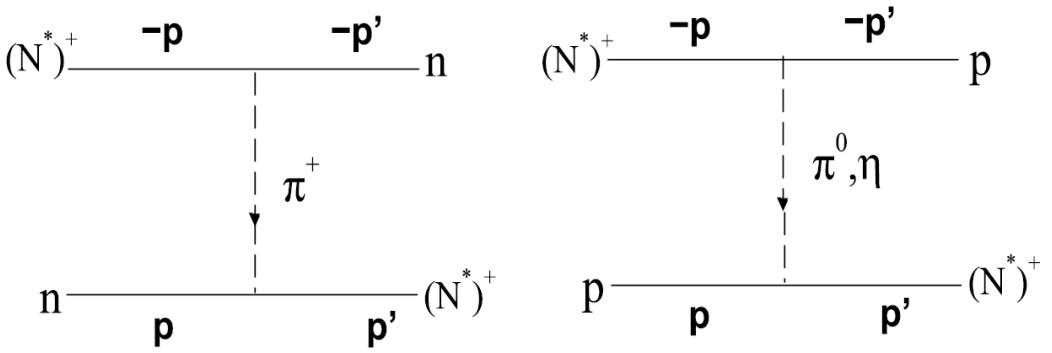

Figure 2.8: Diagrams of elementary NN* $\rightarrow$ NN* interaction with π and η mesons exchange.

The momentum distributions of N*-^{3}He and N*-d for the two binding energy values are shown in the left and right panels of Fig. 2.9, respectively. These distributions are narrower relative to the distribution of the neutron in ^{4}He or the proton in ^{3}He (red solid line), as it can be seen. It results from the fact that the binding energy of N* is lower than the separation energy of nucleons in ^{4}He and ^{3}He. Based on the obtained distributions, Monte Carlo simulations were performed for the $(^4\text{He-}\eta)_{bound} \rightarrow {}^3\text{He}n\pi^0$, $dd \rightarrow (^4\text{He-}\eta)_{bound} \rightarrow {}^3\text{He}p\pi^-$ and $pd \rightarrow (^3\text{He-}\eta)_{bound} \rightarrow dp\pi^0$ processes that are the subject of the analyzes described in Refs. **[H1,H2,H7]**.

Reactions $dd \rightarrow (^3\text{He-}\eta)_{bound} \rightarrow {}^3\text{He}N\pi$ reactions were also studied by the authors of Ref. [64], who determined for the first time the shapes and values of the active cross-sections for these processes in the range of excitation energies relevant to the search for η-mesic nuclei. The developed phenomenological model, which reproduces well the $dd \rightarrow {}^4\text{He}\eta$ reaction data, allows to determine the total cross-sections for a wide range of ^{4}He-η optical potential parameters (V_0,W_0). In the framework of the model, the deuteron-deuteron fusion and η meson production processes are phenomenologically parametrized, and the sum over all ^{4}He-η final states is determined based on the Green's function method. The total cross-section σ for the $dd \rightarrow {}^3\text{He}N\pi$ reaction contains the conversion part σ_{conv} corresponding to the absorption of the η meson in the atomic nucleus

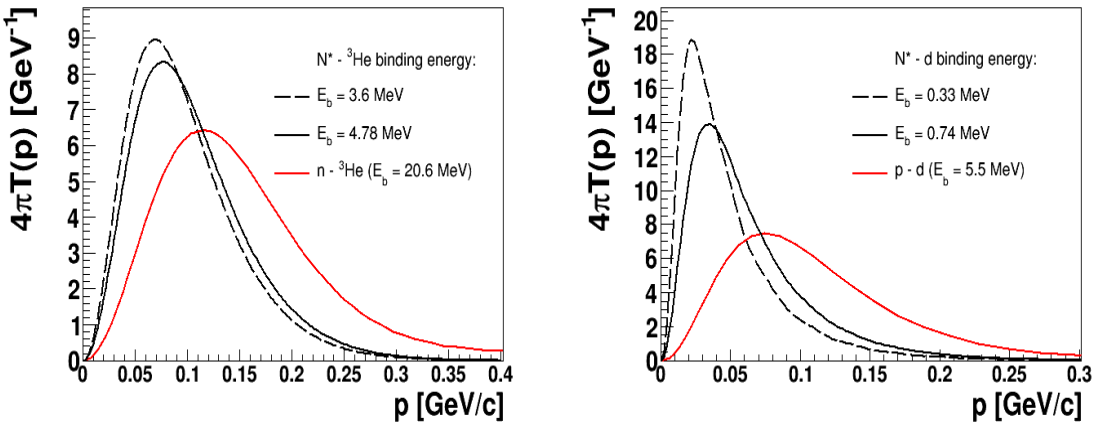

Figure 2.9: (Left) Momentum distribution of N* (black solid and dashed lines) and neutron (red solid line) inside a ^{4}He nucleus calculated with N*-^{3}He potentials giving 3.6 MeV and 4.78 MeV binding energies and n-^{3}He potential giving an n separation energy of 20.6 MeV (red solid line), respectively. (Right) Momentum distribution of the N* (black solid and dashed lines) inside a ^{3}He nucleus calculated with a N*-d potential giving 0.74 MeV and 0.33 MeV binding energies and a p-^{3}He potential giving a p separation energy of 5.5 MeV (red solid line), respectively. The Figures are obtained based on Refs. [65, 66]**[H3,H6]**.

(below the threshold for the η production) and the above-threshold part related to the η meson production (the so-called escape part). The conversion part is determined for various parameters of the ^{4}He-η spherical optical potential, $V(r) = (V_0 + iW_0)\frac{\rho_\alpha(r)}{\rho_\alpha(0)}$ (where ρ_α - α particle density), and the escape part as σ_{esc}=$\sigma - \sigma_{conv}$. An example of the determined total cross-section for three different sets of optical potential parameters after normalizing the σ_{esc} part to the experimental $dd \to {}^4$Heη data is shown in Fig. 2.10. The analysis of a wide range of parameters (V_0,W_0) allowed the determination of the so-called contour plot showing the cross-section of the studied process on the (V_0,W_0) plane (see Fig. 21 in Ref. [64] and Section 2.3.2.3). The value of the cross-section ranges from a few to more than a hundred nb. For comparison, earlier calculations based on scattering amplitude approximation for two-body processes [68] allowed to estimate the cross-section for the $dd \to ({}^4\text{He-}\eta)_{bound} \to {}^3\text{He}p\pi^-$ reaction on $\sigma \sim 4.5$ nb. In contrast, in the case of the $pd \to ({}^3\text{He-}\eta)_{bound} \to$XN$\pi$ reaction cross-section was roughly estimated to be 80 nb based on the hypothesis that the probability of η-mesic nucleus formation below the threshold is primarily equal to the probability of η meson production in the near-threshold region [69, 70]. The cross-sections obtained by the authors of Ref. [64] were used to perform the comparative analysis described in the article **[H2]** (details in Section 2.3.2.3).

The second mechanism of the He-η mesic nucleus decay, occurring through the decay of the η meson when it is bound to the atomic nucleus (see Fig. 2.7), is presented in the article **[H4]**. This first theoretical model of the non-mesonic decay of the η-mesic nucleus was developed for the decay of the ^{3}He-η bound state into ^{3}He2γ(6γ) channels describing

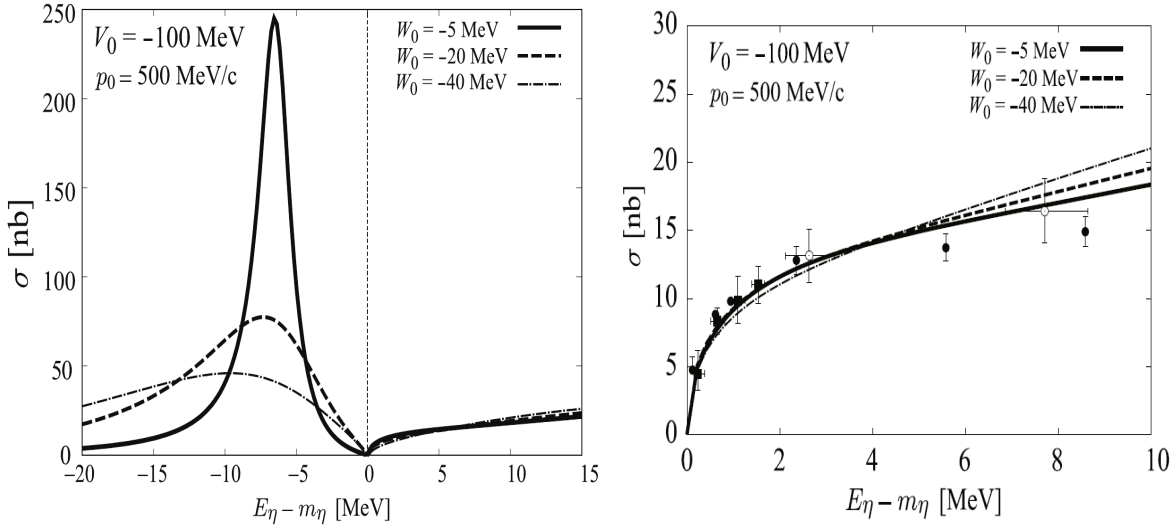

Figure 2.10: (Left panel) Total cross-section determined for the $dd \rightarrow (^4\text{He-}\eta)_{bound} \rightarrow {}^3\text{HeN}\pi$ reaction for the formation of the ^{4}He-η bound system and (right panel) total cross-section σ_{esc} as function of the excess energy $E_\eta - m_\eta$ for ^{4}He-η optical potential parameters (V_0, W_0)=−(100,5), −(100,20), −(100,40) MeV (solid, dashed and dotted lines, respectively). Figures are adapted from Ref. [64].

the bound system by the solution of the Klein-Gordon equation:

$$\left[-\vec{\nabla}^2 + \mu^2 + 2\mu U_{\text{opt}}(r)\right] \psi(\vec{r}) = E_{\text{KG}}^2 \psi(\vec{r}), \tag{2.1}$$

with given optical potential parameters $U_{\text{opt}}(r) = (V_0 + iW_0)\frac{\rho(r)}{\rho_0}$ ($\rho(r)$ denotes the density distribution in ^{3}He while ρ_0 is the normal nuclear density: $\rho_0 = 0.17$ fm^{-3}). The calculations provided the relative momentum distributions of ^{3}He-η in the bound system, as well as the branching ratios (BRs) for $\eta \rightarrow 2\gamma$ and $\eta \rightarrow 3\pi^0$ decay in the nuclear medium for different combinations of optical potential parameters. The momentum distributions determined for various (V_0, W_0) sets are shown in Fig. 2.11. The in-medium branching ratios were determined based on the ratio of the decay width η to 2γ to the decay width $3\pi^0$ $\Gamma_{\eta\rightarrow 2\gamma/\eta\rightarrow 3\pi^0}$ in a vacuum, the total meson width η in a vacuum Γ_η^{tot} (1.31 keV) [27], and the absorption width Γ_{abs} related to the Klein-Gordon energy by the relation Γ_{abs}=−2Im(E_{KG}):

$$\text{BR}^*_{\eta\rightarrow 2\gamma/\eta\rightarrow 3\pi^0} = \frac{\Gamma_{\eta\rightarrow 2\gamma/\eta\rightarrow 3\pi^0}}{(\Gamma_\eta^{\text{tot}} + \Gamma_{\text{abs}})}\ , \tag{2.2}$$

Estimated branching ratios in the nuclear matter range from about $2{\cdot}10^{-5}$ to $7{\cdot}10^{-4}$ depending on the optical potential parameters. The results obtained in this work were crucial for the Monte Carlo simulations and interpretation of experimental data collected by the WASA Collaboration **[H5]**.

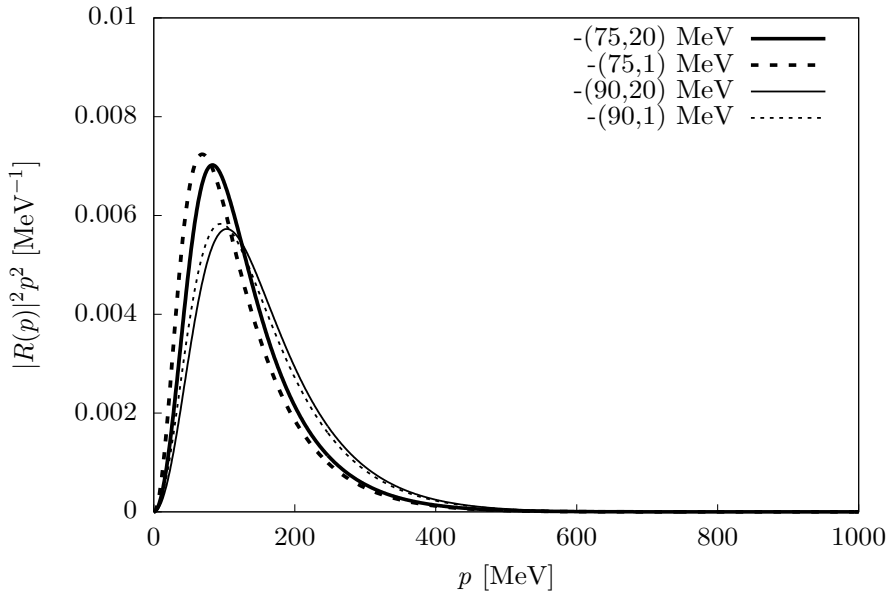

(V_0, W_0) [MeV]	(B_s, Γ_{abs}) [MeV]	$BR^*_{\eta\to 2\gamma}$	$BR^*_{\eta\to 3\pi^0}$
−(75,20)	(4.06, 15.66)	3.30×10^{-5}	2.73×10^{-5}
−(90,20)	(11.16, 20.65)	2.50×10^{-5}	2.07×10^{-5}
−(75,1)	(5.96, 0.76)	6.78×10^{-4}	5.62×10^{-4}
−(90,1)	(12.67, 1.02)	5.06×10^{-4}	4.20×10^{-4}

Figure 2.11: (Upper panel) Momentum distribution of the η meson in ^{3}He-η bound system estimated for (V_0, W_0)=−(75,20) MeV (thick solid line), (V_0, W_0)=−(75,1) MeV (thick dotted line), (V_0, W_0)=−(90,20) MeV (thin solid line), and (V_0, W_0)=−(90,1) MeV (thin dotted line). The distributions are normalized to be 1 in the whole momentum range. (Lower panel) The binding energies B_s and nuclear absorption widths Γ_{abs} values for the ^{3}He-η ground (0s) states obtained by solving the Klein-Gordon equation are listed with the optical potential parameters (V0, W0) assumed in Ref. **[H4]**. Figures are adapted from Ref. **[H4]**.

2.3.2.3 Experimental search for η-mesic nuclei

In parallel with theoretical studies, many experimental groups have attempted to search for hypothetical η-mesic nuclei, a real challenge due to the very weak expected signal and huge background. Initially, the experiments focused on the area of heavy atomic nuclei carrying out measurements mainly using beams of pions [71, 72], photons [73] and hadrons [74, 75]. These studies have been summarized in the publications [7, 12, 13][R5]. Current searches mainly concern light η-mesic nuclei **[H9,H10]**, the existence of which has not been ruled out due to the wide range of ηN scattering lengths values of resulting from the use of different theoretical models/approaches. This section summarizes

the experimental results obtained from measurements dedicated to the search for η-mesic helium nuclei.

As mentioned in section 2.3.2.2, despite the efforts of many theoretical groups, there are no model-independent calculations that unequivocally confirm or deny the existence of η-mesic bound states with helium. However, some experimental observations may suggest the formation of such mesic nuclei, such as the sharp rise in the total cross-section for the $dp \to {}^3\mathrm{He}\eta$ reaction [76–79][R52] and $dd \to {}^4\mathrm{He}\eta$ reaction [80–83] (Fig. 2.12) being a sign of a very strong interaction between helium and the η particle in the final state (FSI). This interaction is much stronger in the case of the ${}^3\mathrm{He}\eta$ system, indicating that η meson binding is more likely to occur in the ^{3}He nucleus than in ^{4}He. Another indication in favor of the ^{3}He-η bound system is the small value of the tensor analyzing power T_{20}, and its weak energy dependence, which is evident from ANKE Collaboration measurements carried out in the excitation energy range of Q$\in$(0.11) MeV. The result confirms the very strong change in the s-wave amplitude for the $dp \to {}^3\mathrm{He}\eta$ process [77, 79, 84, 85] associated with the strong ${}^3\mathrm{He}\eta$ interaction. Moreover, the total cross-section for the ${}^3\mathrm{He}\eta$ production does not depend on the initial channel, namely, for both hadronic production [77, 79] and photoproduction [86, 87] shows similar behavior above the threshold, suggesting an interaction between ^{3}He and η meson.

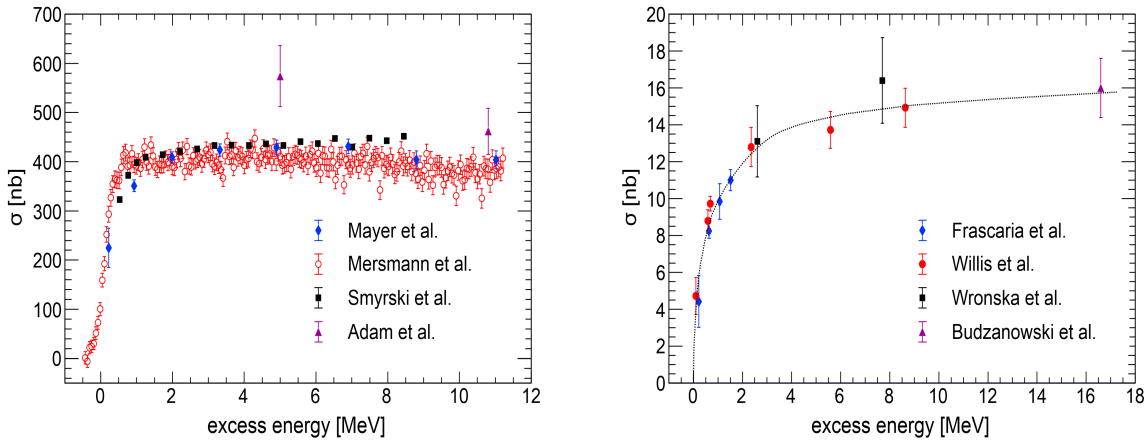

Figure 2.12: The close-to-threshold total cross-section as a function of excess energy: $dp \to {}^3\mathrm{He}\eta$ (left), experimental results correspond to Refs. [76–79] and $dd \to {}^4\mathrm{He}\eta$ (right), experimental results correspond to Refs. [80–83]. The black dotted curve is added for better visualization of the trend. Figures are taken from article [R5].

The first search for a direct signal of the ^{3}He-η bound state was carried out by a TAPS Collaboration for the $\gamma {}^3\mathrm{He} \to \pi^0 p\mathrm{X}$ photoproduction process [86]. An enhancement was observed just below the threshold for the ${}^3\mathrm{He}\eta$ production in the difference of the excitation functions measured for two ranges of angles between the π^0 and the proton ($170^\circ - 180^\circ$ and $150^\circ - 170^\circ$). It suggested the possible formation of the ^{3}He -η bound state and then its subsequent decay by absorption of the η meson in the nucleon (excitation of the

N*(1535) resonance and its decay into a nucleon-pion pair). However, a later experiment with much higher statistics [87] showed that the observed structure is an artifact from complex background behavior.

Promising experiments related to helium meson nuclei have been conducted at the Forschungszentrum Jülich research center using the COSY [88] synchrotron. Measurements to search for the signature of ^{3}He-η nuclei in $dp \rightarrow ppp^-$ and $dp \rightarrow {}^3$He0 reactions were carried out by the COSY-11 Collaboration. The obtained excitation functions allowed to determine the upper limits of the total cross-section for both processes at 270 nb and 70 nb , respectively [70, 77, 89].

The ^{4}He-η and ^{3}He-η bound states were searched for in three dedicated experiments, in 2008 [R94], 2010 **[H1,H2]** and 2014 **[H5,H7]**, carried out using the WASA-at-COSY detection system (shown in Fig. 2.13), described in detail in the article [78]. Measurements were made using a deuteron pellet target (deuterium microdroplets) and a cooled deuteron or proton beam of the COSY accelerator. The measurements aimed to determine the excitation function for selected decay channels of the He-η bound system and to search for the resonance structure corresponding to the η-mesic nuclei below the η meson production threshold. During the experiments, a technique called beam ramping was used, which consisted of a continuous and slow change in beam momentum around the threshold for meson η production in each beam acceleration cycle, thus reducing systematic uncertainties with respect to separate measurements with fixed beam energy [R94] [77]. It is worth emphasizing that the above-described method for searching for η-mesic helium nuclei with the WASA-at-COSY detector was developed by a research group from the Jagiellonian University, to which the author of this work belongs.

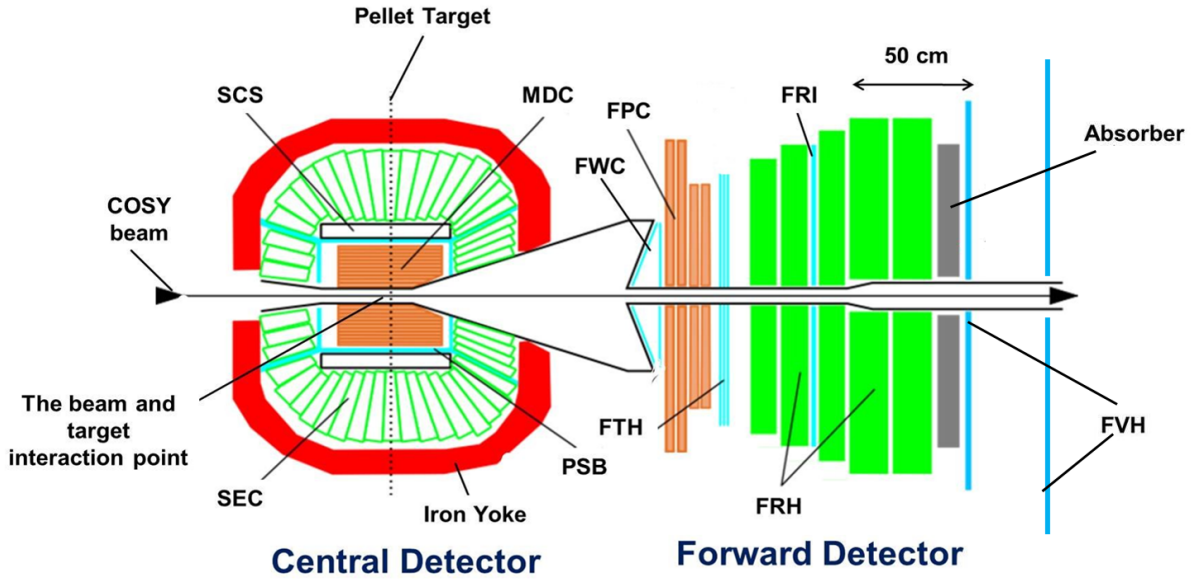

Figure 2.13: Scheme of the WASA-at-COSY detector. A detailed description of the detector can be found in Ref. [78]

The ^{4}He-η bound state signal was searched by investigating the excitation curves for the $dd \to {}^3\mathrm{He}p\pi^-$ [**H1,H2**,R94] and $dd \to {}^3\mathrm{He}n\pi^0$ reactions **[H1,H2]** near the ^{4}Heη production threshold (the beam momentum change around the threshold corresponded to the excitation energy range of Q$\in$ ($-$70.30) MeV **[H1,H2]** and Q$\in$ ($-$51.22) MeV [R94]). Data analyses were performed assuming the mechanism of mesic nucleus decay with the formation of the N* baryon resonance in the intermediate state, described in the previous section and shown in Fig. 2.7. In the Monte Carlo simulations of the signal carried out for purpose of the analyzes described in Ref. **[H1,H2]**, the N* resonance momentum distribution determined by the authors of Ref. [65,66] and shown in Fig. 2.9 (Sec. 2.3.2.2) was applied. Details of the data analysis procedure leading to the determination of the excitation function are described in the articles [R94] and **[H1]**. The obtained excitation functions do not show any narrow structure below the η meson production threshold, which could indicate the bound state existence. Therefore, the upper limit of the total cross-section for the η-mesic ^{4}He production was determined at the 90% confidence level (CL) by fitting the excitation curve with the sum of the Breit-Wigner function (describing the signal), with fixed binding energy (B_s) and width (Γ), and a second-order polynomial (describing the background). For the data from the experiment in 2010 **[H1]**, the fit was made simultaneously for both decay channels $dd \to {}^3\mathrm{He}p\pi^-$ and $dd \to {}^3\mathrm{He}n\pi^0$ considering isospin relationship between $n\pi^0$ and $p\pi^-$ pairs. This analysis allowed for the first experimental determination of the upper limit of the total cross-section for the $dd \to ({}^4\mathrm{He}\text{-}\eta)_{bound} \to {}^3\mathrm{He}n\pi^0$ process, which varies from 2.5 to 3.5 nb. On the other hand, in the case of the $dd \to ({}^4\mathrm{He}\text{-}\eta)_{bound} \to {}^3\mathrm{He}p\pi^-$ reaction the cross-section sensitivity was about 6 nb, which is about four times higher than the result obtained in the previous experiment [R94]. The obtained upper limits of the total cross-sections as a function of the bound state width for both considered reactions are shown in Fig. 2.14. It is worth mentioning that the systematic uncertainty marked in green results primarily from the assumption regarding the N* resonance momentum distribution. Before the Kelkar et al. model [65, 66], it was assumed that the resonance momentum N* had the distribution of the nucleon momentum in the ^{3}He nucleus (red line in Fig. 2.9a). The acceptance of the investigated process using in the simulations the N* momentum distribution determined in Ref. [65, 66] is about 40% lower than that obtained for the nucleon momentum distribution **[H1]**.

Due to the lack of theoretical predictions of cross-sections for the $dd \to ({}^4\mathrm{He}\text{-}\eta)_{bound} \to {}^3\mathrm{HeN}\pi$ reactions below the threshold for the η meson production, the research described above [**H1**,R94] assumed that the Breit-Wigner shape represents the bound state signal (with fixed binding energy B_s and width Γ). However, as presented in Sec. 2.3.2.2, the phenomenological research by Ikeno et al. [64] resulted in the distributions of the cross-sections in the range of excitation energy relevant for the search for He-η nuclei (example in Fig. 2.10). The newly developed model was compared with the experimental results described in Ref. **[H1]**. The measured excitation functions were fit with the theoretical distributions of conversion cross-sections σ_{conv} obtained for different values of the ^{4}He-η optical potential parameters (V_0,W_0) (taking into account the experimental resolution of the excitation energy for theoretical curves). The value of the upper limit of the total cross-section (CL=90%) for the ^{4}He-η bound state formation in $dd \to {}^3\mathrm{HeN}\pi$

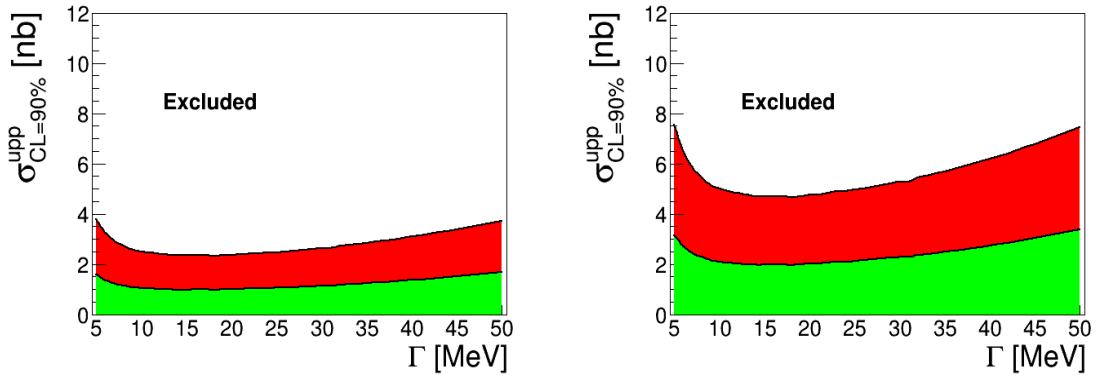

Figure 2.14: Upper limit of the total cross-section for the $dd \rightarrow (^4\text{He-}\eta)_{bound} \rightarrow {}^3\text{He}n\pi^0$ (left panel) and $dd \rightarrow (^4\text{He-}\eta)_{bound} \rightarrow {}^3\text{He}p\pi^-$ reaction (right panel) as a function of the width of the bound state. The binding energy was fixed to 30 MeV. The upper limit was determined via the simultaneous fit for both channels. The green area denotes the systematic uncertainties. The Figures are adapted from **[H1]**.

process was found to vary from 5.2 nb to 7.5 nb **[H2]**. Comparing the experimentally determined upper limits of the cross-section with the cross-sections obtained in Ref. [64] allowed to constrain the ^{4}He-η optical potential parameters. As shown in Fig. 2.15, only very narrow and weakly bound systems are allowed in the model ($|V_0|<$ ∼60 MeV, $|W_0|<$ ∼7 MeV for CL=90%), which rules out most of the predictions for η-mesic halium nuclei in the frame of the optical model (colored circles in Fig. 2.15).

The last experiment using the WASA-at-COSY detection system (in 2014) was devoted to the search for the ^{3}He-η bound states, which creation, according to the experimental indications described in this section, is more probable than the formation of the bound ^{4}He-η system. The measurements resulted in the collection of the world's most significant data sample and allowed the study of the two different bound state decay mechanisms: (i) assuming η meson absorption on the nucleon followed by N*(1535) resonance decay (as assumed in previous analyses) and (ii) by the decay of the bound η meson, shown in Fig. 2.6 and 2.7, respectively.

Data analysis, assuming the first mechanism, allowed for the first determination of the excitation function for the $pd \rightarrow dp\pi^0$ process around the η production threshold **[H7]**. Monte Carlo simulations of the signal were performed based on the N* resonance momentum distribution determined by the authors of Ref. **[H3,H6]** (Fig. 2.9, description in Sec. 2.3.2.2). Although no narrow resonant structure corresponding to the bound states was observed, the performed analysis allowed to conclude the η-nucleon scattering length. The obtained upper limits of the total cross-sections (by fitting the sum of the Breit-Wigner distribution and the polynomial function) vary in the range from 13 to 24 nb depending on the parameters of the mesic nucleus (Γ, B_s), as shown in Fig. 2.16, not excluding predictions of mesic nuclei for the scattering length $a_{\eta N}$ with a real part of about 1 fm. [58, 90].

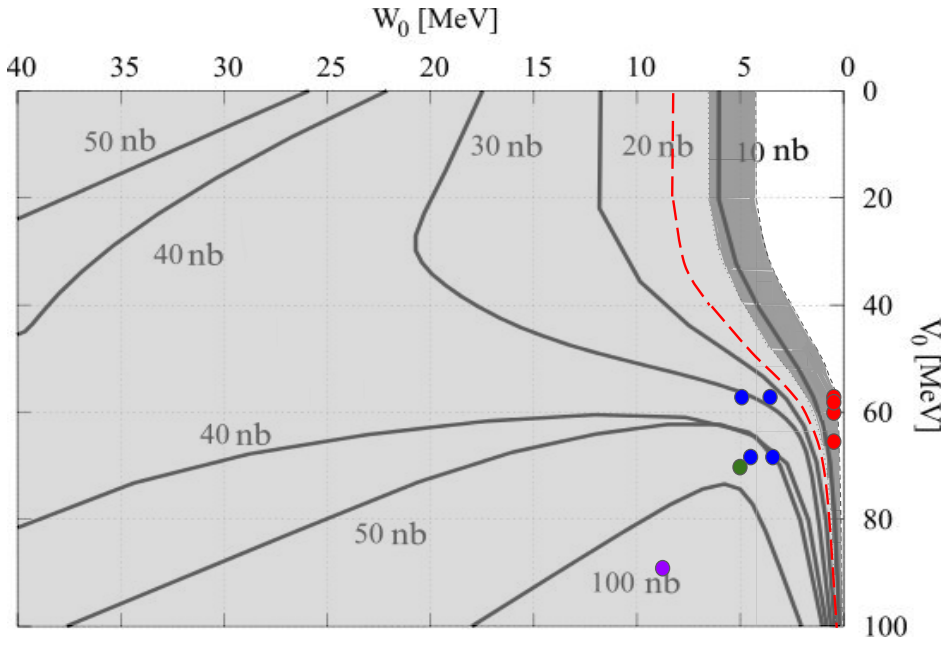

Figure 2.15: Contour plot of the theoretically determined conversion cross-section in the $V_0 - W_0$ plane [64]. The light shaded area shows the region excluded by the analysis presented in Ref. **[H3]**, while the dark shaded area denotes the systematic uncertainty of the $\sigma_{upp}^{CL=90\%}$. The red line extends the allowed region based on a new estimate of errors. Dots denote the optical potential parameters corresponding to the predicted ^{4}He-η bound states obtained for different optical model predictions **[H2]**. The Figure is adapted from Ref. **[H2]**.

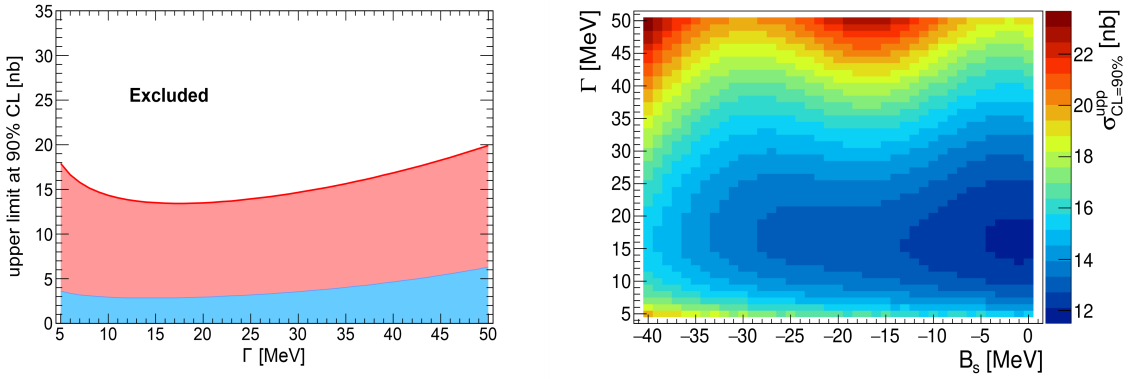

Figure 2.16: The upper limit (at the CL=90%) of the total cross-section for $pd \to (^3\text{He-}\eta)_{bound} \to dp\pi^0$ reaction as a function of the width of the bound state, with the fixed binding energy (left panel) and in (B_s, Γ) plane (right panel). Figures are adapted from Ref. **[H7]**.

The second decay mechanism of the hypothetical η-mesic nucleus, i.e. by direct decay of the bound η meson, was investigated for the first time by analyzing the $pd \rightarrow {}^3\mathrm{He}2\gamma$ and $pd \rightarrow {}^3\mathrm{He}6\gamma$ reactions. Data analysis was based on a recently developed theoretical model presented in Ref. **[H4]** and Sec. 2.3.2.2. The determined Fermi momentum distribution for the bound η meson (Fig. 2.11) was used to simulate the considered processes. The obtained excitation functions for both measured channels reveal a structure that could be interpreted as a bound state signal with a width greater than 20 MeV and a binding energy in the range of 0 to 15 MeV (Fig. 2.17). However, the result is burdened with a large systematic error, which does not allow us to clearly state whether η-mesic nucleus is produced in the considered mechanism. Finally, the upper limit of the total cross-section (CL=90%) was determined for the formation of the ${}^3\mathrm{He}$-η nucleus by fitting the excitation curves for both reactions with the sum of Breit-Wigner function and polynomial (signal+background) taking into account the branching ratio between the $\eta \rightarrow 2\gamma$ and $\eta \rightarrow 3\pi^0$ decays in a vacuum. The estimated upper limit ranges from 2 nb to 15 nb depending on the bound state parameters (binding energy, width) **[H5]**. Fig. 2.17 shows the result for the bound state width Γ=28.75 MeV.

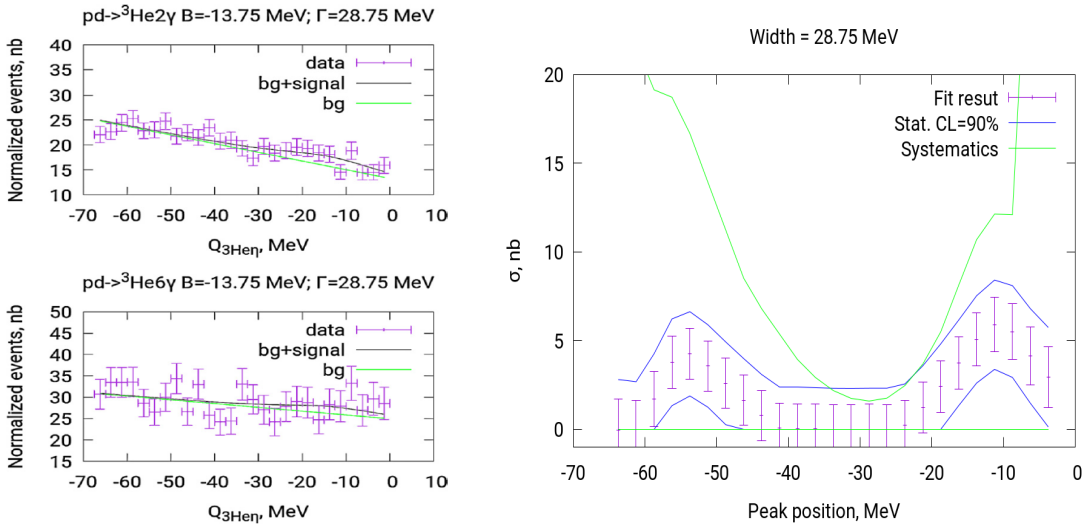

Figure 2.17: (Left panel) The result of the simultaneous fit of the Breit-Wigner function with a polynomial to the experimental data with the assumed binding energy B_s=-13.5 MeV. The black line represents the fit result, and the green line shows the background function. (Right panel) Upper limit for the bound state production cross-section via $pd \rightarrow ({}^3\mathrm{He}\text{-}\eta)_{bound} \rightarrow {}^3\mathrm{He}$ (η decays) as function of the peak position for fixed width Γ=28.75 MeV. The values of the Breit-Wigner amplitude σ are shown with statistical uncertainties. The range of possible bound state production cross-section obtained based on statistical uncertainty corresponding to 90% confidence level is shown by blue lines. The range of possible bound state production cross-section including systematic uncertainty is shown by green lines. Figure is adapted from Ref. **[H5]**.

In the experiments conducted so far, dedicated to the search for η-mesic helium nuclei, no signals confirming their existence has been observed. Nevertheless, the measurements with the WASA-at-COSY detection system (described above and summarized in Refs. **[H9,H10]**) allowed for the first time to determine the upper limits of the total cross-sections for the production of the ^{4}He-η and ^{3}He-η bound states in the *dd* and *pd* collisions, taking into account different decay channels.

Currently, research with the WASA detector is continued (with the participation of the author of this work) at the GSI research center in Darmstadt (Germany) to search for the bound states of η' with carbon nuclei (see Sec. 3.1).

2.3.2.4 My contribution to the study of η-mesic nuclei

A Krakow research group, which I am part of, has developed a method that gives a good chance of discovering a system of η meson bound to a helium atom. These studies were carried out in the frame of the international WASA-at-COSY Collaboration at the Jülich Research Center in Germany with unique accuracy using a cooled proton and deuteron beam of the COSY synchrotron and the WASA detector with a pellet target (see Sec. 2.3.2.3), and in collaboration with theoretical groups from Universidad de los Andes in Colombia and Nara Women's University in Japan. My most significant achievements in research on η-mesic nuclei are presented in the papers **[H1-H7,H9,H10]**, the results of which are summarized in Sec. 2.3.2.3. I present my contribution to the conducted research below.

I began research on η-mesic nuclei during my master's studies by joining the WASA-at-COSY Collaboration. As part of my master's thesis, I performed feasibility studies of ^{4}He-η/^{3}He-η and T-η (quasi-free production) mesic nuclei measurements using the WASA-at-COSY and COSY-TOF detection systems, respectively. The result of the work was to show that both detection systems allow the search for considered bound states with high geometric acceptance.

During my doctoral studies (as a fellowship holder of the Foundation for Polish Science under the MPD project on Applications of Nuclear Physics and Innovative Technologies), I continued my research on the search for ^{4}He-η mesic nuclei using the WASA-at-COSY detection system. I was involved in experimental work, data analysis, and Monte Carlo simulations. I co-coordinated an experiment dedicated to searching for the ^{4}He-η bound state in the *dd* fusion reaction, actively participating in the preparation and testing of the measurement system and data acquisition and experimental shifts (measurements monitoring). As part of my doctoral thesis, based on the Monte Carlo simulations I prepared, and conducted research on the $dd \rightarrow {}^3\mathrm{He}n\pi^0$ reaction measured in the experiment to search for a bound ^{4}He-η system, which resulted in the first experimental estimation of the upper limit of the total cross-section for mesic nucleus production and decay in this process ($\sigma_{upp}^{CL=90\%} \in (21.36)$ nb).

The publications **[H1-H7,H9,H10]** presented in this work concern my post-doctoral research. After my PhD, I developed the study described above by optimizing the analysis of the $dd \rightarrow {}^3\mathrm{He}n\pi^0$ reaction and analyzing the following $dd \rightarrow {}^3\mathrm{He}p\pi^-$ process,

considering the scheme of mesic nucleus production and decay shown in Sec. 2.3.2.2 and in Fig. 2.6. I performed dedicated Monte Carlo simulations of $dd \rightarrow (^4\text{He-}\eta)_{bound} \rightarrow {}^3\text{HeN}\pi$ reaction based on the kinematics of the process developed by me, taking into account the resonance momentum distribution N* (Fig. 2.9, Ref. [65, 66]). The simulations included three stages: (i) event generation, (ii) detector response simulation, and (iii) data reconstruction for experimental conditions. I also developed and simulated reactions that are the principal background contributors, i.e. $dd \rightarrow {}^3\text{HeN}\pi$ and $dd \rightarrow {}^3\text{HeN}^*$. Subsequently, based on the performed MC simulations, I selected events for the experimental data to determine the excitation function for the signal-rich area. This selection included the identification of particles in the output ${}^3\text{He}n\pi^0$ and ${}^3\text{He}p\pi^-$ channels and selection of the kinematic region corresponding to the production of hypothetical η-mesic nuclei. The obtained excitation functions (corrected for efficiency and normalized by the luminosity determined by the quasifree scattering reaction pp [R81]) did not reveal a structure that is a signature of the existence of a bound state. However, they allowed for the first experimental determination of the upper limits of the total cross-section at the 90% confidence level for the $dd \rightarrow (^4\text{He-}\eta)_{bound} \rightarrow {}^3\text{He}n\pi^0$ and $dd \rightarrow (^4\text{He-}\eta)_{bound} \rightarrow {}^3\text{He}p\pi^-$ reactions taking into account the isospin relation between $n\pi^0$ and $p\pi^-$ pairs. The upper limit varies between 2.5 to 3.5 nb and between 5 to 7.5 nb, respectively, for the first and second reactions [**H1**], indicating four times higher sensitivity of the cross-section measurements compared to the previous WASA experiment [R94]. I conducted my research with the support of the PRELUDIUM grant from the National Science Center, which I received as a Ph.D. student and continued after my Ph.D.

I extended the studies on the search for ^{4}He-η bound states by developing and conducting a comparative analysis of the experimental data presented in Ref. **[H1]** with a new theoretical model developed by a research group from Nara Women's University (Japan). Phenomenological studies performed by the authors of Ref. [64] resulted in the world's first distributions of cross-sections below the threshold for the $dd \rightarrow (^4\text{He-}\eta)_{bound} \rightarrow {}^3\text{He}N\pi$ reaction (see Fig. 2.10) for different values of ^{4}He-η optical potential parameters, an alternative to the Breit-Wigner distributions assumed in earlier analyzes describing the bound state signal. As a result of the analysis, the upper limit of the total cross-section (CL=90%) was obtained for the production of the ^{4}He-η nuclei in the $dd \rightarrow {}^3\text{HeN}\pi$ process in the range of 5.2 nb to 7.5 nb **[H2]**. Moreover, the comparison of the experimentally determined upper limits of the cross-section with the theoretical conversion cross-sections [64] allowed to constrain the ^{4}He-η optical potential parameters ($|V_0| < \sim$60 MeV, $|W_0| < \sim$7 MeV). This constrain excludes most predictions for η-mesic helium in the optical model (Fig. 2.15). That indicates the existence of narrow bound states.

I also conducted studies dedicated to the search for ^{3}He-η bound states in the experiment using the WASA detector, which I independently coordinated, taking an active part in the measurements preparations (preparation and tests of the detection system, data acquisition system, triggers, programs for online measurement monitoring) and their implementation and monitoring (participation in experimental shifts). Before starting the experiment, I performed feasibility studies of ^{3}He-η mesic nuclei measurements with the WASA detector (Monte Carlo simulations of the signal and background main

contributions), the results of which were shown in the measurement project [I2] presented at the general meeting of the COSY Scientific Committee in Jülich (PAC Session No. 42 II/2013) and approved for realization. During the experiment, the world's most significant data sample was collected so far for the bound ^{3}He-η system. The collected data allowed for the analysis of the reaction in terms of searching for mesic nuclei, taking into account two possible mechanisms of bound state decay: by excitation of the N* resonance and its decay to a nucleon-pion pair and by direct decay of the bound η meson into 2 γ or 6γ (Fig. 2.6 and Fig. 2.7).

Data analysis assuming the first mechanism, which I developed conceptually and in which I significantly contributed (Ph.D. dissertation of Mr. Aleksander Khreptak under my supervision as an auxiliary supervisor) allowed for the first determination of the excitation function for the $pd \to dp\pi^0$ process around the η production threshold **[H7]**. Dedicated MC simulations for the signal, taking into account the detector response, were performed based on the N*-d momentum distribution (Fig. 2.9) determined based on a theoretical model developed by the research group from the University of Los Andes in Bogotá (Colombia) and published with my contribution in Refs. **[H3,H6]**. The simulations were used to determine the criteria for experimental data selection and to determine efficiency, which together with the luminosity [P39] allowed for the appropriate correction of the experimental excitation functions. The data analysis resulted in the determination of the upper limit of the cross-section for the η-mesic nuclei production and decay in the considered process, which ranges from 13 to 24 nb depending on the parameters of the mesic nucleus (Fig. 2.16). The obtained result does not exclude predictions of mesic nuclei for the scattering length $a_{\eta N}$ with a real part of about 1 fm. [58, 90].

My contribution to the publications **[H3,H6]** was related to the preparation and performance of the MC simulation of the $pd \to dp\pi^0$ reaction, taking into account the determined N* resonance momentum distributions. The simulations were aimed at determining the geometrical acceptance of the WASA detector for the measurement of the process mentioned above, as well as comparing it with the acceptance, assuming that the momentum distribution of N* is described by the distribution of the proton's momentum in ^{3}He nucleus. The conducted analysis allowed to estimate the systematic uncertainty (in Ref.**[H7]**) resulting from the assumption of the N* resonance momentum distribution. It has been shown that this uncertainty is the most significant contribution to the bias in determining the upper limit of the cross-section **[H7]**.

The study of the second decay mechanism of the hypothetical η-mesic nucleus, i.e., by the direct decay of the bound η meson, was carried out in collaboration with the theoretical group from Nara Women's University. I proposed the topic of the work [**H4**] covered the description of a new mechanism of mesic nucleus decay, within which I participated in the theoretical model development (description in Sec. 2.3.2.2). The calculations provided the relative ^{3}He-η momentum distribution in the bound system, as well as the branching ratios for $\eta \to 2\gamma$ and $\eta \to 3\pi^0$ decays in the nuclear medium for various combinations of the optical potential parameters. I also developed and conducted dedicated Monte Carlo simulations to study the feasibility of measuring the proposed mechanism in the WASA-at-COSY experiment. Based on the developed theoretical model **[H4]**, I

elaborated substantially experimental data analysis for the $pd \rightarrow (^3\text{He-}\eta)_{bound} \rightarrow {}^3\text{He}2\gamma$ and $pd \rightarrow (^3\text{He-}\eta)_{bound} \rightarrow {}^3\text{He}6\gamma$ reactions, and I actively participated in it (Oleksandr Rundel's doctoral thesis under under my care as an auxiliary supervisor). The Fermi momentum distribution for the bound η meson determined in **[H4]** (Fig. 2.11) was used in the simulations of the considered processes. As a result of the analysis, the world's first excitation functions for the reaction mentioned above were determined. Although both measured channels revealed a structure that could be a signature of the η-mesic nucleus (for Γ>20 MeV and $B_s \in$(0,15) MeV) (Fig. 2.17), it is covered by the systematic uncertainty, not allowing any conclusion whether the considered processes generate an η-mesic bound state or not. The result of the work is, therefore, the value of the upper limit of the total cross-section (CL=90%) for the formation of the ^{3}He-η nucleus in the considered reactions, which varies from 2nb to 15nb depending on the bound state parameters **[H5]**.

Although the research I carried out using the WASA-at-COSY detection system did not allow observing η-mesic nuclei, it allowed for a significant improvement in the accuracy of the cross-section determination for the production of the exotic bound state of the η meson in the helium nucleus. For the first time, the upper limits of the total cross-sections for the production of the ^{4}He-η and ^{3}He-η bound states were determined in *dd* and *pd* collisions, taking into account different decay channels. The data analyzes I performed were summarized in my publications **[H9,H10]**.

I carried out the activity described above to a large extent during internships and research stays at the Jülich Research Center (Forschungszentrum Jülich), Universidad de los Andes in Colombia and Nara Women's University in Japan.

I am continuing research on η-mesic nuclei as a member of the WASA-FRS Collaboration, which aims to search for bound states of η' and carbon nuclei (see Sec. 3.1).

2.3.3 Research on kaonic bound systems (kaonic atoms and kaonic nuclei)

The study of exotic nuclear matter in the form of systems of kaons bound to atomic nuclei includes the exploration of kaonic atoms and strongly bound kaonic nuclei, also known as kaonic nuclear clusters.

Exotic atoms, where the electron is replaced by a negatively charged muon (μ^-), pion (π^-), kaon (K^-), antiproton, or hyperon Σ bound to the atomic nucleus via Coulomb interaction, were predicted already in the 1940s [91, 92]. The first observations of electromagnetic radiation (X-rays) from the kaonic atoms were made by Burleson et al. 1965 [93], several years after the discovery of muonic [94] and pionic [95] atoms. Since then, many dedicated experiments have been carried out to study kaonic atoms, including kaonic hydrogen K^-H, (also kaonic helium, nitrogen, oxygen, carbon and other heavier elements) [96], which resulted in measurements of strong interaction observables such as shift and width of the K^-H ground state (1s) [97, 98]. Currently, a huge experimental challenge is to measure a tiny signal that will allow for the first determination of observables for kaonic deuterium representing the most crucial experimental information that is missing in the sector of low-energy antikaon-nucleon interactions [96].

The existence of kaonic nuclei K^-pp was first postulated by Prof. Wycech over 30 years

ago [99]. The current theoretical studies, based on various models (phenomenological and chiral SU(3)), have resulted in a wide range of possible binding energies of kaonic nuclear clusters, from a few MeV up to about 100 MeV [100–115]. So far kaonic nuclei have been searched for in several experiments [8, 116–119], e.g., in proton-proton collisions, heavy ion collisions, and kaon induced reactions. The first and only signal so far interpreted as coming from the kaonic K^-pp cluster [113,114] was recently observed in the $^3He(K^-,\Lambda p)n$ reaction measurement conducted at the J-PARC [8] accelerator center. Valuable information on the possibility of producing kaon nuclei is provided by the currently performed studies on the absorption of K^- in the nuclear medium [**H11**,R42,R47].

The study of kaonic atoms, as well as the processes of single- and multi-nucleon absorption of K^- kaons with the possible formation of kaonic clusters, allows to study low-energy kaon-nucleon/atomic nucleus interactions and thus to determine the isospin-dependent antikaon-nucleon scattering amplitudes (at and below the $\bar{K}N$ threshold). They scattering amplitudes are of fundamental importance for understanding the low-energy region of quantum chromodynamics (QCD) in the strangeness sector, and consequently, one of the most important, still unsolved problems of hadronic physics: chiral symmetry breaking that gives mass to the surrounding matter [120, 121]. This research may also contribute to astrophysics, as the interaction of kaons in nuclear matter may affect models describing the structure and density of the neutron stars [122–124], including binaries of neutron stars, considered to be the main sources of gravitational waves.

Experiments devoted to the study of kaonic atoms, as well as the processes of kaon absorption on light atomic nuclei, have been and are carried out at the Laboratori Nazionali di Frascati in Italy with the use of unique low-energy K^- beams delivered by the electron-positron collider DAΦNE [125]. The ongoing SIDDHARTA-2 experiment, which uses the upgraded SIDDHARTA [126] detection system, aims primarily to measure the observables of kaonic deuterium atoms (ground state shift and width) using high-precision X-ray spectroscopy. In turn, data collected by the AMADEUS Collaboration using the KLOE detector [127] give opportunity to first comprehensive study of the absorption processes of K^- mesons in light atomic nuclei, which provides information on the interaction dynamics of K^- with one and few nucleons and the possibility of kaonic nuclei formation. The results of the SIDDHARTA-2 and the AMADEUS researches with my contribution (Refs. **[H8,H11]**) are described in this section after presenting the theoretical outline and the status of experiments devoted to the study of kaonic bound systems.

2.3.3.1 K^--nukleon interaction

$K^\pm$ mesons, also called kaons, like η, η' mesons (Sec. 2.3.2.1), belong to the nonet of pseudoscalar mesons. The K^- particle consisting of anti-up and strange quarks ($\bar{u}s$) and its antiparticle K^+ ($u\bar{s}$) [27] live much longer than most of the mesons ($\sim 1.24 \cdot 10^{-8}$s) decaying through electroweak interactions mainly into muons and π mesons [27]. The mass of the charged kaon is about 493.68 MeV [27], and the precision of its determination in comparison to the mass of charged pions is one order of magnitude worse, which is caused

by a significant discrepancy in the results of the latest and most precise measurements [128, 129]. An experiment aimed at very precise determination of the charged kaons mass by measuring the energy of X-ray transitions in kaonic atoms is planned using fixed targets (e.g. lead) and HPGe germanium detector at Laboratori Nazionali di Frascati in Italy [R32].

The interaction of K^+ and K^- mesons with nucleons is very different due to their quark composition. The K^+N interaction strength is small and changes slightly with energy. For low energies, the interaction of K^+ kaons occurs through elastic and charge exchange processes. The K^+-nucleon scattering process can be described in terms of the perturbation approach, which gives information about the parameters of the chiral perturbation theory SU(3) [130].

In the case of the K^- meson, due to the $\bar{u}s$ quarks content, its interaction with the nucleon is dominated by the wide $\Lambda(1405)$ (I=0) and $\Sigma(1385)$ (I=1) resonances appearing just below the $\bar{K}N$ threshold. Their presence makes the $\bar{K}N$ interaction attractive in the far subthreshold region and repulsive at the threshold, as shown by the SIDDHARTA measurements of the a_{K^-p} scattering length [98]. The Chiral Perturbation Theory (ChPT), which is an Effective Field Theory (EFT) describing the πN, $\pi\pi$ and NN interactions in the low energy region [131, 132] can, therefore, not be used to describe the dynamics interactions $\bar{K}N$.

K^- interactions with nucleons are considered within two main theoretical approaches: phenomenological models based on $\bar{K}N$ and NN interactions [100–106] and chiral unitary models involving non-perturbative SU(3) dynamics [107–115]. Fitting these models to existing scattering data [133] describes the $\bar{K}N$ dynamics above the threshold very well. However, there is a significant inconsistency between the chiral and phenomenological models when extrapolating the scattering amplitude to the subthreshold region, which is shown in Fig. 2.18 for an example of models taken from Ref. [115] and [101], respectively. In the chiral approach, where the $\bar{K}N$ interaction is energy-dependent, the kaon-nucleon attraction is weaker than that resulting from energy-independent phenomenological potentials [133]. It leads to contradictory predictions regarding the $\Lambda(1405)$ (I=0) resonance structure and the kaonic nuclei formation.

Although the $\Lambda(1405)$ resonance has been observed in many experiments, its structure and behavior in the nuclear medium are still poorly understood. The key issue is the explanation of its mass, which cannot be described based on a simple three quarks picture (uds). According to the phenomenological approach, the $\Lambda(1405)$ particle is a strongly bound $\bar{K}N$ system with a mass, binding energy, and width of approximately 1405 MeV/c^2, 30 MeV and 40 MeV/c^2 [100, 101], respectively. On the other hand, chiral models predict that $\Lambda(1405)$ is a molecular meson-baryon state resulting from the superposition of two poles in the scattering matrix: the narrower coupled mainly to the $\bar{K}N$ channel and the wider coupled to the $\Sigma\pi$ channel. The positions of these poles vary depending on the chiral models used, as shown in Fig. 2.19. The wider pole corresponds to a state with a mass in the range of 1410 - 1440 MeV/c^2, and the narrower one with a mass of 1320 - 1440 MeV/c^2 [135].

Two different scenarios describing the $\Lambda(1405)$ structure reflect the strength of the $\bar{K}N$ interaction, thus affecting the possibility of kaonic bound states creation. The strong $\bar{K}N$

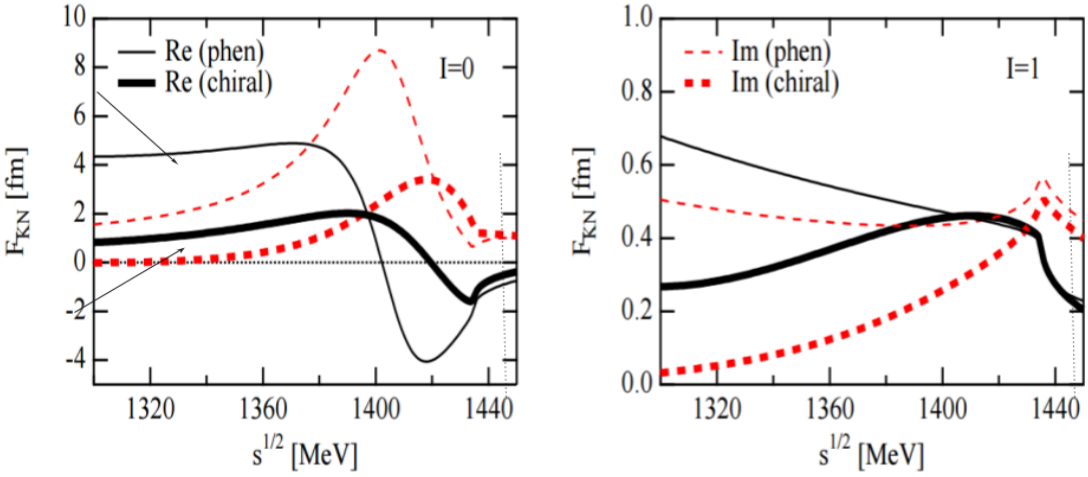

Figure 2.18: The real (black solid) and imaginary (red solid) parts of $\bar{K}N$ scattering amplitude for I=0 (left panel) and I=1 (right panel) obtained for the phenomenological potential model [101] and chiral SU(3) model [115]. Figures are taken from Ref. [134].

attraction resulting from phenomenological models leads to predictions of deeply bound kaonic clusters (binding energy up to 100 MeV/c^2), while SU(3) models predicting weaker K^-N interaction, postulate weakly bound kaonic nuclei.

Recent studies of K^-p correlations in proton-proton collisions in the ALICE experiment at the LHC are consistent with the prediction of the couple-channel character of the $\bar{K}N$ interaction [136] indicating that the $(\Sigma\pi)^0$ invariant mass spectral shape depends not only on the decay channel (isospin interference term contributes to $\Sigma^{\pm}\pi^{\mp}$ cross-section with opposite sign and vanishes for $\Sigma^0\pi^0$) but also on the production channel. In this case the absorption process $\bar{K}N$ represents the so-called golden channel for examining of the predicted $\Lambda(1405)$ high mass pole. Experimental studies of K^-N absorption (above, on, and below the $\bar{K}N$ threshold) are crucial for the verification of existing chiral models (Fig. 2.19). Current chiral calculations constrained only by the measurement of a_{K^-p} by SIDDHARTA Collaboration [98] and the measurements of elastic and inelastic cross-sections ($K^-p \to K^-p$, $K^-p \to \Sigma^{\pm}\pi^{\mp}$, $K^-p \to \Sigma^0\pi^0$,$K^-p \to \Lambda\pi^0$), show a large discrepancy in scattering amplitudes in the subthreshold region for I=0 and I=1, as well as on and above the threshold in the case of the K^-n channel.

2.3.3.2 Kaonic atoms and nuclei - theoretical outline

Mesonic atoms, including kaonic atoms, were predicted as early as the 1940s [91, 92] after Yukawa and Okayama showed that the capture of mesons by atomic nuclei occurs after their energy loss for ionization stops them, and its probability increases with the material density [137].

A kaonic atom is formed when the K^- kaon stops in the target is captured in the outer orbit of the atom, knocking an electron out of it (the overlap of the kaon wave function

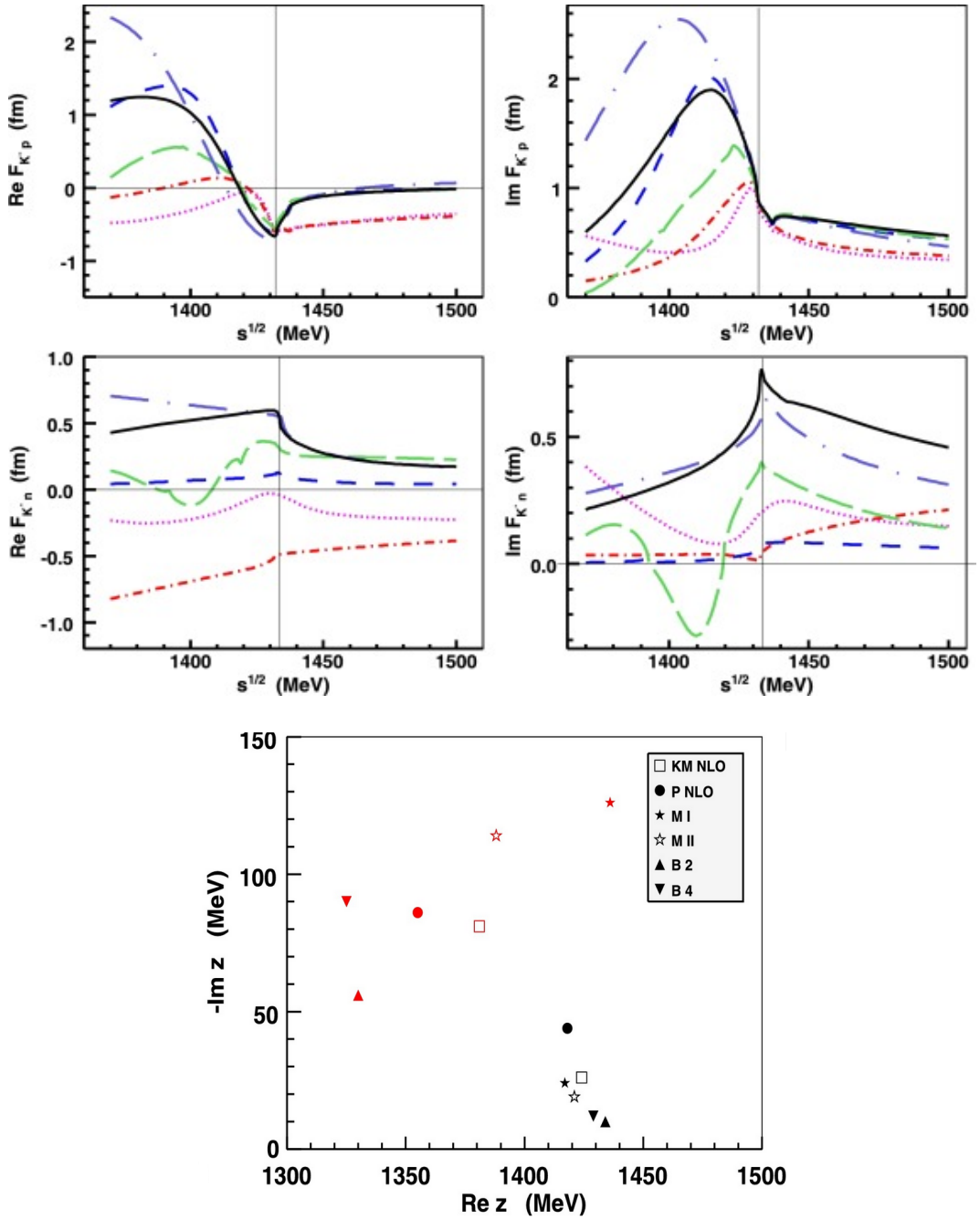

Figure 2.19: The K^-p (upper panel) and K^-n (mid panel) elastic scattering amplitudes obtained for the chiral models: B2 (dotted, purple), B4 (dot-dashed, red), MI (dashed, blue), MII (long-dashed, green), PNLO (dot-long-dashed, violet), KMNLO (continuous, black) and corresponding positions of the $\Lambda(1405)$ resonance poles (lower panel). Figures are adapted from Ref. [135].

with the outer atomic orbit is then maximum). The kaon capture occurs in a highly excited quantum state since its mass is much greater than the mass of the electron. This

process depends on the element type, the range of values of the principal quantum number n, and the angular momentum l [138]. The initial principal quantum number n of the exotic atom is proportional to the principal quantum number of the outermost electron shell of the atom (n_e) and the square root of the ratio of the kaonic atom reduced mass (μ) to the electron mass (m_e), $n \sim \sqrt{\frac{\mu}{m_e}} n_e$ (for kaonic hydrogen n =25) [139]. Binding energies and radii of the kaonic atom individual levels according to the Bohr formula are proportional to μ and $1/\mu$, respectively (for the 1s state of kaonic hydrogen, they are $B_{1s} = 8.61\ keV$ and $r_B = 81\ fm$) [140].

The kaonic atom experiences a series of de-excitation processes (and Auger electron emission) that bring it to its ground state. As a result, γ radiation is emitted, which is in the X-ray energy regime for transitions to the lowest levels. Such a kaon cascade, shown schematically in Fig. 2.20 for the example of kaonic hydrogen, continues until the atomic nucleus absorbs the kaon. Because the kaon lifetime is much longer than the time needed for its deceleration in nuclear matter and the de-excitation process, it is possible to measure the effects of the strong kaon - atomic nucleus interaction [96].

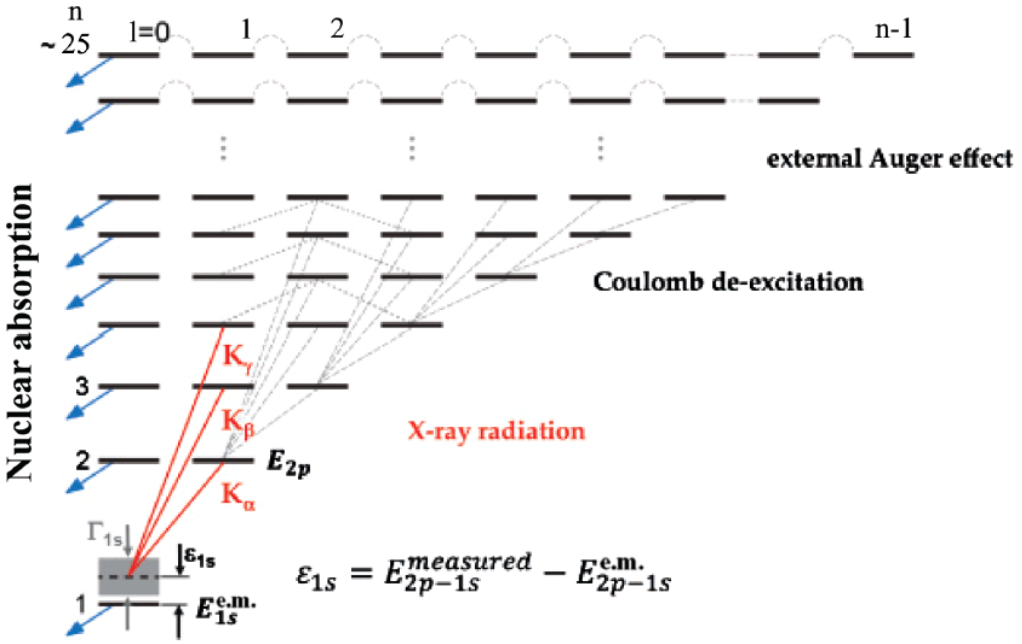

Figure 2.20: Cascade processes for K^-H, starting when the kaon is captured in a highly excited state, down to the 1s ground state, which is shifted due to strong interaction and broadened due to nuclear absorption of the kaon by the proton. The figure is adapted from Ref. [96].

Not all kaons can reach the fundamental level due to other processes, such as the Stark effect, which results in the mixing of levels with the same principal quantum number (and different 1) belonging to different atoms. It allows the absorption of the kaon even from a further orbit. This effect increases with the density of the target material. Cascade models taking into account the Stark mixing effect were introduced by the authors of

Ref. [141, 142].

When a kaon is close enough to an atomic nucleus, it interacts strongly with it, what results in a energy levels shift with respect to the values determined for well-known electromagnetic interaction (for which the energy levels can be calculated with precision of eV by solving the Klein-Gordon equation) and their broadening (Fig. 2.20). The broadening results from the absorption of the kaon by the nucleus and implies the limited kaonic atom lifetime. The shift and broadening effect is greatest for the 1s ground state and negligible for higher atomic levels. The observables of the strong kaon - atomic nucleus interactions are shift ϵ_{1s} and width Γ_{1s} of the ground state. The shift ϵ_{1s} is the difference between the $2p \to 1s$ (line K_α) transition energy measured experimentally and calculated for the purely electromagnetic interaction (ϵ_{1s}=$E^m_{2p\to 1s} - E^{em}_{2p\to 1s}$).

Essential for understanding the K^-N interactions is the precise measurement of the shift and width of the 1s level in the lightest kaonic atoms, i.e., kaonic hydrogen (K^-H) and kaonic deuterium (K^-D). These observables allow us to determine isospin-dependent antikaon-nucleon scattering lengths a_0 (I=0) and a_1 (I=1) based on Deser's formula, which has the following form:

$$\epsilon_{1s} + \frac{i}{2}\Gamma_{1s} = 2\alpha^3\mu^2 a_{K^-X}[1 - 2\alpha\mu(\ln\alpha - 1)a_{K^-X} + ...], \tag{2.3}$$

where a_{K^-X} is the complex K^-p or K^-d scattering length, α - the fine-structure constant, $a_{K^-p} = 1/2(a_0 + a_1)$, and $a_{K^-n} = a_1$, $a_{K^-d} = \frac{4[m_N+m_K]}{2m_N+m_K}\frac{1}{2}(a_{K^-p} + a_{K^-n}) + C$ (C denotes higher-order contributions).

The SIDDHARTA Collaboration has measured $-\epsilon_{1s}$ and Γ_{1s} for K^-H [98] with high precision (see Sec. 2.3.3.3). On the other hand, no signal from K^-D atoms has been observed so far. Theoretically predicted shift and width of the kaonic deuterium ground state oscillate around $\epsilon_{1s} \in$(-1100,-670) eV and $\Gamma_{1s} \in$ (505.2280) eV [96, 143], respectively. A few of them are shown in Fig. 2.21, including values determined by the authors of Ref. [143] based on Hamiltonian Effective Field Theory (HEFT) with and without the nucleon recoil effect assumption in the deuteron.

Kaonic atoms studies have shown the attractive nature of the nuclear potential for K^- mesons (see review article [121]), thus initiating predictions concerning the formation of hypothetical kaonic nuclei. First theoretical work in 1986 [99] demonstrated very strong K^- binding (approximately 100 MeV) in heavy atomic nuclei resulting from the presence of the $\Lambda(1405)$ resonance and small bound states widths. Deeply bound and narrow kaonic nuclei were later predicted for light nuclei such as He [100]. The strong, attractive interaction in the kaonic nucleus was attributed to the strong K^-N interaction in the channel with the isospin I=0 generated by the $\Lambda(1405)$ resonance being the K^-p bound state. That and other models based on (energy-independent) phenomenological potentials predict the existence of K^-pp kaonic clusters with binding energies and widths in the range $B_s \in (40, 95)$ MeV and $\Gamma \in (32, 110)$ MeV, respectively. In turn, chiral models postulate weakly bound kaonic clusters with $B_s \in (9, 50)$ MeV and $\Gamma \in (16, 80)$ MeV [144]. The parameters of the kaonic nuclei are summarized in Table 2.1 for the phenomenological and chiral approaches, specifying the methods used in the calculations. The discrepancy in the binding energy and the width values of kaonic nuclei results both from the uncertainty

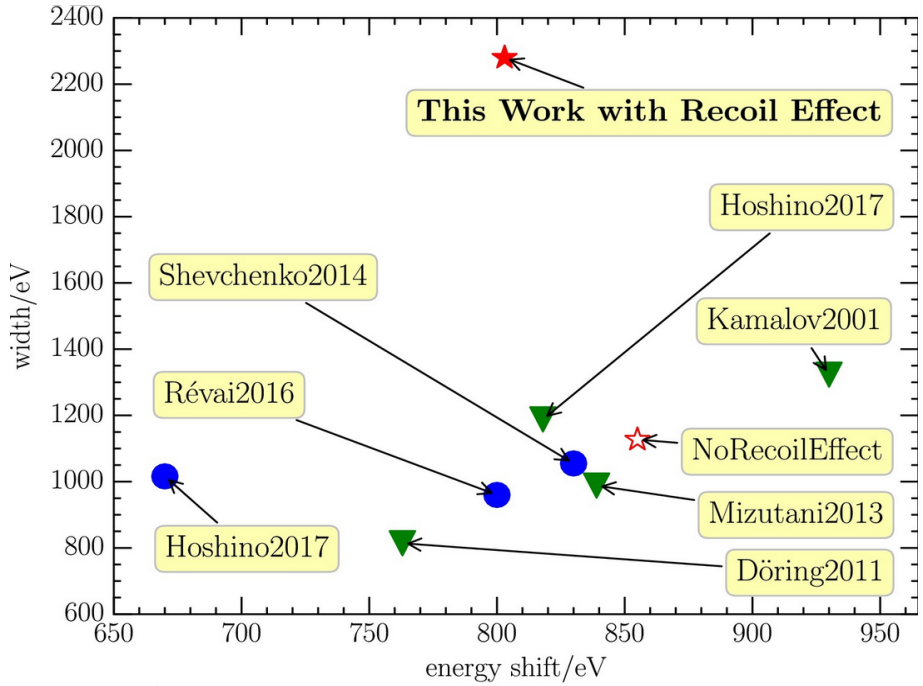

Figure 2.21: Shift and width for the kaonic deuterium atom ground state obtained for different theoretical models. Green triangles correspond to ϵ_{1s}, Γ_{1s} determined from a_{K^-d} based on Deser formula, and the blue circles to parameters determined directly from the solution of the Schrödinger equations. Asterisks indicate the results of work with and without considering the recoil effect. The figure is taken from Ref. [143].

of the $\bar{K}N$ interaction extrapolation to the subthreshold region (the $\bar{K}N$ interaction is weaker in the case of chiral models, as shown in Fig. 2.18), as well as the choice of the calculation method. In summary, the properties of kaonic nuclei (binding energy and width) are related to the still unknown $\Lambda(1405)$ structure and, from a more general point of view, to the modification of the $\bar{K}N$ interaction in the nuclear medium.

The search for kaonic bound states in low-energy kaon induced reactions comes with the study of multinucleon K^- absorption processes because they overlap in a wide range of the phase space. The study of the single and multinucleon kaon absorption processes is crucial for constraining the theoretical models predicting various $\bar{K}N$ scattering amplitude dependences below the threshold, affecting the description of the $\Lambda(1405)$ resonance structure and thus on the values of kaonic nuclei parameters. The depth of kaon interaction in nuclear matter may, in turn, influence models describing the structure and density of the neutron stars [144].

Reference	B_s [MeV]	Γ [MeV]	Method	Potential
Yamazaki et al. (2002)	48	61	variational	phenomenological
Shevchenko et al. (2007)	50-70	90-110	Faddeev	phenomenological
Ikeda et al. (2007)	60-95	45-80	Faddeev	phenomenological
Wycech et al. (2009)	40-80	40-85	variational	phenomenological
Dote et al. (2017)	51	32	ccCSM	phenomenological
Revai et al. (2014)	32/47-54	50-65	Faddeev	chiral/phenomenological
Barnea et al. (2012)	16	41	variational	chiral
Dote et al. (2009)	17-23	40-70	variational	chiral
Dote et al. (2018)	14-50	16-38	ccCSM	chiral
Ikeda et al. (2010)	9-16	34-46	Faddeev	chiral
Bayar et al. (2013)	15-30	75-80	Faddeev	chiral
Sekihara et al. (2016)	15-20	70-80	Faddeev	chiral

Table 2.1: Binding energy B_s and width Γ of K^-pp clusters for diffeerent chiral and phenomenological calculations using variational, Faddeev 3-body equations, or ccCSM+Feshbach methods (details in Ref. [144]). The table was prepared based on Ref. [144].

2.3.3.3 Experimental studies of kaonic atoms and nuclei

Measurements of kaonic atoms, especially with light elements such as hydrogen, deuterium, or helium, are a major experimental challenge. They require (i) the production of low-energy K^- beams, which can be stopped in the target, (ii) the construction of cryogenic gas targets with high density (to make the probability of kaonic atom production as high as possible), and (iii) the use of very sensitive X-ray detectors with excellent energy and time resolution.

The first experiments dedicated to kaonic atoms were carried out at the CERN accelerator center and the Rutherford Laboratory in the years 1970-1980 [145–147] using liquid hydrogen targets and Si(Li) detectors [96]. Due to low statistics and a large background (e.g., related to the Stark effect in liquid hydrogen), identifying signals from X-ray transitions in kaonic atoms was challenging. In the measurements, excitations assigned to the lines K_α [145–147], K_β [146, 147], K_γ [146, 147] and K_δ [147] were observed. In all cases, a positive ground level shift (K_α) was obtained with respect to the calculated electromagnetic value, which suggested that the interaction of the kaon with the proton at the threshold is strongly attractive. The result was inconsistent with the low-energy K^-p [148, 149] scattering analyses. This kaonic hydrogen puzzle was solved in the 1990s thanks to measurements made wit the KEK Proton Synchrotron in Japan. In the experiment (E228, KpX) [6], a gas target was used for the first time, which allowed for a significant reduction of the Stark effect. Moreover, to identify and reduce the background originating from pions produced by kaon absorption, several detectors,

such as Cherenkov counters, multiwire proportional chambers (MWPC), or hodoscope scintillation counters, were used. Two distinct excitations were observed in the X-ray energy spectrum: the first corresponding to the K_α transition and the second being the sum of all other transitions (K_β,K_γ,K_δ,...) [96]. The 1s shift obtained for kaonic hydrogen (negative sign), consequently the $\bar{K}N$ scattering length, is consistent with the results [148,149], confirming the repulsive nature of the K^-p interaction on the threshold.

Other experiments devoted to the kaonic atoms studies, DEAR [97] and SIDDHARTA [98], were carried out in the DAΦNE [125] accelerator complex at the Laboratori Nazionali di Frascati (LNF-INFN). DAΦNE is a unique apparatus in the world that allows the production of low-energy charged kaons beams through the ϕ mesons decay (BR($\phi \rightarrow K^+K^-$)=48.9%), which in turn are produced in collisions of e^+e^- opposite beams. The ability to produce charged kaons with momentum around 127 MeV/c (ϕ particle decay almost at rest) and momentum resolution $< 0.1\%$ makes the K^- beam from DAΦNE ideal for kaonic atoms measurement.

The DEAR detection system consisting of a cryogenic target system and a system of X-ray detectors, the so-called CCDs (*charged-coupled devices*) embedded in a vacuum, and a kaon monitor that also was used as a luminosity detector (details in Ref. [96]) were used to measure kaonic atoms using hydrogen and nitrogen gas targets [97]. The experiment allowed the observation of the K_α, K_β, K_γ transitions and the sum of the remaining lines for kaonic hydrogen, as well as lines coming from the kaonic atoms of elements forming the detection system, such as Fe, Ti, Zn, Au. The obtained ϵ_{1s} and Γ_{1s} values for kaonic hydrogen are consistent with the KpX [6] experiment values within their uncertainty of 2σ. In the case of kaonic nitrogen measurement, three lines corresponding to the $7\rightarrow 6$, $6 \rightarrow 5$ and $5 \rightarrow 4$ transitions were identified and their yields were determined for the first time [150].

The SIDDHARTA Collaboration, using a low-energy kaon beam provided by the DAΦNE and a detection system consisting of a kaon trigger, a cryogenic target system and a silicon drift detector (SDD) system, has performed the most precise so far measurement of the shift and width of the K_α line for kaonic hydrogen [96,98]. During the experiment, 144 SDD detectors arranged in 48 modules (each containing 3 SDD targets) were employed. They are characterized by high energy (approx. 160 eV (FWHM) for 6 keV energy) and time (of the order μs) resolution. They are surrounded by a cylindrical target filled with gaseous hydrogen (high density), in which, previously slowed down (by using a degrading material) kaons, K^- were stopped, creating kaonic hydrogen atoms. The charged kaon detector (trigger) allowed the measurement of K^-K^+ pairs, based on the coincidence of signals from two plastic scintillators, one of which was located above and the other below the DAΦNE interaction point. The use of the so-called triple coincidence, i.e., the coincidence between the X-ray signal from the SDD detector and the correlated K^-K^+ pair allowed for a significant reduction of the asynchronous background improving the signal/background ratio. The measured X-ray energy spectrum is shown in Fig. 2.22 (left panel, b)). To determine the shift and the width of the ground level of the K^-H atom, the obtained spectrum of hydrogen and the first ever measured spectrum of deuterium (Fig. 2.22, left panel, c)) were fitted simultaneously, which allowed to determine the background lines originating from the kaons captured in the setup material. The

analysis allowed for the clear observation of the K_α line of kaonic hydrogen (Fig. 2.22, left panel, a)), determining the parameters of the strong K^--proton interaction with a large accuracy [98]:

$$\epsilon_{1s} = -283 \pm 36(stat) \pm 6(syst)eV, \tag{2.4}$$

$$\Gamma_{1s} = 541 \pm 89(stat) \pm 22(syst)eV. \tag{2.5}$$

This measurement of the K^-H atom, the most precise so far, confirmed the repulsive nature of the strong interaction between the kaon and the proton that had been observed in earlier experiments [6, 97, 148, 149].

The SIDDHARTA group measured as well the L_α ($3d \rightarrow 2p$) transition in kaonic helium atoms using ^{4}He and ^{3}He gas targets, as shown in Fig. 2.22 b), c) and d) (right panel) [151–153]. The following parameters for $2p$ state were determined:

$$K^{-4}\mathrm{He} : \epsilon_{2p} = 5 \pm 3(stat) \pm 4(syst)eV, \tag{2.6}$$

$$K^{-4}\mathrm{He} : \Gamma_{2p} = 14 \pm 8(stat) \pm 5(syst)eV, \tag{2.7}$$

$$K^{-3}\mathrm{He} : \epsilon_{2p} = -2 \pm 2(stat) \pm 4(syst)eV, \tag{2.8}$$

$$K^{-3}\mathrm{He} : \Gamma_{2p} = 6 \pm 6(stat) \pm 7(syst)eV. \tag{2.9}$$

Very small $2p$ level shift in K^{-4}He atom caused by the strong interaction (consistent with the result obtained in the E570 experiment in KEK-PS [154]) confirmed theoretical predictions based on phenomenological potentials [121] and chiral SU(3) models [155], while ruling out earlier measurements of shifts of about -40 eV [156, 157]. In turn, for K^{-3}He atoms, for the first time in history, the X-ray spectrum was measured and the strong interaction parameters were experimentally determined.

Using the SIDDHARTA detection system, the first exploratory experiment was performed to measure the series of K transitions for kaonic deuterium (Fig. 2.22, left panel, c). However, the collected data did not reveal structures originating from transitions in the K^-D atom due to the expected tiny and wide signal. Instead, they allowed to determine the upper limits for the yields for the series of K transitions and for the K_α line, which are 0.0143 and 0.0039 [159], respectively. As mentioned earlier, these data were also used to estimate background contributions to the X-ray spectrum of kaonic hydrogen [96, 98].

In 2019, the SIDDHARTA-2 [R20,R31] detection system, which is an improved version of the SIDDHARTA detector, was installed at the DAΦNE collider, aimed at performing the world's first measurement of the shift and width of the 1s level in kaonic deuterium atoms with a precision similar to that achieved by the SIDDHARTA collaboration for the kaonic hydrogen [98]. Such a measurement is challenging because the expected X-ray signal from K^-D atoms is one order of magnitude smaller than the signal from K^-H, and the line width of the K transitions is of the order of the keV. The new experiment aims to significantly improve the signal-to-background ratio using the following enhancements:

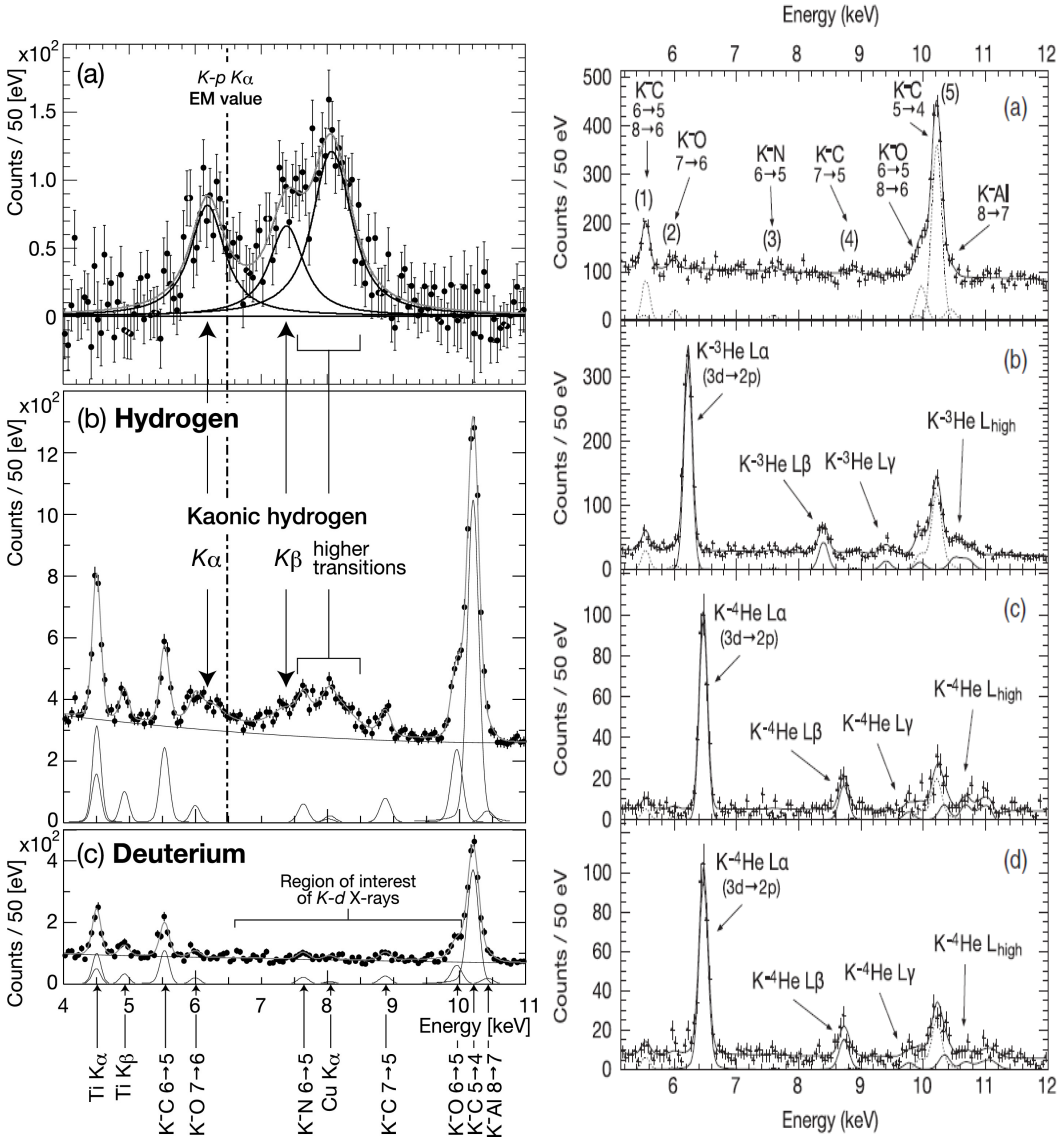

Figure 2.22: (Left panel) The global simultaneous fit of the X-ray energy spectra of hydrogen (b) and deuterium (c) and the measured kaonic-hydrogen X-ray spectrum after subtraction of the fitted background (a). (Right panel) X-ray energy spectra measured for gasous deuteron target (a), ^{3}He target (b) and ^{4}He target for two different gas density (c) i (d). Details one can find in Ref. [96]. Figures are adapted from Ref. [158].

- The increase the solid angle using (i) dedicated silicon drift detectors SDD (with integrated CMOS charge sensing amplifier - CUBE) [160] with excellent energy (140 eV for 6 keV photon energy) and time (drift time 400 ns) resolution [R14] densely packed around a cylindrical cryogenic target. It is constitued by 384 SDD detector with a surface of 0.64 cm^2 and 450 μm of thickness. They are arranged in 48 monolithic modules, each containing 2 x 4 square SDD targets, (details on the characteristics of silicon detectors and their calibration can be found, in

Ref. [R14,R16,R17,R22,R23,P4]). Moreover, (ii) a simultaneous reduction of the distance of the target from the DAΦNE interaction point (IP) (relative to the SIDDHARTA detection system) is used.

- The application of a new light cryogenic target cell of cylindrical shape (ϕ=144 mm and h=125 mm) made of high purity aluminum rods and Kapton walls (125μm thick) [R16] is embed, together with surrounding SDD detectors, in a vacuum chamber (the target is cooled to -145°C at a pressure of about 1.2 ba), able to store high-density gaseous deuterium (about 3% liquid deuterium (LD)); X-ray transmittance through the target chamber is approx. 85% at energies of 7 keV.

- The application of additional Veto-1 [161] and Veto-2 [P37] systems to reduce the background from hadronic processes. They consist of, respectively, twelve pairs of plastic scintillators read by photomultiplier tubes (PM) placed around the target outside the chamber, and plastic scintillator tiles read by silicon photomultipliers (SiMP) installed inside the vacuum chamber right after the SDD detectors, respectively. Veto-1 system allows to separate events corresponding to kaons trapped in the setup material from cases where the kaon is absorbed in the gas, while Veto-2 system allows for the elimination of signals from charged particles (mainly π) outgoing from nuclear kaons absorption.

- The use of two lead shielding blocks to protect the apparatus against particles, mainly MIPs (Minimum Ionizing Particles), formed in the DAΦNE rings mostly by the Touschek effect [R16].

The SIDDHARTA-2 detection system includes also the previously mentioned kaon trigger, which is a pair of two plastic scintillators read by the PM, as well as a new luminosity detector [**H8**]. The SIDDHARTA-2 apparatus is schematically presented in Fig. 2.23 (details can be found in Ref. [**H8**,R12-R14,R17,R22,R23,P4,P37]).

The configuration of the SIDDHARTA-2 detection system (moving the target closer to the interaction point e^+e^-) required the elimination of the old DAΦNE luminosity detector, constructing a new dedicated luminometer. This detector marked in Fig. 2.23 (red color and module scheme) was designed and manufactured at the Jagiellonian University in Krakow **[H8]**. It is constitued by two parallel detection modules installed on opposite sides of the DAΦNE beam pipe on the collision plane (one side corresponds to the boost and the other to the anti-boost direction of the ϕ meson), which allows the measurement of kaon K^+K^- pairs outgoing from the decay of the ϕ meson in opposite directions. Each module consists of an organic scintillator (80×40×2) mm^3, which both ends are connected to fast photomultipliers (PMTs) with a 6 cm plastic optical fiber. The contact surfaces of the optical fiber - scintillator form a 38° angle to match the geometry of the SIDDHARTA-2 system.

The luminosity detector with a dedicated data acquisition DAQ system is characterized by high efficiency and excellent time resolution, which makes it ideal for precise $K^\pm$ pairs counting, i.e, for the luminosity determination. That is crucial for determining the transitions yields in kaonic deuterium atoms. Moreover, the luminosity monitor allows

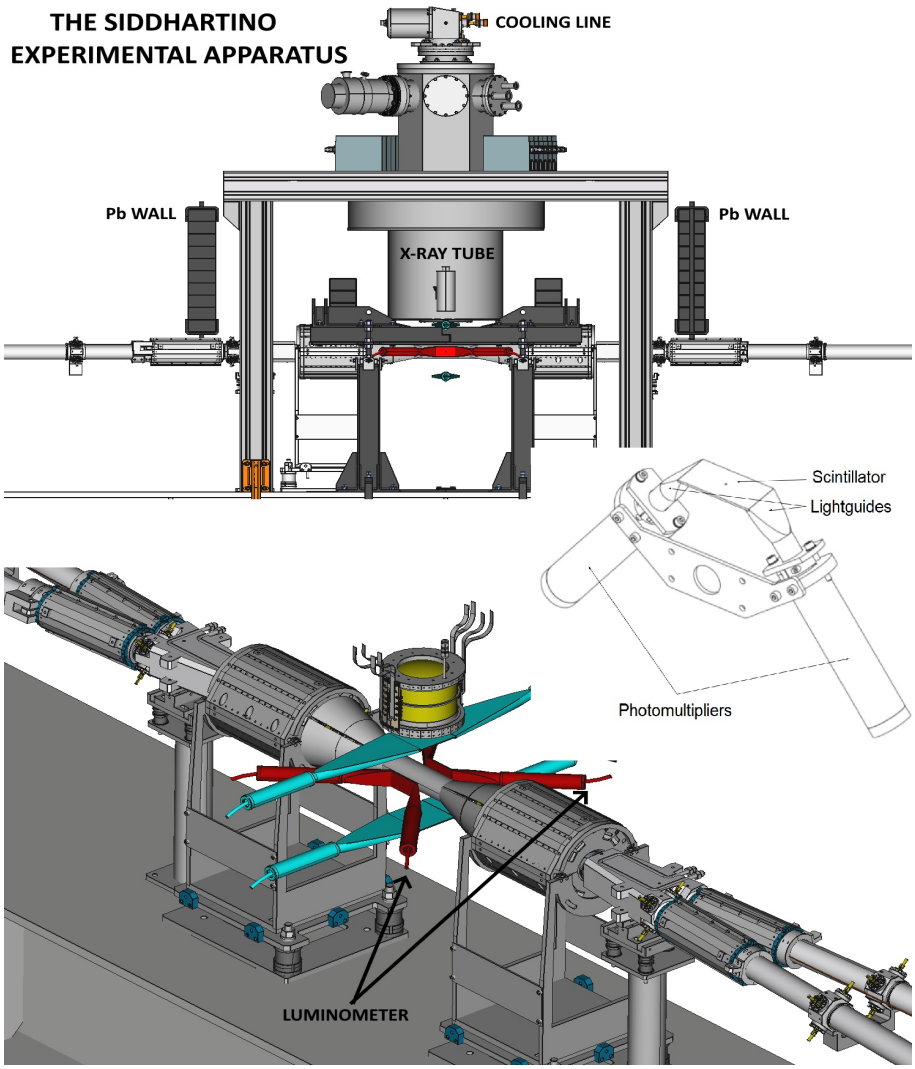

Figure 2.23: (Upper panel) Scheme of the SIDDHARTA-2/SIDDHARTINO detection system installed at the DAΦNE collider interaction point (IP). (Lower panel) a view of the target, the kaon trigger (blue), the luminosity detector (red), and a scheme of one of its modules. The schemes are taken from Ref. [R16].

optimization of the beam optics of the DAΦNE collider by providing a real-time kaon to MIPs ratio. The distance of the luminometer from the DAΦNE interaction point (7.2 cm) was optimized based on the time of flight of the K^- kaons and MIPs particles to ensure the best possible separation between these two components (Fig. 2.24 left pane).

The luminosity detector was tested during the DAΦNE commissioning phase SIDDHARTA-2 in 2020. Based on the collected data sample, the average luminosity value was estimated at $(3.26\pm0.05(\text{stat.})^{+0.17}_{-0.15}\ (\text{sys.}))\cdot10^{31}cm^{-2}s^{-1}$ projecting the two-dimensional spectrum of the average TDCs for signals in coincidence recorded by the detector module installed on the boost and the anti-boost side of IP (Fig. 2.24 left panel) on the diagonal and extracting the number of kaons fitting the signal and background as

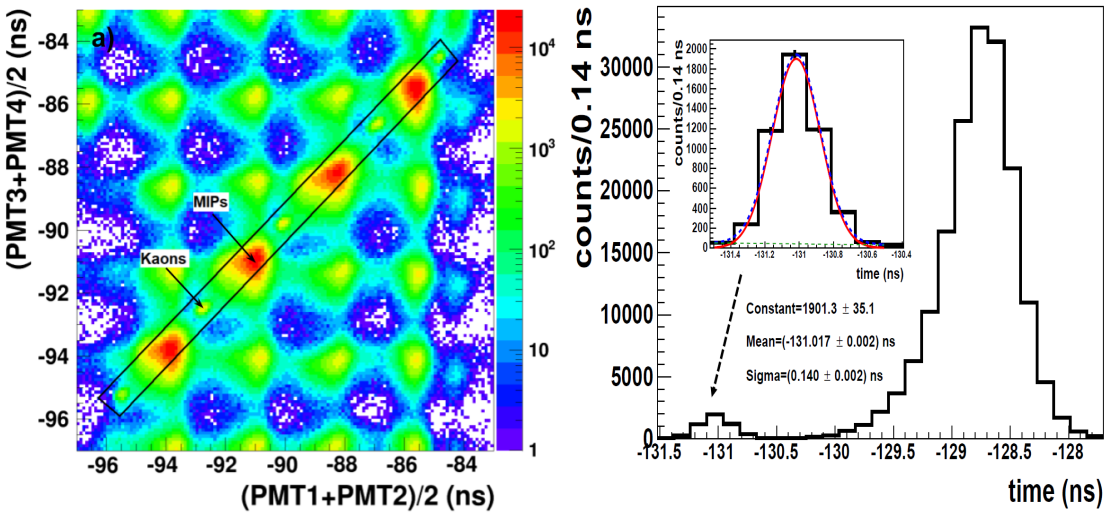

Figure 2.24: (Left panel) 2D plot representing the average TDCs for the signals in coincidence registered on the boost ((PMT1+PMT2)/2) and anti-boost ((PMT3+PMT4)/2) sides of DAΦNE IP for collision. (Right panel) Projection on the diagonal time coordinate of the 2D plot. The inner pad shows the fit to kaon peak (blue dashed line). The signal and background components are marked with the solid red and dashed green lines, respectively. Figures are adapted from Ref. **[H8]**

shown in the right panel of Fig. 2.24. This method is used to determine the luminosity during the SIDDHARTA-2 experiment (online monitoring). The concept of the luminosity monitor, its laboratory characteristics, and the first results at DAΦNE are presented in Ref. **[H8]**.

Before the measurement dedicated to the kaonic deuterium atoms study (during the commissioning accelerator phase from January to July 2021), the SIDDHARTA-2 Collaboration conducted a pilot experiment, SIDDHARTINO, with a reduced number of SDD detectors using a gaseous ^{4}He target with different densities. The primary purpose of the measurement was to optimize the working conditions of the detection system and to estimate the background level. The SIDDHARTINO experiment also allowed for a much more precise measurement of the shift and width of the L_α line in kaonic helium atoms [R16] compared to the SIDDHARTA measurement [152], as well as the absolute yield of the L_α transition and the L_β/L_α and L_γ/L_α ratios [R4]. The shift and width of $3d \rightarrow 2p$ line obtained for the data sample corresponding to the luminosity of 26 pb^{-1} [R16] is equal to:

$$K^{-4}\mathrm{He} : \epsilon_{2p} = 0.2 \pm 2.5(stat) \pm 2(syst)eV, \tag{2.10}$$

$$K^{-4}\mathrm{He} : \Gamma_{2p} = 8 \pm 10(stat)eV. \tag{2.11}$$

Measurement with helium after installing the entire configuration of the

SIDDHARTA-2 detector [R3,R12,R13] brought even greater accuracy in the L lines parameters determination, as well as observations of the M lines in the kaonic helium (article in preparation). What is more, allowed for the first time to determine the energies of a series of transitions in kaonic atoms with intermediate masses (O,C,N,Al) with high precision [R3]. The SIDDHARTA-2 Collaboration carried out measurements with a neon target (125 pb^{-1}), which data is currently being analyzed. Measurements with a 1.4% LD deuterium target began at the beginning of this year and will continue into the next year. So far, collected data correspond to the luminosity of about 200 pb^{-1}, which is 1/4 of the sample, which, according to the simulations, will allow the observation of structures originating from transitions in the kaonic deuterium atom.

After completing the measurements dedicated to the study of K^-D atoms, the SIDDHARTA-2 Collaboration plans to conduct several new experiments, including (i) measurements of X-ray transitions in kaonic atoms using fixed targets (Pb) and HPGe germanium detector to determine very precisely the mass of kaon K^- [R32], (ii) measurements of radiation transitions for kaonic atoms with medium and high masses using CdZnTe detectors with excellent energy resolution [R2], and (iii) studies of the E2 nuclear resonance effect in the kaonic molybdenum atom (KAMEO) [P1].

Several research groups have carried out measurements dedicated to the search for light kaonic nuclei K^-pp using various experimental approaches. Potential kaonic clusters were searched for in their decays to Λp and $\Sigma^0 p$ pairs.

The DISTO collaboration measured the ΛpK^+ channel in the proton-proton collision and observed the structure for $T_p = 3.5$ GeV in the K^+ missing mass and Λp invariant mass spectrum, which corresponds to the binding energy (B_s) and the kaonic cluster width (Γ) B_s=103 $\pm$ 3($stat.$) $\pm$ 5($syst.$) MeV and Γ=118 $\pm$ 8($stat.$) $\pm$ 10($syst.$) MeV, respectively [116]. The HADES experiment at GSI on the same process revealed no significant structure for $T_p = 3.5$ GeV [162] and determined the upper limit of the cross-section for the $\bar{K}NN$ bound state production using the partial wave analysis of the final state. It took into account resonant and non-resonant intermediate processes leading to the formation of the ΛK^+ pair. The OBELIX group at CERN, analyzing the antiproton-^{4}He annihilation process, registered a peak in the Λp invariant mass spectrum suggesting a deeply bound K^-pp cluster with B_s=160.9$\pm$4.9 MeV and Γ<24.4$\pm$8.0 MeV (the upper limit of Γ was determined due to low experimental resolution). Experiment E27 in the pion induced reaction $\pi^+ d \rightarrow K^+X$ observed a broad enhancement in the Λp missing mass spectrum corresponding to $B_s = 95^{+18}_{-17}(stat)^{+30}_{-21}(syst)$ MeV and $\Gamma = 162^{+87}_{-45}(stat)^{+66}_{-78}(syst)$ MeV [163], while the analysis of the photoproduction reaction d(γ,$K^+\pi^-$)X by the LEPS/SPring-8 group allowed determination of the upper limit of the cross-section for the K^-pp production [164].

Among the experiments dedicated to bound K^-pp systems in kaon K^- induced reactions, one can mention the experiments carried out at the DAΦNE collider at LNF-INFN (FINUDA [117] and AMADEUS [165][R42]), in the KEK-PS (E549 [118]), and J-PARC (E15 [8, 166]) accelerator centers. The FINUDA Collaboration measured kaons stopped in ^{6,7}Li and ^{12}C targets. In the invariant mass $m_{\Lambda p}$ spectrum determined for back-to-back Λp pairs ($cos_{\Lambda p}$<-0.8) a structure around 2.5 GeV/c^2 was observed

(Fig. 2.25 upper left panel), which was attributed to the existence of a kaonic nucleus [117] with B_s=$115^{+6}_{-5}(stat.)^{+3}_{-4}(syst.)$ MeV and Γ= $67^{+14}_{-11}(stat.)^{+2}_{-3}(sys.)$ MeV. In the E549 experiment at KEK performed with the ^{4}He target, the Λp invariant mass spectrum revealed three main components: low-mass component coming from pions, high-mass component interpreted as a two-nucleon absorption process (2NA) in He, and the intermediate mass region interpreted as a signal originating from a kaonic nucleus or 2NA followed by a conversion process. These three contributions are marked in Fig. 2.25 (upper right panel) in blue, green, and red, respectively [118]. Experiment E15 was carried out twice by bombarding the ^{3}He target with a K^- beam with a momentum of 1 GeV/c. The analysis was performed by selecting the Λpn events based on the neutron missing mass spectrum and then fitting the invariant mass $m_{\Lambda p}$ and momentum transfer spectra $q_{\Lambda p}$ with the sum of signal (corresponding to the K^-pp cluster) and background functions. The result of the first measurement [166] was the observation of a signal that could correspond to the kaonic nuclei with binding energy and width B_s=$15^{+6}_{-8}(stat.) \pm 12(syst.)$ MeV and Γ= $110^{+19}_{-17}(stat.) \pm 27(sys.)$ MeV, respectively. A similar signal was observed in the later measurement (red color in Fig. 2.25 bottom panel). However, due to the much greater statistics of the collected data, it gave the possibility of a more refined analysis, which allowed for a significant background reduction (e.g., by selecting the area corresponding to the range $q_{\Lambda p}$ ∈(0.35,0.65) GeV/c). This signal is, so far, the first and only interpreted as originating from the K^-pp mesic nucleus [8,113,114] having B_s=$47 \pm 3(stat.)^{+3}_{-6}(syst.)$ MeV and Γ= $115 \pm 7(stat)^{+10}_{-20}(syst.)$ MeV.

For over a decade, the AMADEUS Group has been conducting experimental research on the processes of single- and multi-nucleon absorption of low-energy K^- kaons in light atomic nuclei, allowing for a better understanding of the meson-baryon interaction at low energies. Yhat limits the theoretical predictions regarding the $\bar{K}$N interaction below the threshold, which in turn affects the description of the Λ(1405) resonance structure and the formation of kaonic bound states [**H11**,R1,R42,R47] [165]. The conducted analyses are based on a sample of experimental data, corresponding to a total integrated luminosity of 1.74 fb^{-1}, collected with the KLOE detector [127] installed at the DAΦNE collider. The measurement carried out using a unique monochromatic low-momentum kaon beam allows the study of K^- nuclear absorptions in light elements of the active KLOE material, such as hydrogen, helium, or carbon, whether at rest or in flight.

One of the studies carried out by the AMADEUS Collaboration focuses on the measurement of K^- absorption processes on two or more nucleons, which play a significant role in determining the optical potential of K^--atomic nuclei and are also associated with the search for K^-pp kaonic bound states. K^--nucleus optical potentials determined based on existing single-nucleon K^- absorption potentials (1NA) and phenomenologically determined multi-nucleon absorption potentials (based on global absorption bubble chamber data [167]) do not reproduce the kaonic atom data along the periodic table of elements [168, 169]. Therefore, it is necessary to improve the theoretical model by providing complete characteristics of the absorption processes, separating individual components, i.e., two-, three- and four-nucleon absorptions (2NA, 3NA, and 4NA). The AMADEUS group provided the first characterization of such processes for K^- absorption in ^{12}C nuclei by examining the Λ(Σ^0)p channels [165] [R42]. Comprehensive data analysis

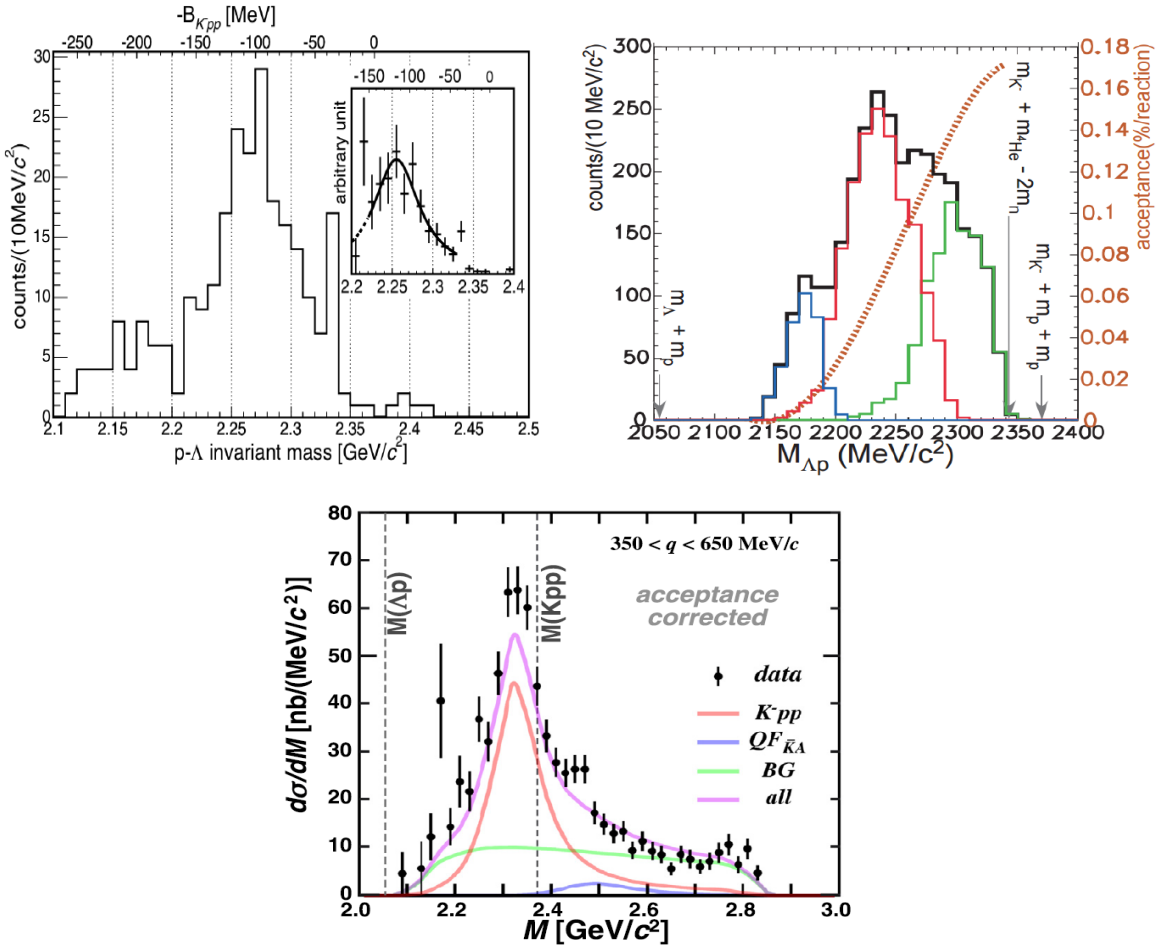

Figure 2.25: Λp invariant mass measured by FINUDA experiment at DAΦNE (left upper panel), by E549 in KEK (right upper panel), and by E15 experiment (run 2) at J-PARC (lower panel). Figures are taken from Refs. [8, 117, 118].

was performed [R42] based on a phenomenological model of K^- capture in light nuclei at rest and in flight [170]. For this purpose, spectra of experimental invariant mass $m_{\Lambda p}$, angular correlation $\cos(\Lambda p)$, and particle momenta p_Λ and p_p were simultaneously fitted with simulated distributions of processes. The reactions are the Σ^0 productions followed by $\Sigma^0 \to \Lambda\gamma$ decay and for the 2NA: (i) the Quasi-Free (QF) processes, (ii) elastic Final State Interaction (FSI) processes, and (iii) inelastic FSI processes due to conversion ($\Sigma N \to \Lambda N'$). It allowed for the extraction of branching ratios (BR) for the 2NA, 3NA, and 4NA processes (based on the K^- absorption processes at rest) and cross-sections (for kaons captured in flight) in the final Λp and $\Sigma^0 p$ states, which are shown in Table 2.2. The determined global branching ratio BR is consistent with that obtained in previous experiments [167].

The AMADEUS group determined also for the first time the total BR for the two-nucleon K^- absorption in ^{12}C equal to $21.6 \pm 2.9(\text{stat.})^{+4.4}_{-5.6}(\text{syst.})\%$ [R28]. They

Process	Branching Ratio (%)	σ (mb)	@	p_K (MeV/c)
2NA-QF Λp	0.25 ± 0.02 (stat.) $^{+0.01}_{-0.02}$(syst.)	2.8 ± 0.3 (stat.) $^{+0.1}_{-0.2}$ (syst.)	@	128 ± 29
2NA-FSI Λp	6.2 ± 1.4(stat.) $^{+0.5}_{-0.6}$(syst.)	69 ± 15 (stat.) ± 6 (syst.)	@	128 ± 29
2NA-QF Σ^0p	0.35 ± 0.09(stat.) $^{+0.13}_{-0.06}$(syst.)	3.9 ± 1.0 (stat.) $^{+1.4}_{-0.7}$ (syst.)	@	128 ± 29
2NA-FSI Σ^0p	7.2 ± 2.2(stat.) $^{+4.2}_{-5.4}$(syst.)	80 ± 25 (stat.) $^{+46}_{-60}$ (syst.)	@	128 ± 29
2NA-CONV Σ /Λ	2.1 ± 1.2(stat.) $^{+0.9}_{-0.5}$(syst.)	-		
3NA Λpn	1.4 ± 0.2(stat.) $^{+0.1}_{-0.2}$(syst.)	15 ± 2 (stat.) ± 2 (syst.)	@	117 ± 23
3NA Σ^0pn	3.7 ± 0.4(stat.) $^{+0.2}_{-0.4}$(syst.)	41 ± 4 (stat.) $^{+2}_{-5}$ (syst.)	@	117 ± 23
4NA Λpnn	0.13 ± 0.09(stat.) $^{+0.08}_{-0.07}$(syst.)	-		
Global: $\Lambda(\Sigma^0)$p	21 ± 3(stat.) $^{+5}_{-6}$(syst.)	-		

Table 2.2: Branching ratios (for the K^- captured at-rest) and cross-sections (for the K^- captured in-flight) of the K^- multi-nucleon absorption processes. The Table is adapted from Ref. [R42].

combined the obtained BRs for the processes leading to the Λp pair production (16.1± 2.9(stat.)$^{+1.0}_{-0.9}$(syst.))% [R42] with a component corresponding to processes without Λp in the final state (5.5± 0.1(stat.)$^{+1.0}_{-0.9}$(syst.))% [R28] (obtained based on theoretical and experimental information [167, 171]). The conducted research showed that the experimental branching ratio for the quasi-free Λp production in the 2NA reaction is lower than the quasi-free Σ^0p production: $R = \frac{BR(K^-(pp)\to\Lambda p)}{BR(K^-(pp)\to\Sigma^0 p)} = 0.7 \pm 0.2(static)^{+0.2}_{-0.3}(syst.)$. It indicates the dominance of the Σ^0p final state and contradicts the $R' = 1.22$ obtained from the phase space. This result is in agreement with the theoretical predictions assuming an additional effect in the nuclear medium caused by the Pauli blocking [171].

To investigate in the Λp spectrum the contribution originating from the K^-pp bound system, the authors of Ref. [R42] repeated the data analysis assuming the measurement conditions as in the case of the previously mentioned FINUDA experiment ($\cos\theta_{\Lambda p} <$ -0.8), which claimed the observation of a kaonic nucleus. Fitting the Λp spectra with an additional K^-pp component showed a complete overlap of the signal associated with the kaonic nucleus formation with the 2NA-QF process [R42]. It means that even if a bound system exists, it is not possible to distinguish it from a two-nucleon absorption process.

New experimental constraints for the strong $\bar{K}N$ interactions, which affect the description of the $\Lambda(1405)$ resonance and thus the possibility of kaonic nuclei creation, are also provided by the AMADEUS Collaboration in the studies of single-nucleon K^-n and K^-p absorption processes. The K^- absorption process on a single nucleon in ^{4}He, i.e. $K^-n \to \Lambda\pi^-$ was analyzed to investigate the non-resonant contribution in invariant mass spectrum $(\Sigma\pi)^0$, subtraction of which is necessary to determine the shape and characteristics of the $\Lambda(1405)$ resonance. The non-resonant transition amplitude below the $\bar{K}N$ threshold was determined for the first time, based on the well-known resonant formation process of $\Sigma^-(1385)$ (I=1). A multidimensional fit of $\Lambda\pi^-$ experimental spectra was performed with dedicated Monte Carlo simulations for contributing processes [170]. Modulus of non-resonant transition amplitude $|A_{K^-n\to\Lambda\pi^-}| = (0.334 \pm 0.018$ stat $^{+0.034}_{-0.058}$ syst.) fm [R47] was determined (33±6) MeV/c^2 below the $\bar{K}N$ threshold. It was possible due to the binding energy of the absorbing nucleon as well as to the recoil energy

of the K^-n pair with respect to the residual ^{3}He nucleus. The obtained result allowed to test (strongly model-dependent) chiral predictions in the subthreshold region, which will allow to constrain the appropriate non-resonant background for the channel with I=0 $(\Sigma\pi)^0$, and thus to study the properties of the $\Lambda(1405)$ resonance and kaonic nuclei. Details on data analysis are presented in Ref. [R47].

The latest analysis of the AMADEUS Collaboration allowed for independent determination of cross-sections for the $K^-p \to \Sigma^0\pi^0$ and $K^-p \to \Lambda\pi^0$ processes for the kaon momentum below 100 MeV/c **[H11]**, which are missing in the literature. They are the key information for the non-perturbative chiral SU(3) models. So far, $K^-p \to \Sigma^0\pi^0$ cross-sections near the threshold have been determined only in bubble chamber experiments [172, 173], by indirect estimations using isospin symmetry for the measured $K^-p \to \Lambda\pi^0$ process. Three cross-sections were obtained for the average kaon momentum of p_K =120, 160, and 200 MeV/c with uncertainties greater than 30% (uncertainty for p_K is 12.5 MeV/c).

The AMADEUS group used a sample of $\Sigma^0\pi^0$ events from the K^- absorption in the gas filling the KLOE drift chamber (a mixture of isobutane C_4H_{10} and ^{4}He in a volume ratio of 90% and 10%). To determine the cross-section for $K^-p \to \Sigma^0\pi^0$ and $K^-p \to \Lambda\pi^0$ reactions selection of events corresponding to the K^- absorption in flight in the hydrogen nuclei of the isobutane molecule was performed. The selection was based on several stages described in detail in the article **[H11]** and in Sec. 2.3.3.4. The final one involved the simultaneous fit of the selected experimental spectra using contributions corresponding to various physical processes, e.g., K^-H absorption in flight, as a signal, and background reactions such as the absorption of K^-H at rest or the absorption in helium and carbon nucleus. For the $\Sigma^0\pi^0$ channel, total momentum $p_{\Sigma^0\pi^0}$, invariant mass $m_{\Sigma^0\pi^0}$ and angular correlation $\cos\theta_{\Sigma^0\pi^0}$ were fitted, as shown in Fig. 2.26, while for $\Lambda\pi^0$ channel, the spectra of $p_{\Sigma^0\pi^0}$, $m_{\Sigma^0\pi^0}$ and p_{Σ^0} and p_{π^0}.
After selecting the signal, the following cross-sections for the kaon momentum (98 ± 10)MeV/c **[H11]** were obtained:

- $\sigma_{K^-p\to\Sigma^0\pi^0} = 42.8 \pm 1.5(stat.)^{+2.4}_{-2.0}(syst.)$ mb
- $\sigma_{K^-p\to\Lambda\pi^0} = 31.0 \pm 0.5(stat.)^{+1.2}_{-1.2}(syst.)$ mb

They are characterized by relative errors about one order of magnitude smaller than the results presented in Ref. [172, 173]. Moreover, they were determined in a way of two simultaneous and independent analyses for the lowest kaon momentum value so far. The achieved precision, the vicinity to the threshold $\bar{K}N$, and the best momentum resolution p_{K^-} will undoubtedly improve the fit of theoretical models. The first analysis using the results of the cross-sections **[H11]** (as well as that described in Ref. [R47]) resulted in 20% higher precision of $\Lambda(1405)$ resonance position determination [174].

The research from experimental groups SIDDHARTA-2 [**H8**,R2,R3,R12,R13,R16,R32,P1] and AMADEUS [**H11**,R1,R42,R47] [165] significantly contribute to the investigations of the K^-n and K^-p scattering amplitudes at the $\bar{K}N$ threshold and in the subthreshold region. It is extremely important for a better understanding of the non-perturbative

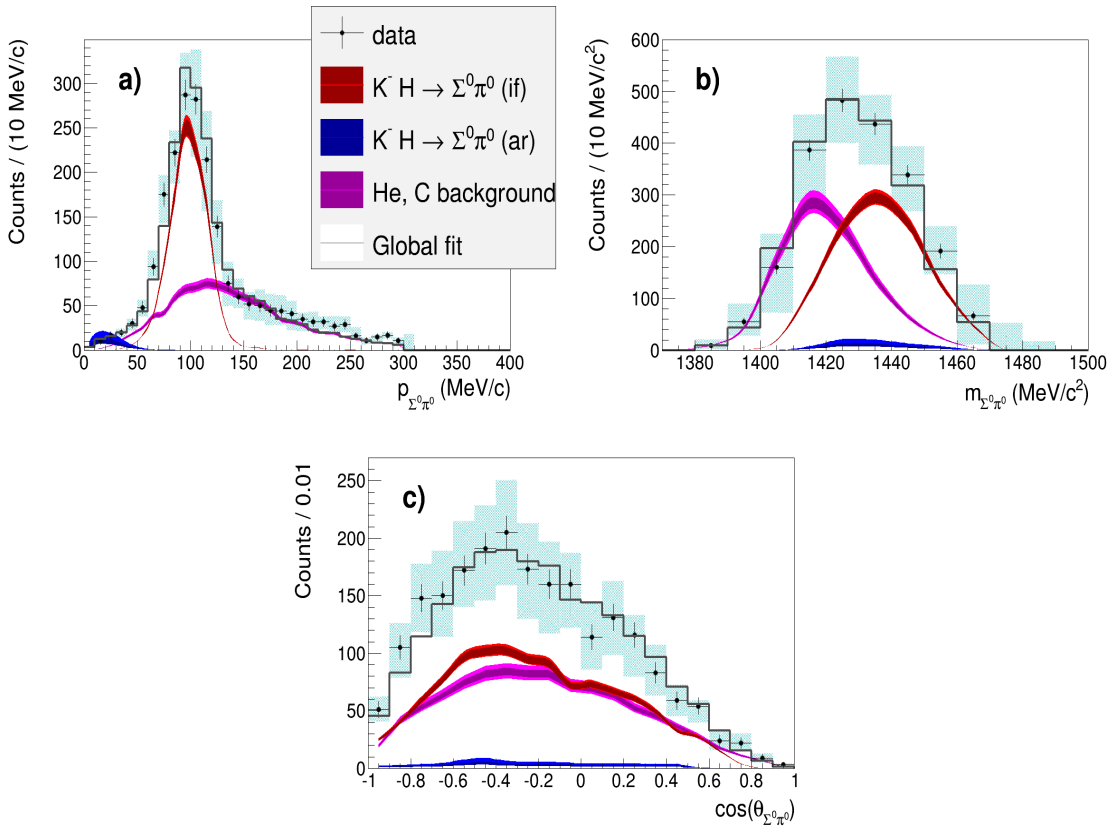

Figure 2.26: The result of the simultaneous fit of $p_{\Sigma^0\pi^0}$ (a), $m_{\Sigma^0\pi^0}$ (b) and $\cos\theta_{\Sigma^0\pi^0}$ (c). The experimental data and the corresponding statistical errors are represented by black crosses, the systematic errors are light blue boxes. The contributions of the various physical processes are shown as colored histograms, according to the color code shown in Ref. [**H11**]. The light and dark bands correspond to systematic and statistical errors, respectively. The gray distribution reproduces the global fit function. The Figure is adapted from Ref. [**H11**].

QCD in the strangeness sector, leading to the solution of long-standing problems ranging from nuclear physics to astrophysics.

2.3.3.4 My contribution to the study of kaonic bound systems

I have been conducting research on the interactions of low-energy kaons with nuclear matter for almost ten years as part of the SIDDHARTA-2 and AMADEUS Collaborations operating at the Laboratori Nazionali di Frascati in Italy, focusing on the experimental study of kaonic atoms and the exploration of K^--nucleon/atomic nucleus absorption processes affecting the possibility of kaonic clusters formation. My greatest achievements in this field of research have been included in the publications **[H8,H11]**, the results of which are summarized in Section 2.3.3.3. I present my contribution to the conducted research below.

As part of the research carried out by the SIDDHARTA-2 Collaboration, I was involved in the work related to the upgrade of the existing SIDDHARTA detection system [96, 98], to perform the first ever extremely precise measurement of the deuterium kaonic atom. I participated in the preparation and testing of the detector system (SDD detectors, veto systems, kaon trigger, luminosity detector - details in Sec. 2.3.3.3), installation of the system on the DAΦNE collider, and its optimization in the initial phase of the experiment. In particular, I was responsible for the construction, testing and implementation of a new dedicated detection system for luminosity measurement (beam monitoring) based on plastic scintillation detectors [**H8**], which was described in Section 2.3.3.3 and shown in Fig. 2.23. Luminosity determination in the SIDDHARTA-2 experiment is crucial for determining the transition yields in kaonic atoms.

I developed the design of the luminosity detector, and the device was built at the Institute of Physics of the Jagiellonian University in Krakow under my supervision. The detector was constructed taking into account the geometrical limitations of the SIDDHARTA-2 measurement system while maintaining the highest possible acceptance of the measurement of correlated K^+K^- pairs emitted in the ϕ meson decay. Before integration with the SIDDHARTA-2 apparatus, I participated in a series of laboratory tests which were aimed, among several tasks, at optimization of the voltage value on the photomultipliers to obtain the best time resolution for each module. Efficiencies determined for each of the modules range from about 96% to 99%, which, together with the obtained resolution t_{MT} ∼140 ps (σ), confirm that the proposed device can be successfully used to determine the luminosity in the SIDDHARTA-2 experiment. Subsequently, I actively participated in installing the luminosity monitor modules on the DAΦNE accelerator beam and then in its integration with the dedicated DAQ data acquisition system. The DAQ system requires three coincidences. The first one is that both the PMTs of each module fire. The second requirement is the coincidence between both modules. Finally, the modules must be synchronized with one-fourth of the DAΦNE RF signal (368.7 MHz). The RF signal represents the precise e^+e^- collision time clock. Thanks to that, it is possible to measure the frequency of signal coincidence from the luminosity detector as a function of time in the DAΦNE reference system, which is extremely important mainly when monitoring measurements during the experiment. It allows for optimizing the DAΦNE beam optics by providing a real-time ratio of the number of kaons to MIPs particles.

Test measurements with the detection system for the luminosity monitoring, which I coordinated, were carried out during the commissioning phase of the SIDDHARTA-2 experiment. I conducted an independent analysis to determine the luminosity based on the collected data. I developed a method for the effective kaons separation from the background (Fig. 2.24) and determined the average luminosity for the measurement, taking into account the systematic uncertainty (Fig. 2.3.3.3). It is equaled to $(3.26 \pm 0.05(\text{stat.})^{+0.17}_{-0.15}(\text{sys.})) \cdot 10^{31} cm^{-2} s^{-1}$. I implemented the developed method of determining the luminosity in the program that monitors the luminosity in real time of the SIDDHARTA-2 experiment (online). Details on data analysis, construction, tests, and characterization of the luminosity detector and the logic of the integrated DAQ system

are described in [**H8**].

The luminosity detector was successfully used to measure the luminosity in the pilot experiment with the SIDDHARTINO system [R16], as well as in the following SIDDHARTA-2 measurements [R3,R12,R13] (the results are presented in Section 2.3.3.3). Moreover, the authors of Ref. [R2] showed that the luminosity monitor could be used as a trigger (significant background reduction from MIPs particles) in measurements of medium and high mass kaonic atoms planned using CdZnTe detectors characterized by excellent energy resolution. Similarly, in the scheduled precise mass measurements of kaon K^- [R32] (by measuring X-ray transitions in kaonic atoms in solid targets), as well as for the study of the E2 nuclear resonance effect in the kaonic molybdenum atom [P1], the luminosity detector will be used as a trigger for the HPGe germanium detector.

In the framework of the SIDDHARTA-2 Collaboration, I also participated in developing the dedicated Monte Carlo simulations to optimize the detection system for the kaonic deuterium atoms measurement and in the analysis of experimental data. I took part in experimental shifts at the BTF (beam test facility), during the commissioning phase of the experiment, during the SIDDHARTINO pilot experiment, and the SIDDHARTA-2 experiment. I plan to participate in the future measurements of SIDDHARTA-2, which will start in September this year and continue in 2024 .

As part of my activity in the AMADEUS group, I participated in experimental studies of low-energy kaons absorption in the light atomic nuclei, which allow for a better understanding of the $\bar{K}N$ interaction in the subthreshold region, and, consequently, the properties of the $\Lambda(1405)$ baryon resonance and kaonic clusters. The results of these studies are presented in Ref. [**H11**,R42,R47] and summarized in Ref. [R1] and Section 2.3.3.3.

The research was based on data collected using the KLOE detection system (description in Section 2.3.3.3). Thanks to the excellent quality of the low-energy K^- beam provided by the DAΦNE collider and the high acceptance of the KLOE detector was able to obtain unique results, allowing the new experimental constraints on the strong kaon-nucleon interaction at low energies, which is crucial for the verification of existing theoretical models.

My participation in the research presented in the papers [R42,R47] (Sec. 2.3.3.3) concerned mainly conceptual work, discussion on the methods of the experimental data analysis and Monte Carlo simulations, as well as interpretation of the obtained results. In turn, in the case of the studies presented in the article [**H11**], I developed and conducted a complete analysis of the $K^-p \to \Sigma^0\pi^0$ and $K^-p \to \Lambda\pi^0$ reactions to determine, for the first time in the world, their cross-sections for kaons momentum below 100 MeV/c, which are a fundamental contribution to non-perturbative QCD models. I prepared and conducted dedicated Monte Carlo (MC) simulations for all possible K^- absorption processes in the gas filling the KLOE drift chamber (DC), which can produce $\Sigma^0\pi^0$ and $\Lambda\pi^0$ pairs in the final state, taking into account the appropriate theoretical models [170, 175]. The simulation included (i) event generation, (ii) detector response simulation, and (iii) data reconstruction for experimental conditions. MC simulations allowed optimization of the selection conditions in the experimental data to separate the signal processes

($K^- + H \rightarrow \Sigma^0/\Lambda + \pi^0$ absorptions in flight) from competing background reactions. Then, I selected events in the experimental data to reconstruct and identify particles in the final state: correlated $\Sigma^0\pi^0$ and $\Lambda\pi^0$ pairs, using several criteria and kinematics cuts. The cuts have been optimized to maximize the signal/background ratio while maintaining sufficient statistics of $\Sigma^0\pi^0$ ($\Lambda\pi^0$) events from the K^- absorption in helium and carbon. In the case of a small number of K^-He and K^-C events, it is impossible to separate them from the signal because they overlap. The kinematic distributions of the selected $\Sigma^0\pi^0$ ($\Lambda\pi^0$) events in the experimental data were fitted with appropriate simulated processes to determine the signal contribution. This allowed to determine the cross-sections for the $K^-H \rightarrow \Sigma^0\pi^0$ and $K^-H \rightarrow \Lambda\pi^0$ reactions, which are equal to:

- $\sigma_{K^-p\rightarrow\Sigma^0\pi^0} = 42.8 \pm 1.5(stat.)^{+2.4}_{-2.0}(syst.)$ mb
- $\sigma_{K^-p\rightarrow\Lambda\pi^0} = 31.0 \pm 0.5(stat.)^{+1.2}_{-1.2}(syst.)$ mb ,

and correspond to kaon momentum $p_K = (98 \pm 10)$ MeV/c **[H11]**.

The obtained cross-sections are characterized by relative errors of about one order of magnitude smaller than the results obtained so far (experiments with bubble chambers) [172, 173]. In addition, the analysis provided the first simultaneous and independent measurement of two inelastic cross-sections $K^-p \rightarrow \Lambda\pi^0$ and $K^-p \rightarrow \Sigma^0\pi^0$ for momentum of kaons below 100 MeV/c. In previous measurements, the $K^-p \rightarrow \Sigma^0\pi^0$ cross-section was determined indirectly assuming isospin symmetry of the measured $K^-p \rightarrow \Lambda\pi^0$ process for higher kaon momentum values (above 120 MeV/c).

The results presented in Ref. **[H11]** will allow to put new experimental constraints on the strong kaon-nucleon interaction at low energies, which is crucial for the verification of existing theoretical models (Sec. 2.3.3.1). Analysis carried out by the authors of Ref. [174] shows that the application of the cross-sections obtained by me **[H11]** together with the results of Ref. [R47] increases the precision of the $\Lambda(1405)$ resonance position determintion by 20% [174].

I carried out the activity described above within the SIDDHARTA-2 and AMADEUS groups mainly during the postdoctoral fellowship at the LNF-INFN (2018 - 2020), as well as during scientific visits to the LNF-INFN, including those realized as part of the NAWA Canaletto project (Joint Projects between Poland and Italy). The research I conducted as part of the AMADEUS Collaboration received support from the SONATA grant, which I obtained from the National Science Center.

2.3.4 Summary

In conclusion, I believe that my work has significantly contributed to studying mesic nuclei and mesonic atoms. Some of my most significant achievements are:

- Determination for the first time in the world the upper limit of the total cross-section ($\sigma^{CL=90\%}_{upp}$) for the ^{4}He-η bound state production and decay in $dd \rightarrow {}^3\mathrm{He}n\pi^0$ reaction

and lowering $\sigma_{upp}^{CL=90\%}$ for $dd \rightarrow {}^3\mathrm{He}p\pi^-$ process by about four times [**H1**] compared to the previous measurement [R94].

- Constraining the ^{4}He-η optical potential parameters by performing a comparative analysis of the experimental data with the current theoretical model. It excludes most predictions for helium mesic nuclei within the optical model, indicating the existence of narrow bound states ($|V_0|<$ ∼60 MeV, $|W_0|<$ ∼7 MeV) [**H2**].

- Determination, for the first time, of the upper limit of the total cross-section for the bound state ^{3}He-η production and the decay in the $pd \rightarrow dp\pi^0$ reaction **[H7]** by applying, in the data analysis, the momentum distribution N*-d (Fig. 2.9) based of the theoretical works **[H3,H6]** in which I contributed. The obtained result does not exclude predictions of mesic nuclei for the scattering length $a_{\eta N}$ with a real part of about 1 fm.

- Evaluation of a new mechanism for the mesic nuclei decays via direct decay of the bound η meson ($pd \rightarrow {}^3\mathrm{He}2\gamma/6\gamma$), and development of a dedicated theoretical model that provided the momentum distribution of the η meson in the bound ^{3}He-η system as well as the branching ratios for $\eta \rightarrow 2\gamma$ and $\eta \rightarrow 3\pi^0$ decays in the nuclear medium for various combinations of the optical potential parameters **[H4]**. The model was developed to analyze experimental data **[H5]**.

- Determination, for the first time, of the upper limit of the total cross-section for the bound state ^{3}He-η production and decay in the $pd \rightarrow {}^3\mathrm{He}2\gamma$ and $pd \rightarrow {}^3\mathrm{He}6\gamma$ reactions **[H4]** by applying, in the data analysis, the η meson momentum distribution determined based on Ref. **[H4]**.

- Development of the concept of the luminosity monitor for the SIDDHARTA-2 experiment, coordination of its construction, testing, integration with the dedicated DAQ system, and implementation in the SIDDHARTA-2 apparatus at the DAΦNE beam [**H8**]. This detector was successfully used to measure the luminosity in the SIDDHARTINO/SIDDHARTA-2 experiment, and, in the planned measurements [R2,R32,P1] will be used as a trigger.

- Determination, for the first time, of the cross-sections for $K^-H \rightarrow \Sigma^0\pi^0$ and $K^-H \rightarrow \Lambda\pi^0$ reactions for the kaon momentum p_K below 100 MeV/c [**H11**]. These two independently obtained cross-sections characterized by small uncertainties will allow to put new experimental constraints on the strong $\bar{\mathrm{K}}$N interaction at low energies testing existing theoretical models.

The results of my studies were discussed in detail at international conferences, as well as at scientific seminars in research centers in the country and abroad.

References:

[1] M. Danysz and J. Pniewski, Phil. Mag. **44**, 348 (1953).

[2] S.-K. Choi et al., Phys. Rev. Lett. **100**, 142001 (2008).

[3] R. Aaij et al., Phys. Rev. Lett. **115**, 072001 (2015).

[4] R. Aaij et al., Phys. Rev. Lett. **122**, 222001 (2019).

[5] T. Yamazaki et al., Z. Phys. **A355**, 219 (1996).

[6] M. Iwasaki et al., Phys. Rev. Lett. **78**, 3067 (1997).

[7] V. Metag, M. Nanova and E. Ya. Paryev, Prog. Part. Nucl. Phys. **97**, 199 (2017).

[8] S. Ajimura et al., Progr. Theor. Exp. Phys. **789**, 620 (2018).

[9] E. Czerwiński et al., Phys. Rev. Lett. **113**, 062004 (2014).

[10] Q. Haider and L. C. Liu, Phys. Lett. **B172**, 257 (1986).

[11] R. S. Bhalerao and L. C. Liu, Phys. Rev. Lett. **54**, 865 (1985).

[12] N. G. Kelkar, K. P. Khemchandani, N. J. Upadhyay and B. K. Jain, Rept. Prog. Phys. **76**, 066301 (2013).

[13] H. Machner, J. Phys. **G42**, 043001 (2015).

[14] B. Krusche and C. Wilkin, Prog. Part. Nucl. Phys. **80**, 43 (2015).

[15] S. D. Bass and P. Moskal, Rev. Mod. Phys. **91**, 015003 (2019).

[16] S. D. Bass, V. Metag, P. Moskal, in Handbook of Nuclear Physics. Editors I Tanihata, H Toki, T Kajino (Singapore: Springer), 1 (2022).

[17] S. D. Bass and A. W. Thomas, Phys. Lett. **B634**, 368 (2006).

[18] S. D. Bass and A. W. Thomas, Acta Phys. Polon. **B45**, 627 (2014).

[19] C. DeTar and T. Kunihiro, Phys. Rev. **D39**, 2805 (1989).

[20] D. Jido, H. Nagahiro, S. Hirenzaki, Phys. Rev. **C66**, 045202 (2002).

[21] H. Nagahiro, D. Jido and S. Hirenzaki, Phys. Rev. **C80**, 025205 (2009).

[22] N. Kaiser, P. B. Siegel and W. Weise, Phys. Lett. **B362**, 23 (1995).

[23] T. Inoue and E. Oset, Nucl. Phys. **A710**, 354 (2002).

[24] C. Garcia-Recio et al., Phys. Lett. **B550**, 47 (2002).

[25] T. Hyodo, D. Jido, and A. Hosaka, Phys. Rev. **C78**, 025203 (2008).

[26] E. J. Garzon and E. Oset, Phys. Rev. **C91**, 025201 (2015).

[27] R. L. Workman et al., Prog. Theor. Exp. Phys. **2022**, 083C01 (2022).

[28] P. Ball, J. M. Frere, M. Tytgat, Phys. Lett. **B365**, 367 (1996)

[29] F. Ambrosino et al., J. High Energ. Phys. **0907**, 105 (2009)

[30] F. J. Gilman, R. Kauffman, Phys. Rev. **D36**, 2761 (1987); Erratum [Phys. Rev. **D37**, 3348 (1988)]

[31] P. Moskal et al., Eur. Phys. J. **A43**, 131 (2010).

[32] P. Moskal et al., Phys. Rev. **C79**, 015208 (2009).

[33] S. Prakhov et al., Phys. Rev. **C72**, 015203 (2005).

[34] R. A. Arndt et al., Phys. Rev. **C72**, 045202 (2005).

[35] Q. Haider and L. C. Liu, Int. J. Mod. Phys. **E24**, 1530009 (2015).

[36] W. Deinet et al., Nucl. Phys. **B11**, 495 (1969).

[37] A. Sibirtsev et al., Phys. Rev. **C65**, 044007 (2002).

[38] A. M. Green and S. Wycech, Phys. Rev. **C71**, 014001 (2005).

[39] A. Cieply and S. Smejkal, Nucl. Phys. **A919**, 46 (2013).

[40] M. Mai, P. C. Bruns, U.-G. Meissner, Phys. Rev. **C86**, 015201 (2013).

[41] T. Inoue and E. Oset, Nucl. Phys. **A710** (2002) 354.

[42] J. Mares et al., EPJ Web Conf **130**, 03006 (2016).

[43] A. Gal et al., Acta Phys. Polon. **B45**, 673 (2014).

[44] W. Cassing, M. Stingl, A. Weiguny, Phys. Rev. **C26**, 22 (1982).

[45] Q. Haider and L. C. Liu, Phys. Rev. **C66**, 045208 (2002).

[46] E. Friedman, A. Gal and J. Mares, Phys. Lett. **B725**, 334 (2013).

[47] K. Tsushima, D. H. Lu, A. W. Thomas, K. Saito, Phys. Lett. **B443**, 26 (1998).

[48] K. Tsushima, Nucl. Phys. **A670**, 198 (2000).

[49] C. Wilkin, Phys. Rev. **C47**, 938 (1993).

[50] S. A. Sofianos, S. A. Rakityansky, arXiv:nucl-th/9707044 (1997).

[51] S. A. Rakityansky et al., Phys. Rev. **C53**, R2043 (1996).

[52] T. Ueda, Phys. Rev. Lett. **66**, 297 (1991).

[53] A. M. Green, J. A. Niskanen and S. Wycech, Phys. Rev. **C54**, 1970 (1996).

[54] N. V. Shevchenko, S. A. Rakityansky, S. A. Sofianos, V. B. Belyaev, W. Sandhas, Phys. Rev. **C58**, R3055 (1998).

[55] N. V. Shevchenko, V. B. Belyaev, S. A. Rakityansky, S. A. Sofianos, W. Sandhas, Eur. Phys. J **A9**, 143 (2000).

[56] N. G. Kelkar, Phys. Rev. Lett. **99**, 210403 (2007).

[57] N. Barnea, E. Friedman and A. Gal, Phys. Lett. **B747**, 345 (2015).

[58] N. Barnea, E. Friedman and A. Gal, Nucl. Phys. **A968**, 35 (2017).

[59] M. Schäfer, N. Barnea, E. Friedman, A. Gal, J. Mares, EPJ Web Conf. **199**, 02022 (2019).

[60] J. Mares et al., Acta. Phys. Polon. **B51**, 129 (2020).

[61] J. J. Xie et al., Phys. Rev. **C95**, 015202 (2017).

[62] J. J. Xie et al., Eur. Phys. J. **A55**, 6 (2019).

[63] A. Fix and O. Kolesnikov, Phys. Rev. **C97**, 044001 (2018).

[64] N. Ikeno, H. Nagahiro, D. Jido, S. Hirenzaki, Eur. Phys. J. **A53**, 194 (2017).

[65] N. G. Kelkar et al., Acta Phys. Polon. **B47**, 299 (2016).

[66] N. G. Kelkar, Eur. Phys. J. **A52**, 309 (2016).

[67] M. Lacombe et al., Phys. Lett. **B101**, 139 (1981).

[68] S. Wycech and W. Krzemien, Acta Phys. Polon. **B45**, 745 (2014).

[69] W. Krzemien, J. Smyrski, AIP Conf. Proc. **950**, 265 (2007).

[70] P. Moskal and J. Smyrski, Acta Phys. Polon. **B41**, 2281 (2010).

[71] R. E. Chrien et al., Phys. Rev. Lett. **60**, 2595 (1988).

[72] J. D. Johnson et al., Phys. Rev. **C47**, 2571 (1993).

[73] G. A. Sokol and L. N. Pavlyuchenko, arXiv:nucl-ex/0111020 (2011).

[74] S. V. Afanasiev et al., Nucl. Phys. **B219/220**, 255 (2011).

[75] A. Budzanowski et al., Phys. Rev. **C79**, 012201 (2009).

[76] B. Mayer et al., Phys. Rev. **C53**, 2068 (1996).

[77] J. Smyrski et al., Phys. Lett. **B649**, 258 (2007).

[78] H. H. Adam et al., Phys Rev **C75**, 014004 (2007).

[79] T. Mersmann et al., Phys. Rev. Lett. **98**, 242301 (2007).

[80] R. Frascaria et al., Phys. Rev. **C50**, 537 (1994).

[81] N. Willis et al., Phys. Lett. **B406**, 14 (1997).

[82] A. Wrońska et al., Eur. Phys. J. **A26**, 421 (2005).

[83] A. Budzanowski et al., Nucl. Phys. **A821**, 193 (2009).

[84] J. Berger et al., Phys. Rev. Lett. **61**, 919 (1988).

[85] M. Papenbrock et al., Phys. Lett. **B734**, 333 (2014).

[86] M. Pfeiffer et al., Phys. Rev. Lett. **92**, 252001 (2004).

[87] F. Pheron et al., Phys. Lett. **B709**, 21 (2012).

[88] C. Wilkin, Eur. Phys. J. **A53**, 114 (2017).

[89] W. Krzemien et al., Int. J. Mod. Phys. **A24**, 576 (2009).

[90] N. Barnea, B. Bazak, Phys. Lett. **B771**, 297 (2017), Erratum: [Phys. Lett. **B775**, 364 (2017)].

[91] S. Tomonaga and G. Araki, Phys. Rev. **58**, 90 (1940).

[92] E. Fermi and E. Teller, Phys. Rev. **72**, 399 (1947).

[93] G. R. Burleson, et al., Phys. Rev. Lett. **15**, 70 (1965).

[94] V. Fitch and J. Rainwater, Phys. Rev. **92**, 789 (1953).

[95] M. Camac, A. D. McGuire, J. B. Platt and H. J. Schulte, Phys. Rev. **88**, 134 (1952).

[96] C. Curceanu et al., Rev. Mod. Phys. **91**, 025006 (2019).

[97] G. Beer et al., Phys. Rev. Lett. **94**, 212302 (2005).

[98] M. Bazzi et al., Phys. Lett. **B704**, 113 (2011).

[99] S. Wycech, Nucl. Phys. **A450**, 399c (1986).

[100] Y. Akaishi, T. Yamazaki, Phys. Lett. **B535**, 70 (2002).

[101] Y. Akaishi, T. Yamazaki, Phys. Rev. **C65**, 044005 (2002).

[102] S. Wycech, A. M. Green, Phys. Rev. **C79**, 01400 (2009).

[103] Y. Ikeda, T. Sato, Phys. Rev. **C76**, 035203 (2007).

[104] S. Maeda, Y. Akaishi, T. Yamazaki, Proc. Jpn. Acad. **B89**, 418 (2013).

[105] N. V. Shevchenko, A. Gal, J. Mares, Phys. Rev. Lett. **98**, 082301 (2007).

[106] J. Revai, N.V. Shevchenko, Phys. Rev. **C90**, 034004 (2014).

[107] A. Dote, T. Hyodo, W. Weise, Phys. Rev. **C79**, 014003 (2009).

[108] A. Dote, T. Inoue, T. Myo, Phys. Lett. **B784**, 405 (2018).

[109] N. Barnea, A. Gal, E.Z. Liverts, Phys. Lett. **B712**, 132 (2012).

[110] Y. Ikeda, H. Kamano, T. Sato, Prog. Theor. Phys. **124**, 533 (2010).

[111] P. Bicudo, Phys. Rev. **D76**, (2007).

[112] M. Bayar, E. Oset, Nucl. Phys. **A914**, 349 (2013).

[113] T. Sekihara, E. Oset, A. Ramos, Prog. Theor. Exp. Phys. **2016**, (2016).

[114] T. Sekihara, E. Oset, A. Ramos, J.P.S. Conf. Proc. **26**, 023009 (2019).

[115] Y. Ikeda, T. Hyodo, W. Weise, Nucl. Phys. **A881**, 98 (2012).

[116] M. Maggiora et al., Nucl. Phys. **A835**, 43 (2010).

[117] M. Agnello et al., Phys. Rev. Lett. **94**, (2005).

[118] T. Suzuki et al. Mod. Phys. Lett. **A23**, 2520 (2008).

[119] R. Del Grande et al., Eur. Phys. J. **C79**, 190 (2019).

[120] E. Friedman, A. Gal, Phys. Rep. **452**, 89 (2007).

[121] C. J. Batty, E. Friedman, A. Gal, Phys. Rep. **287**, 385 (1997).

[122] L. Tolos, L. Fabbietti, Progr. Part. Nucl. Phys. **112**, 103770 (2020).

[123] T. Muto, T. Maruyama, T. Tatsumi, Phys. Lett. **B820**, 136587 (2021).

[124] D. Cabrera, L. Tolos, J. Aichelin, E. Bratkovskaya, Phys. Rev. **C90**, 055207 (2014).

[125] M. Zobov et al., Phys. Rev. Lett. **104**, 174801 (2010).

[126] M. Bazzi et al., Phys. Lett. **B704**, 113 (2011).

[127] F. Bossi et al., Rivista del Nuovo Cimento **31**, 531 (2008).

[128] K. P. Gall et al., Phys. Rev. Lett. **60**, 186 (1988).

[129] A. S. Denisov et al., JEPT Lett. **54**, 558 (1991).

[130] L. Bosisio et al., *Interacting Kaons on Nucleons (IKON)*, Scientific Report LNF-INFN (2010) i cytowania wewnątrz.

[131] V. Bernard, N. Kaiser, U. G. Meisner, Nucl. Phys. **A615**, 483 (1997).

[132] S. Scherer, M. R. Schindler, Theory. Lect. Notes Phys. **830**, 1 (2012).

[133] S. Ohnishi, Y. Ikeda, T. Hyodo, and W. Weise, Phys. Rev. **C93**, 025207 (2016) i cytowania wewnątrz.

[134] T. Hyodo and W. Weise, Phys. Rev. **C77**, 035204 (2008).

[135] A.Cieplý, M. Mai, U-G.Meissner, J.Smejkal, Nucl. Phys. **A954**, 17 (2016).

[136] S. Acharya et al, Phys. Rev. Lett. **124**, 092301 (2020).

[137] H. Yukawa and T. Okayama, Sci. Papers Inst. Phys. and Chem. Research **36**, 385 (1939).

[138] D. Horvath and F. Entezami, Nucl. Phys. **A407**, 297 (1983).

[139] J. Zmeskal, Prog. Part. Nucl. Phys. **61**, 512 (2008).

[140] D. Gotta, Prog. Part. Nucl. Phys. **52**, 133 (2004).

[141] M. Leon, H.A. Bethe, Phys. Rev. **2**, 127 (1962).

[142] E. Borie, M. Leon, Phys. Rev. **A21**, 1460 (1980).

[143] Z. W. Liu, J.J. Wu, D. B. Leinweber and A. W. Thomas, Phys. Lett. **B808**, 135652 (2020).

[144] L. Tolos, L. Fabbietti, Prog. Part. Nucl. Phys. **112**, 103770 (2020).

[145] J. D. Davies et al., Phys. Lett. **B83**, 55 (1979).

[146] M. Izycki et al., Z. Phys. **A297**, 11 (1980).

[147] P. M. Bird et al., Nucl. Phys. **A404**, 482 (1983).

[148] J. K. Kim, Phys. Rev. Lett. **14**, 29 (1965).

[149] A. D. Martin, Nucl. Phys. **B179**, 33 (1981).

[150] T. Ishiwatari et al., Phys. Lett. **B593**, 48 (2004).

[151] M. Bazzi et al., Phys. Lett. **B681**, 310 (2009).

[152] M. Bazzi et al., Phys. Lett. **B697**, 199 (2011).

[153] M. Bazzi et al., Phys. Lett. **B714**, 40 (2012).

[154] S. Okada et al., Phys. Lett. **B653**, 387 (2007).

[155] S. Hirenzaki, Y. Okumura, H. Toki, E. Oset and A. Ramos, Phys. Rev. **C61**, 055205 (2000).

[156] C. E. Wiegand and R. H. Pehl, Phys. Rev. Lett. **27**, 1410 (1971).

[157] S. Baird et al., Nucl. Phys. **A392**, 297 (1983).

[158] M. Bazzi et al., Eur. Phys. J. **A50**, 91 (2014).

[159] M. Bazzi et al., Nucl. Phys. **A907**, 69 (2013).

[160] L. Bombelli et al., IEEE Nucl. Sci. Symp. Med. Imag. Conf., 135 (2010).

[161] M. Bazzi et al., J. Instrum. **8**, T11003 (2013).

[162] G. Agakishiev et al., Phys. Lett. **B742**, 242 (2015).

[163] Y. Ichikawa et al., Prog. Theor. Exp. Phys. **2015**, 021D01 (2015).

[164] A. O. Tokiyasu et al., Phys. Lett. **B728**, 616 (2014).

[165] O. Vazquez Doce et al., Phys. Lett. **B 758**, 134 (2016).

[166] Y. Sada et al., Prog. Theor. Exp. Phys. **2016**, 051D01 (2016).

[167] C. Vander, II Nuovo Cimento **A39**, 538 (1977).

[168] J. Hrtankova and J. Mares, Phys. Rev. **C96**, 015205 (2017).

[169] E. Friedman and A. Gal, Nucl. Phys. **A959**, 66 (2017).

[170] K. Piscicchia and S. Wycech, Nucl. Phys. **A954**, 75 (2016).

[171] J. Hrtankova and A. Ramos, Phys. Rev. **C101**, 035204 (2020).

[172] W. E. Humphrey and R. R. Ross, Phys. Rev. **127**, 1305 (1962).

[173] J. K. Kim, Columbia University Report No. NEVIS-149 (1966).

[174] D. Sadasivan et al., Front. Phys. **11**, 1139236 (2023).

[175] R. Del Grande, K. Piscicchia, S. Wycech, Acta Phys. Polon. **B48**, 1881 (2017).

[176] F. James and M. Roos, Comput. Phys. Commun. 10 (1975) 343; F. James and M. Roos, Minuit: Function Minimization and Error Analysis, CERN Program Library Long Writeup D506 (1994); F. James and M. Winkler, Minuit User's Guide: C++ Version (2004).

3 Other scientific and research achievements

3.1 Research not contributing to the habilitation

My scientific activities and the most important achievements that do not contribute to the habilitation achievement described in Section 2 are presented below. They concern participation in the WASA-at-COSY and WASA-at-FRS experiments, research conducted by the J-PET group, and research performed at the Laboratori Nazionali di Frascati (LNF-INFN). Citations refer to the list of scientific publications presented at the end of this section and included in section 2.1 of *List of Achievements*.

As part of the WASA experiment operating on the COSY beam (WASA-at-COSY) in Forschungszentrum Jülich in Germany, I took an active part in measurements (experimental shifts) dedicated primarily to the study of the light mesons (η, ω, π) production and decay, and in discussions devoted to individual data analyses. The measurements provided a significant contribution, e.g., to the fundamental symmetries studies in the light mesons decay, as well as allowed the discovery of dibarion resonance $d^*(2380)$ and the study of its properties or the study of breakup processes. The obtained results are the basis of over twenty scientific articles [R34,R35,R44,R49-R54,R65,R66,R78-R80,R82,R83,R89-R93,R95-R98,R100-R103].

Research using the central part of the WASA detector is currently being carried out at the GSI Darmstadt research center in Germany. In 2022, as part of the S490 EtaPrime Collaboration, I participated in the WASA-at-FRS experiment, the aim of which was to observe for the first time the system of the η' meson bound to the atomic nucleus (η'-mesic nuclei) [I1,R36]. Integration of the WASA detector with the FRS magnetic spectrometer allowed the measurement of the $^{12}\mathrm{C}(p, dp)$ process [P2] whith simultaneous high-resolution missing mass spectroscopy for $^{12}\mathrm{C}(p, d)$ process and detection of particles emitted in the decay of hypothetical ^{11}C-η' mesic nuclei. It allowed for a significant increase in the experiment's sensitivity compared to the inclusive measurement carried out a few years earlier [1], which gives high hopes for observing the signature of mesic nuclei in the excitation function spectrum. The measurement of the mass of the η' meson bound in nuclear matter will provide key information for understanding the mechanism of particle mass generation (chiral symmetry breaking). A detailed analysis of the collected data is currently being carried out.

For seven years, I have also been involved in research in the J-PET (Jagiellonian PET) project operating at the Institute of Physics of the Jagiellonian University, whose primary goal is to build, launch, and test the first PET scanner for medical diagnostics, enabling simultaneous spatial imaging of the patient's entire body, using organic scintillation materials [2]. The prototype of the J-PET detector is used not only for bio-medical measurements but also due to the very high geometrical efficiency and the excellent

angular and time resolution for photon measurement. It is an ideal system for precise measurements of positronium atom decays, which, as the lightest, purely lepton objects, are a unique laboratory for discrete symmetries studies: C, CP, CPT [3, 4][R26].

Within the framework of the J-PET experiment, I participated in the construction of the tomograph in the measurements carried out, and I evaluated and carried out the time synchronization of the entire detection system based on measurements performed with a reference detector and a radioactive sodium source ^{22}Na. The calibration method is described in the article [R69]. I am also a co-author of a new data analysis software module that enables efficient calibration of the J-PET detector. This calibration was used during the analysis of experimental data, being the subject of several articles on medical diagnostics and discrete symmetries studies, including publications in prestigious journals [R24, R25].

I am currently studying the decay of the positronium atom, focusing on the experimental determination of the Dalitz plot in the angular and energy representation for the ortho-positronium (positronium triplet state) decay into three gamma quanta. So far, only three possible configurations of photons produced in o-Ps $\rightarrow 3\gamma$ decays have been measured, with little statistics (experiment conducted in 1967 by Mills and Berko [5]). The analysis of the data collected using the J-PET detector, which I carried out, allowed for the first determination of the Dalitz distribution for the investigated process in almost the entire available phase space. The obtained result is significant, as it provides a complete description of the studied reaction's dynamics, which will allow to test Quantum Electrodynamics (QED). I am currently preparing an article on the above research. The next step I started to implement is the study of the Dalitz distribution in terms of testing the charge symmetry (C), and, thus the search for the forbidden decay of the parapositonium p-Ps $\rightarrow 3\gamma$.

Another topic I pursue as part of the J-PET project is cancer imaging through the use of, for the first time in the world $3\gamma/2\gamma$ positronium annihilation ratio as an image-driven biomarker. It is one of the properties of positronium, in addition to its average lifetime or production probability [R25], which allows the assessment of tissue pathology "in vivo" at the molecular level [6]. Data from the first measurements of patients, carried out in 2022 using a mobile, modular J-PET tomograph and a CT tomograph (at the Medical University of Warsaw), is currently being analyzed with my participation. At this year's end, patients with liver cancer measurements are planned at the Nuclear Medicine Department of the University Hospital in Krakow. I am involved in their preparation. My task in the project will be active participation in measurements and data analysis.

These topics are included in the OPUS 18 grant titled *Precise tests of matter-antimatter symmetry by measuring the decay of positronium atoms with a J-PET modular tomograph* and MAESTRO 13 titled *Whole-body Jagiellonian Positron Emission Tomography - development of imaging biomarkers* (under the supervision of Prof. Paweł Moskal from the Jagiellonian University).

As part of my activity at Laboratori Nazionali di Frascati, I participated in the TASTE (Transportable and Agile Spectrometer for metal Trace in Edible liquids) project, led by Dr. Alessandro Scordo, which aims to create a Bragg spectrometer with mosaic

pyrolytic graphite crystals (HAPG) in the Von Hamos configuration, capable of working with liquid sources, for testing the concentration of heavy metals (mainly iron) in food products such as wine or olive oil. I participated in preparing the experiment proposal submitted to the National Committee for Technology Transfer in Italy and worked on optimizing the measurement system and the measurements themselves. Data analysis is currently ongoing.

It is also worth mentioning that I joined the research presented in articles [R61, R67]. My contribution to Ref. [R67] is related to the systematization and elaboration of experimental data (cross-sections for $pd(dp) \rightarrow {}^3\mathrm{He}\eta$ process), which were used for comparison with the newly developed theoretical model. As a result of the analysis, the ${}^3\mathrm{He}\eta$ scattering amplitude was determined, which indicates the existence of a weakly bound ^{3}He-η mesic nucleus. As part of the work [R61], I performed a fit of experimental data from the measurements of reactions of polarized photons with protons to determine the effective intersection points for the spin-dependent Regge theory.

References:

[1] Y.K. Tanaka, *et al.*, Phys. Rev. Lett. 117, 202501 (2016).

[2] P. Moskal, E. Stępień, PET Clin. 15, 439 (2020).

[3] P. Moskal, *et al.*, Acta Phys. Polon. B 47, 509 (2016).

[4] S. Bass, Acta Phys. Polon. B 50, 7 (2019).

[5] A. P. Mills and S. Berko, Phys. Rev. Lett. 18, 420 (1967).

[6] B. Jasińska, P. Moskal, Acta Phys. Polon. B 48, 1577 (2017).

3.2 International collaboration

- Collaboration with WASA-at-COSY group started in 2008 (spokesperson Prof. Magnus Wolke) concerns:
  - experimental search for He-η mesic nuclei in Forschungszentrum Jülich (Germany). The results of the collaboration are the publications [**H1,H2,H5,H7,H9,H10**].
- Collaboration with Prof. Neelima Kelkar from Universidad de los Andes, Bogota, Colombia. The collaboration, initiated in 2016, concerns the production model of He-η mesic nuclei with the N* resonance excitation (N* momentum distributions in helium nuclei). The collaboration results are works [**H1-H3,H5,H6,H7**].
- Collaboration with Prof. Satoru Hirenzaki and Prof. Hideko Nagahiro from Nara Women's University, Nara, Japan. The collaboration, initiated in 2014 concerns:

  - the formulation of a new theoretical model of ^{3}He-η bound state production and decay, so-called non-mesonic decay,
  - theoretical interpretation of experimental results obtained for the search for ^{4}He-η mesic nuclei.

    The collaboration results are works [**H2,H4,H5,H7**].

- Collaboration with group of Prof. Catalina Curceanu from Laboratori Nazionali di Frascati INFN, Frascati, Italy. The collaboration, initiated in 2014 concerns:

  - investigation of kaonic atoms (i.a. kaonic deuterium) in frame of the SIDDHARTA-2 Collaboration,
  - studies of low-energy kaon-nucleon/nuclei interactions focusing on the search for kaonic clusters and the properties of the baryon resonance $\Lambda(1405)$ in frame of the AMADEUS Collaboration.

    The collaboration results are works [**H8,H11**,R42,R47].

- Collaboration with WASA-at-FRS group (spokesperson Prof. Kenta Itahashi) concerns:

  - experimental search for η'-mesic nuclei in Research Center GSI Darmstadt (Germany).

3.3 Didactic activity

Teaching activities:

- In years 2010-2015, as a Ph.D. student, and then Research Assistant at the Faculty of Physics, Astronomy and Applied Computer Science of Jagiellonian University, I conducted:

  - Statistical Methods of Measurement Processing class for Physics students,
  - classes in the 1st Physics Laboratory for students from the following fields: Physics, Chemistry, Biotechnology, and Environmental Protection,
  - laboratory classes for secondary and high school students.

- In 2020 I conducted lecture *Relativistics Kinematics* for Ph.D. students of the first and the second year at the Faculty of Physics, Astronomy and Applied Computer Science of Jagiellonian University.

- In years 2021 -2023 as Assistant Professor at the Faculty of Physics, Astronomy and Applied Computer Science of Jagiellonian University, I conducted:

  - Termodynamics classes for Physics and Biophysics students,

  - Physics class for Applied Computer Science students,
  - classes in the 1st Physics Laboratory for students from the following fields: Physics, Physics for Business, Chemistry, and Sustainable Chemistry,
  - classes in the 2nd Physics Laboratory for Physics students,
  - classes in the Electronic Laboratory, i.e. Digital Electronics for Physics and Applied Computer Science students.

- In 2021, 2022, 2023, supervisor of Summer Student Internships at the M. Smoluchowski Institute of Physics of the Jagiellonian University (in the Department of Experimental Particle Physics and Applications).

Supervision:

- In years 2016-2019, scientific supervision of Ph.D. student Oleksandr Rundel as an auxiliary supervisor.
- In years 2016-2020, scientific supervision of Ph.D. student Aleksander Khreptak as an auxiliary supervisor.
- From 2022 scientific supervision of Ph.D. student Kavya Valsan Elyian as an auxiliary supervisor.
- In 2023, scientific supervision of bachelor student Kamila Kasperska as a supervisor of the bachelor thesis.

3.4 Organizational activity

My organizational activity is related to organizing the following conferences and scientific meetings:

- **Main organizer (Chair):** *Symposium on new trends in nuclear and medical physics*, Jagiellonian University, Center for Theranostics, Cracow (Poland), will be held in period 18-20.10.2023.
- Co-organizer: *Applications of radiation detection techniques in fundamental physics, food control, medicine and biology*, Laboratori Nazionali di Frascati (LNF-INFN), Frascati (Italy), 8-12.05.2023.
- **Scientific Secretary:** *4th Jagiellonian Symposium on Advances in Particle Physics and Medicine*, Jagiellonian University, Cracow (Poland), 10-15.07.2022.
- Co-organizer: *Is Quantum theory Exact? Exploring Quantum Boundaries*, Laboratori Nazionali di Frascati (LNF-INFN), Frascati (Italy), 10-11.12.2020.
- **Main organizer:** *Investigating the Universe with exotic atomic and nuclear matter*, Laboratori Nazionali di Frascati (LNF-INFN), Frascati (Italy), 29-30.09.2020.

- Co-organizer: *Strange Matter Workshop - Strangeness studies in Italy and Japan*, Laboratori Nazionali di Frascati (LNF-INFN), Frascati (Italy), 15-17.10.2019.
- Co-organizer: *Is Quantum Theory exact? From quantum foundations to quantum applications*, Laboratori Nazionali di Frascati (LNF-INFN), Frascati (Italy), 23-27.09.2019.
- Co-organizer: *3rd Jagiellonian Symposium on Fundamental and Applied Subatomic Physics*, Jagiellonian University, Cracow (Poland), 23-28.06.2019.
- Co-organizer: *Low-energy strangeness studies at DAΦNE and J-PARC*, Laboratori Nazionali di Frascati (LNF-INFN), Frascati (Italy), 19-20.12.2018.
- Co-organizer sympozjum *2nd Jagiellonian Symposium on Fundamental and Applied Subatomic Physics*, Jagiellonian University, Cracow (Poland), 4-9.06.2017.
- **Main organizer:** *AMADEUS Collaboration Workshop*, Jagiellonian University, Cracow (Poland), 4.06.2017.
- Co-organizer: *Jagiellonian Symposium on Fundamental and Applied Subatomic Physics*, Jagiellonian University, Cracow (Poland), 7-13.06.2015.
- Co-organizer: *II Symposium on Applied Nuclear Physics and Innovative Technologies*, Jagiellonian University, Cracow (Poland), 24-27.09.2014.
- Co-organizer: *Symposium on Positron Emission Tomography*, Jagiellonian University, Cracow (Poland), 21-24.09.2014.
- Co-organizer: *II International Symposium on Mesic Nuclei*, Jagiellonian University, Cracow (Poland), 22-25.09.2013.
- Co-organizer: *Symposium on Positron Emission Tomography*, Jagiellonian University, Cracow (Poland), 19-22.09.2013.
- Co-organizer: *The 22nd European Conference on Few-Body Problems In Physics*, Jagiellonian University, Cracow (Poland), 09-13.09.2013.
- Co-organizer: *Symposium on Applied Nuclear Physics and Innovative Technologies*, Jagiellonian University, Cracow (Poland), 04-05.06.2013.
- Co-organizer: *MESON 2012 (12th International Workshop on Meson Production, Properties and Interaction)*, Jagiellonian University, Cracow (Poland), 31.05-05.06.2012.

Since 2021, I have been the Scientific Secretary of the Cluster of Nuclear Physics Departments at the Marian Smoluchowski Institute of Physics at the Jagiellonian University.

3.5 Popularization of science

- In 2022, popular science lecture as part of the *Closer to Science* series of lectures organized at the Faculty of Physics, Astronomy and Applied Computer Science of the Jagiellonian University, *Search for Exotic Nuclear Matter*

- In 2021, popular science lecture for students of Da Vinci's International School in Cracow, *What is strange matter and where can we find it?*

- In 2021, popular science lecture in frame of Women's Day *Scienziate a confronto dai quark ai buchi neri*, online, in italian.

- In 2020, I participated in the International Day of Women and Girls in Science, organized in Laboratori Nazionali di Frascati LNF-INFN (Italy). I gave a popular science talk for Italian students: *A Nuclear Physicist inspired by Maria Skłodowska-Curie* (11.02.2020).

- In 2013, as a Ph.D. student, I took part in a series of demonstrations of experiences in frame of the Festival of Science and Arts in Cracow.

- In 2009, as a Master student, I participated in the organization and gave a talk at the summer school at the Research Center Jülich (Germany) for students in the third year of Master's Studies *Is Radon really Budding in a Can?*.

- In 2009, as a Master student, I developed instructions for the experiment *Measurement of Radon Activity in Building Materials* for students of the 2nd Physics Laboratory of the Jagiellonian University based on the conducted studies.